Universitat Autònoma de Barcelona

Doctoral thesis

EXPLORING THE MECHANISM OF ACTION OF HUMAN ANTIMICROBIAL RIBONUCLEASES

VIVIAN ANGÉLICA SALAZAR MONTOYA

Barcelona, 2015

DISCUSSION AND FUTURE PERSPECTIVES

5. DISCUSSION AND FUTURES PERSPECTIVES

The innate immunity system or “non–specific” inmunity plays a critical role in fighting infection. The innate immune system relies upon a limited repertoire of receptors to detect invading pathogens, but compensates for this limited number of invariant receptors by targeting conserved microbial components that are shared by large groups of pathogens. Indeed, numerous elements constitute this network of protection, cells of haematopoietic and non-haematopoietic origin. Concerning to haematopoietic cells, the innate responses comprise macrophages, dendritic cells, mast cells, neutrophils, eosinophils, natural killer cells and natural killer T cells. In addition to haematopoietic cells, innate immune responsiveness is a property of the skin and the epithelial cells lining the respiratory, gastrointestinal and genitourinary tracts (Turvey & Broide 2010).

To increase these cellular defences, innate immunity additionally has a humoral component that involves well-characterized components as complement proteins, lipopolysaccharide binding protein (LBP), C-reactive protein and a variety of antimicrobial peptides. We have focused our investigation on human ribonucleases that can be regarded as antimicrobial proteins involved in innate immunity, displaying a remarkable antimicrobial ability against helminths, protozoa, bacteria and fungi (Boix and Noguès, 2007). The current research tries to clarify the biological activities of the eosinophil RNase 3 also called the Eosinophil Cationic Protein (ECP), the skin derived RNase 7 and the human placental RNase 8. Structural-functional studies are focused towards the pharmacological design of peptides derived antimicrobial agents (Torrent et al. 2011); (Pulido et al. 2013).

5.1 Analysis of the contribution of posttranslational modifications of RNase 3/ECP native forms in antimicrobial activity.

One of the most studied cells of innate immunity are eosinophils. Historically, they have been considered a primary effector mechanism against specific parasites, and are likewise implicated in tissue damage accompanying allergic responses (Shamri et al.

2011). The most characteristic feature of eosinophils are their cytoplasmic content of specific granules. The main constituents of eosinophil specific granules are the cationic proteins, such as major basic protein (MBP), eosinophil peroxidase (EPO), eosinophil-derived neurotoxin (EDN) and eosinophil cationic protein (ECP), or RNase 3. The release of granules content implicates a regular process -piecemeal degranulation-, where small spherical vesicles and larger tubular vesicles emerge from mobilized intracellular granules and travel through the cytoplasm to the cell membrane. Simultaneously to this process, RNase 3/ECP suffers a series of post-translational modifications that generate a cytotoxic active molecule (Woschnagg et al. 2009). Previous work reported that native ECP heterogeneity is mostly due to distinct glycosylation degrees (Rubin and Venge 2013), wherethree potential N-glycosylation sites are found in ECP sequence . The location of these potential glycosylation sites on native ECP are shown in Figure 52.

Previously, numerous studies conducted in our laboratory have allowed us to describe the recombinant RNase 3/ECP activity on both bacterial and eukaryotic mammalian cells. The present research is focused on determining the activity of native ECP forms on bacterial cells and a membrane model. The native protein was directly purified from eosinophils with the subsequent characterization of protein fractions by SELDI-TOF MS mass spectrometry. The fractions were sorted by molecular weight and grouped into 7 samples (nECP1- nECP7). Also, the protein fractions were classified into high and low molecular weight pools for comparison purposes (HMW-ECP and LMW-ECP fractions). Recombinant protein expressed in a prokaryote system and previously characterized (Torrent et al. 2007); (Torrent et al. 2009a) was always used as reference.

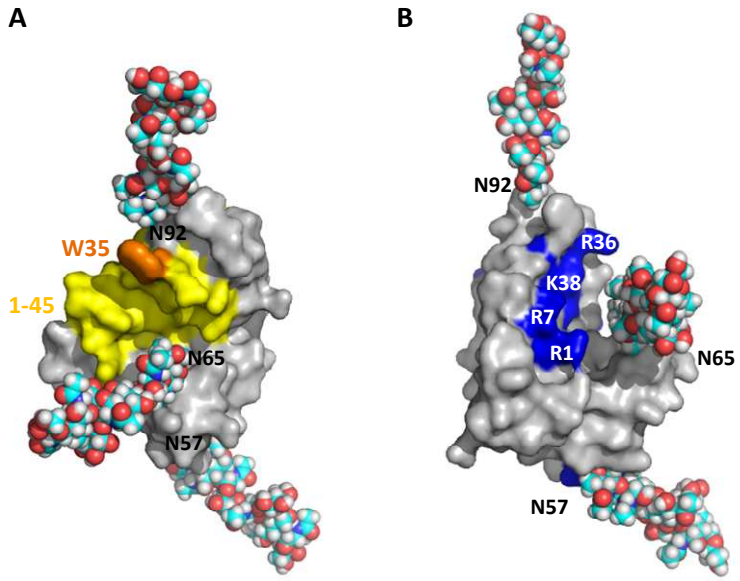

Figure 52: Model showing the location of putative ECP N-glycosylation.
A reference glycan structure (2K33.pdb) was attached to Asn residues at potential glycosylation sites. A) The main ECP region involved in the protein antimicrobial activity is coloured in yellow and key residue for membrane interaction in orange. B) Cationic residues involved in the bactericidal activity are coloured in blue. Residues potentially under the oligosaccharide influence are labelled in white.

Our results highlight an inverse correlation between antibacterial activity against *E.coli* and the grade of glycosylation, where a higher grade of glycosylation corresponds to less cytotoxicity. These results were compared with the action reported previously in eukaryotic cells (Woschnagg et al. 2009), (Rubin & Venge 2013), where LMW-ECP pools presented enhanced cytotoxic activity. Additionally, ability to bind LPS and aggregate bacteria cells as an initial stage for antibacterial activity are progressively reduced as a function of post-translational modifications. Results suggest that the glycosylation in ECP molecule may be blocking the protein-aggregation prone zone and thereby modulate the protein-membrane interaction, especially at the glycosylation site in N65 residue. The intracellular traffic of ECP from granule-stored to cell membrane and posterior degranulation, involves serial glycosylation modifications, converting the protein progressively into a cytotoxic form. In a general context, the post-translational protein modification would modulate intracellular trafficking and final biological properties. Hence, additional studies are in process to clarify the specific biological abilities of each native ECP form.

5.2 Analysis of the antifungal activity of RNase 3/ECP and RNase 7. Candida albicans as an eukaryotic pathogen model.

Several secretory vertebrate RNases were previously reported to display antifungal activity. In particular, RNase 5, RNase 7 and RNase 8 were reported as antifungal, with referred lethal doses close to the ones for bactericidal activity, or only slightly higher values (Hooper et al. 2003); (Abtin et al. 2009); (Harder & Schroder 2002); (Rudolph et al. 2006). Here, the activity towards *Candida albicans* of RNase 7 and RNase 3/ECP, the two main human antimicrobial RNases, was studied. RNase 7, expressed in cutaneous tissues, as a first protection barrier against infection, and RNase 3/ECP secreted by eosinophils secondary granules. Both proteins have previously been associated to expression in the host defence induced by fungal infections (Rothenberg 2009); (Harder and Schroder 2002).

Considering the increment of cutaneous infection caused by *Candida* in healthy and immunocompromised individuals, there is an urgent need to develop new antifungal therapies. Also, *C. albicans* has a remarkable ability to grow in several distinct morphological forms: yeast, hyphae, and pseudohyphae, according to environmental conditions, facilitating evasion of the host immune response (Sudbery et al. 2004). Therefore, this opportunistic yeast, representing a suitable eukaryotic cell model to study the antimicrobial mechanism of action, was chosen.

The results obtained in this study confirm that both ribonucleases were able to inhibit *Candida* growth in a low micromolar range. The present results highlight the proteins dual mode of action. Indeed, antimicrobial RNases would represent an interesting example of a multifunctional protein, combining an enzymatic activity with a mechanical action at the membrane level.

Previous work conducted in our laboratory, demonstrated how RNase 3/ECP and RNase 7 display bactericidal activity, identifying the mechanism of action at the bacterial envelope (Torrent et al. 2010a); (Pulido et al. 2013); (Torrent et al. 2012). However, these studies determined RNase antibacterial activity at high protein concentration, giving as a result, a drastic reduction of bacterial growth. Here we assayed and observed the protein mechanism against *C. albicans* using a RNase concentration below

the protein IC_{50} values to also analyse the potential protein cell internalization and intracellular action.

On the one hand, RNase 7 displayed a particularly high antifungal activity, maybe related to a putative function in physiological conditions as a protector against skin infections (Harder and Schroder 2002); (Köten et al. 2009). Harder and co-workers have determined that RNase 7 is able to inhibit the *Candida albicans* growth using a slightly higher protein concentration in comparison with the values used for antibacterial activity (Harder & Schroder 2002). We also reported the protein antifungal activity, showing an effective concentration slightly above the required for the antibacterial activity. Additionally, we observed the RNase 7 uptake by *Candida* yeast cells. The main events suggested to take place during RNase action on *C. albicans* yeast cells are illustrated in Figure 53. The RNase antifungal activity would start with an electrostatic association to the cell surface, interaction at membrane level,followed by a subsequent internalization that probably concludes with the binding to nucleic acids and RNA degradation by the protein enzymatic activity. The RNase mutant H15A forms devoid of catalytic activity preserve the membrane-binding ability but display a delay in their effective cytotoxicity.

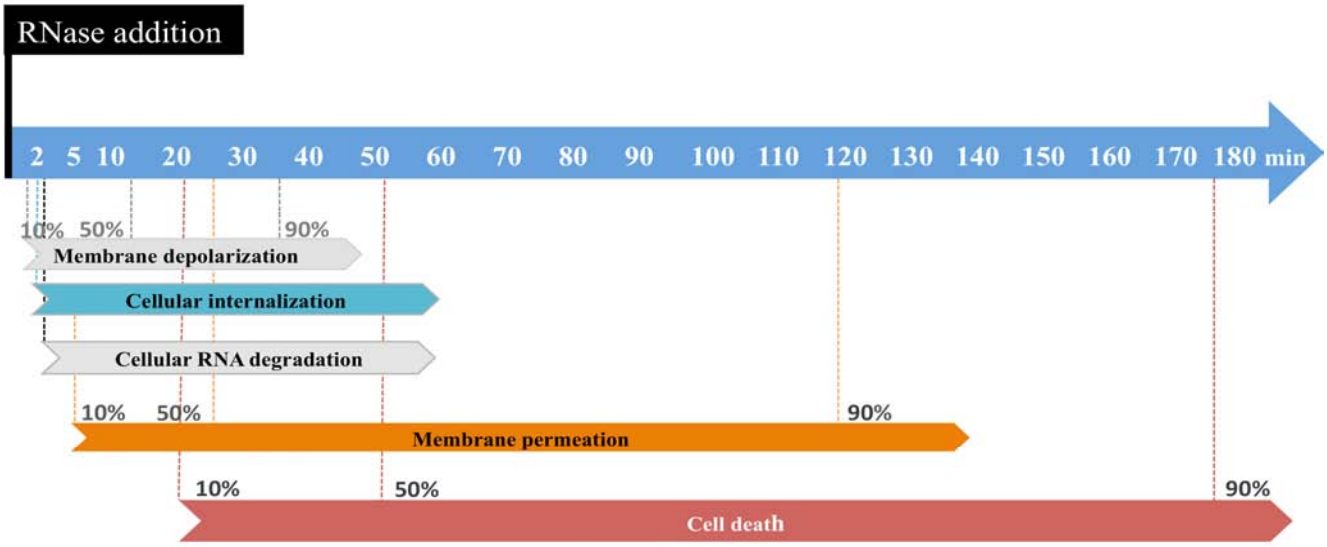

Figure 53: Timing of main events after RNase 3/ECP and RNase 7 addition.
Membrane-depolarization was analysed by monitoring the $DiSC_3(5)$ fluorescence intensity change. Cell permeabilization analysis was monitored by using a SYTOX® Green uptake assay. Intracellular localization was observed using Alexa Fluor labelled RNases and subsequent RNA degradation was evaluated. Cell death was evauated by the Live/Dead staining kit.

Complementary, a point-mutant variant RNase 3-W35A, with reduced cell binding activity (Carreras et al. 2005), (Carreras et al. 2003), (Torrent et al. 2007), was chosen to analyse the protein-cell interaction step. Results on *Candida* yeast cells confirmed that W35 also plays an important role in the protein binding onto the surface of the yeast cell. W35 substitution prevents the RNase cellular internalization and reduces considerably the protein antifungal effect.

Cell entrance is a reported ability shared by various RNase A family members such as onconase, bovine seminal ribonuclease and RNase 3/ECP (Benito et al. 2008); (Nicolas 2009); (Fang et al. 2013). The current experiments confirm that RNase 3/ECP and RNase 7 have the ability to promote cell uptake, perhaps by the interaction of the protein cationic domains with exposed anionic components at the extracellular matrix, which would mediate an unspecific cell entrance. Indeed, both human ribonucleases are strongly cationic due to their high number of either Arg or Lys, a feature common to cell-penetrating peptides (CPPs) (Schmidt et al. 2010); (Patel et al. 2007) with membrane-translocating properties. Following cell internalization, human ribonucleases may have access to potential intracellular targets and in particular cellular RNA. Cationic and amphipathic proteins as human antimicrobial ribonucleases can thus be considered as an example of cell-penetrating peptides. Many CCPs have been reported as internalization vehicles into mammalian-eukaryotic cells lines, but interaction with eukaryotic pathogens is underrepresented. Indeed, the study of CPPs in yeast is an emerging field offering promising biotechnological applications (Mochon & Liu 2008); (Marchione et al. 2014).

In conclusion, antimicrobial RNases have proven a suitable model to study the protein membrane interaction, cellular uptake and subsequent blockage of vital intracellular pathways leading to cell death. Therefore, the studied human antimicrobial RNases provide a promising model towards the design of new applied therapies against fungal infections.

5.3 Exploring RNase 8 structure-function. Design of a new expression protocol and functional characterization.

Human RNase 8 is the eight and last identified member of the Ribonuclease A gene superfamily. However, it should be pointed out that RNase 8 has not yet been detected as a native protein in the tissues analysed, and its existence has only been demonstrated at the gene coding level. First, protein expression by northern analysis identified RNase 8 mRNA prominently in placental tissue (Zhang et al. 2002). Recent analysis by Chan and colleagues detected significant expression level in adult tissues such as spleen, lung, testes, ovary and in foetal tissues as spleen, thymus, brain, kidney and heart (Chan et al. 2012). Notwithstanding, the RNase 8 biological function is still unknown. In fact, Chang and colleagues could not identity the mature protein expression and secretion in the studied tissues and blood cell types. Besides, human genetic diversity of RNase 8 gene suggests that the presence of pseudogenes in human and primate genomes might indicate that the evolutive selection pressure to acquire new physiological functions are still underway (Chang et al. 2012).

On the other hand, subsequent works have been focused on obtaining RNase 8 as a recombinant protein. Zhang and co-workers managed the expression of the protein using the vector pFLAGCTS (Zhang et al. 2002). Afterwards, Rudolph and co-workers cloned RNase 8 gen into pQE-2 vector to express RNase 8 as a histidine-tagged protein in order to purify it by a Ni^{2+} affinity chelate chromatography (Rudolph et al. 2006). However, up to now, no high-yield method of preparation of recombinant RNase 8 has been reported.

In our research group, RNase 8 was initially cloned into the pET 11c vector for the protein expression in *E.coli*. In the first preparation process, very little or no protein was obtained, neither from soluble fraction nor from inclusion bodies fraction. Protocols applied successfully for the preparation of other RNase family members in our group proved inappropriate for RNase 8.

In this work, the plasmid pET45(+) based on the expression of a fusion protein with an N-terminus His-tag coding sequence has been used for the expression in *E.coli* BL21 (λDE3) and subsequent protein purification by an Ni^{2+} affinity chelate chromatography.

This kind of chromatography allowed an effective capture of the target protein and a high yield recovery of the eluted protein. However, severe aggregation problems have been observed at this step of purification leading to a major loss of the recombinant protein. Addition of 5 mM DTT and 5 mM EDTA to the eluted fraction prevented protein aggregation (Bondos & Bicknell 2003); and allowed to continue the process of purification of the histidine-tagged protein and the subsequent downstream processing of the fusion protein for removal of the fusion partner. The method developed for the purification of RNase 8 consisted on a affinity chelate chromatography, a gel filtration chromatography and an optional reverse-phase chromatography; allowing a yield of approximately 4 mg per litre of culture at the end of the purification process.

Protein aggregation tendency has been analysed by dynamic light scattering technique and by computational prediction. Dynamic light scattering has been applied to analyse the effect of the protein concentration on the protein aggregation. The results showed that aggregation occurs at a concentration above 1mg/mL of protein. By applying the *Aggrescan* software, aggregation prone regions in RNase 8 structure were identified. RNase 8 structure presents less aggregation zones than RNase 3/ECP whose aggregation is already observed at concentrations 5 to 10-folds higher than RNase 8. For the structural analysis a 3D model has been predicted for RNase 8 based on RNase 7 known structure, the closest RNase 8 homologue.

Disulphide bonds are important to the folding and stability of some proteins, usually those secreted to the extracellular medium. Because of their structural importance, disulphide bonds tend to be evolutionary conserved (Thornton 1981). In fact, cysteine is the second most conserved amino acid (after tryptophan) in protein evolution (Jones et al. 1992) and cysteine that form disulphide bonds are much more conserved that those not forming disulphide bonds (Thornton 1981). The majority of the canonical RNases of mammals, like RNase A, have 8 conserved cysteines. A notable exception is RNase 5 (also known as angiogenin), which has only 6 cysteines, forming 3 disulphide bonds (Strydom et al. 1985). Zhang and colleagues reported that human RNase 8 lost the sixth (C6) of the 8 conserved cysteines but gained another one leading to a positional change of one cysteine, when compared with other canonical RNases. Our computational prediction of disulphide bonds has been applied assuming that human RNase 8 and RNase 7, with a 78% of sequence identity, share an equivalent overall three-

dimensional structure. The disulphide bond prediction showed that only three disulphide bonds are able to form since cysteine 23 and cysteine 66 residues are too far away to connect (Figure 54). Effectively, the experimental quantitative determination of free sulfhydryl groups in RNase 8 showed the presence of two free sulfhydryl groups in the protein.

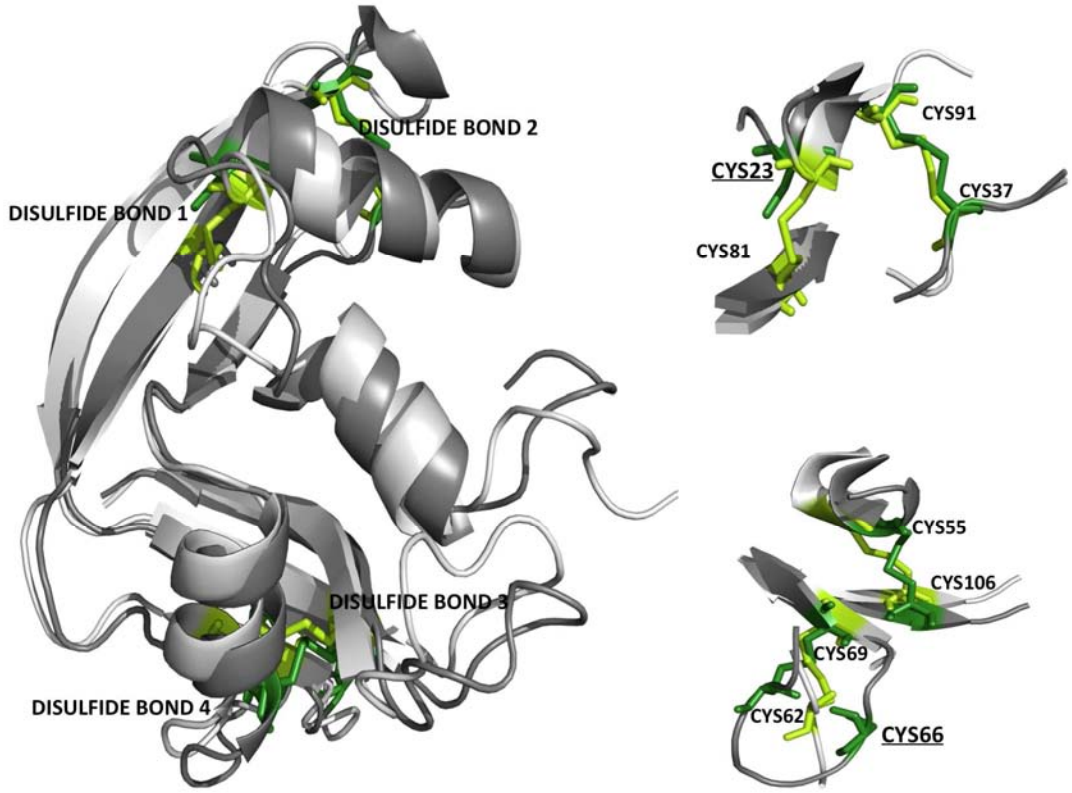

Figure 54: Computational prediction of disulphide bonds reshuffling in RNase 8. The three-dimensional structure of RNase 8 is based on the NMR 3D structure reported for RNase 7. Underline residues correspond to non-paired cysteines.

Because RNase 8 is a paralog of RNase A, the classic model for studying the role of disulphide bonds in protein folding and stability, the potential alterations of RNase 8 function by disulphide-bond reshuffling must be considered in future structure and functional analysis.

Following, we characterized RNase 8 biological properties. Zhang and colleagues 2002 analysed the enzymatic activity of recombinant human RNase 8 against yeast tRNA and found that RNase 8 was ribonucleolytically active, but the detected activity was significantly lower than all the other human canonical RNases, except RNase 5.

In this work, the RNase 8 substrate specificity and the polymeric cleavage mode were analysed. Main base specificity was shown by activity staining electrophoresis. RNase 8 was active against pyrimidinic substrates showing higher activity for poly(C) than poly(U), while no activity was observed for the purinic substrate. However, RNase 8 activity was significantly much lower than the activity observed for RNase A with both pyrimidinic substrates. The results showed that RNase 8 is a pyrimidine specific ribonuclease and presents a clear preference for cytidine, indicating a similar base specificity to RNase A.

Previously, RNase A kinetic studies revealed the presence of several phosphate and base subsites, in particular a main base binding subsite named (B_1), which is specific for pyrimidines, and a secondary (B_2) binding subsite, which can bind preferably a purine (Parés et al. 1991). Further, structural and kinetic studies were undergone to characterize RNase 8 binding subsites.

Following, the RNase 8 catalytic cleavage pattern was studied by means of polymeric substrates. RNase 8 displays an endonucleolytic activity as reported for RNase A, however with slight tendency towards an exonucleolytic activity as assessed by the amount of mononucleotide formation. Previous studies with high molecular mass substrates such as poly (C), identified many binding substrates including basic amino acids located at the protein surface. RNase A shows a characteristic cleavage pattern with intermediate steps with an accumulation of oligonucleotides containing six to seven residues (Moussaoui et al. 1996). RNase 8 showed a cleavage pattern similar to RNase A but with the accumulation at the intermediate stages of the cleavage process of shorter oligonucleotides (containing four or five nucleotides). Moussaoui and colleagues reported that the endonuclease activity and the accumulation of oligonucleotides of intermediate size are due to the presence in RNase A of secondary phosphate-binding subsites. Further kinetic studies and site-directed mutagenesis analysis are needed to confirm the presence of secondary subsites in RNase 8.

Up to now, no clearly-defined physiological function has been reported for RNase 8. However, the high similarity of RNase 8 to the antimicrobially active RNase 7 suggests that RNase 8 might also act as an antimicrobial protein. Rudolph and colleagues reported that the recombinant RNase 8 exhibited a broad spectrum microbial activity

against potential pathogenic microorganisms and identified RNase 8 as a novel antimicrobial protein that may contribute to host defence (Rudolph et al. 2006).

Therefore, after conformational and enzymatic characterization of RNase 8, we analysed the antibacterial activity towards various Gram-positive and Gram-negative species. Controversial results were previously reported. Prior studies by Zhang and co-workers reported that RNase 8 was inactive (Zhang et al. 2002), while studies by Rudolph and co-workers described RNase 8 as a potent antimicrobial protein against clinically relevant microorganisms at concentrations of micro to nanomolar. RNase 8 exhibited a broad spectrum of potent antimicrobial activity against various bacterial species. In particular, many pathogenic bacteria such as *Staphylococcus aureus, Enterococcus faecium, Enterococcus faecalis, Pseudomonas aeruginosa*, and *Klebsiella pneumoniae* were killed by small amounts of RNase 8. Also, the yeast *Candida albicans* was efficiently killed by RNase 8. Furthermore, the antimicrobial activities of RNase 8 compared with the action of native RNase 7 indicated a slightly higher activity for RNase 7 on *Staphylococcus aureus* and *Pseudomonas aeruginosa* (Harder et al. 2002). In this work, the human RNase 8 action against *E. coli, S. aureus, A. baumannii* and *M. luteus* strains was tested and compared with the RNase 3/ECP and 7 counterparts.

Previous work reported that RNase 7 bacterial mechanism was dependant on unspecific electrostatic interaction and subsequent membrane disruption (Torrent et al. 2009b). The present comparative characterization of RNase 8 with other RNase counterparts corroborated that RNase 7 has no significant membrane aggregation capacity compared to RNase 3/ECP, although it displayed a much higher leakage capacity. Interestingly, we have found that RNase 8 also did not display membrane aggregation activity, although the leakage capacity was less effective than RNase 7. Analysis of membrane damage using lipid vesicles with entrapped dye markers of variable size showed that RNase 8 caused only moderate membrane local disturbance.

On the other hand, membrane-depolarizing assays confirmed that RNase 8 was also able to cause cytoplasmatic membrane disturbance, as reported for RNase 3/ECP (Torrent et al. 2008). RNase 7 displayed slightly lower cell membrane depolarization, than RNase

3/ECP. In contrast, RNase 8 depolarization profile was much worse than RNase 7 and RNase 3/ECP. However, ultrastructural analysis visualized how RNase 8 promoted cell disruption, intracellular spillage and membrane detachment, with a similar pattern to the one observed for RNase 7.

Structural comparison of RNase 3/ECP, RNase 7 and RNase 8 predicted model demonstrated particular unique features on RNase 3/ECP structure promoting protein aggregation. Moreover, bacteria agglutinating efficiency was also correlated with the presence of hydrophobic patches by *de novo* designed RNase 3/ECP derived antimicrobial peptides (Torrent et al. 2011). The absence of hydrophobic patches may be responsible for the lack of agglutinating capacity for both RNase 7 and RNase 8.

Human ribonucleases 3 and 7 are currently regarded as antimicrobial proteins involved in innate immunity, as first line protectors against pathogen invasion. Now, we can conclude that RNase 8 might also contribute to the innate immunity system. On going studies are being carried out to fully characterize RNase 8 structure-function relationship.

Interestingly, the three examined RNases contain a high number of cationic residues: Arg and/or Lys, suggesting that the cationicity of the three proteins has been acquired independently during evolution. However, although the initial protein interaction with the bacterial cell (bacteria wall and cytoplasmatic membrane) would be conducted by electrostatic interactions, our results demonstrate that potential intracellular targets as cellular RNA many also have a key role in the protein cytotoxicity.

Further comparative studies on the distintict antimicrobial RNases would help to understand their multitask mechanism of action and their phyisiological role in human host defence.

CONCLUSIONS

6. CONCLUSIONS

Analysis of the antimicrobial mechanism of action of RNase 3/ECP native forms

- Analysis of purified RNase3/ECP native forms from healthy blood donors reveals the protein heterogeneity due to posttranslational modification. Seven fractions grouped according to their molecular weight (nECP1 to nECP7), from lower to higher MW, corresponding to distinct glycosylation degrees were identified and characterized.

- ECP native forms differ in their antimicrobial properties. Low and heavy glycosylated forms display a distinct antimicrobial profile, where heavy glycosylation significantly reduces the protein toxicity. The lowest glycosylated form (nECP7) shows an equivalent, or even slightly higher cytotoxic activity than the recombinant protein (rECP).

- Bacteria cell agglutination and liposome aggregation are gradually hindered by the protein glycosylation, achieving close to total activity inhibition by the heaviest glycosylated form.

- Heavy glycosylation correlates with a moderate reduction of the protein affinity to lipopolysaccharides. However, lack of major differences in the proteins' LPS binding affinity suggests that glycosylation mostly hinders the protein cell agglutination by blocking the protein self-aggregation activity rather than by reducing its binding towards the bacteria wall.

- Comparison of bacteria cell leakage indicates a moderate reduction as a function of the protein glycosylation degree.

- Comparison of liposome leakage activity using distinct MW markers indicates that heavy glycosylation interferes with the protein membrane disruption action.

- The gradual liposome leakage process of Tb^{3+} and ANTS is directly correlated to the lipid/protein ratio.

- The total vesicle content release for high MW entrapped dextran is only accomplished for the LMW fractions, pointing to an overall "carpet-like" mechanism.

- A three-dimensional representation model of RNase 3/ECP putative glycosylated forms suggests that the glycosylation branch at Asn65 would block the protein membrane binding and aggregation prone region.

- We hypothesize that glycosylation modulates RNase 3/ECP physiological role.

Analysis of the antifungal activity of RNase 3/ECP and RNase 7*. Candida albicans *as an eukaryotic pathogen model.

- Both human RNase 3/ECP and RNase 7 display antifungal activity at micromolar concentration; the protein concentration necessary for antifungal activity being slightly higher in comparison to the values reported for antibacterial.

- Results indicate that the fluorescent-labelled protein is associated to the yeast cells already few minutes after addition.

- Membrane depolarization followed by membrane destabilization preceeds the yeast cell viability decrease.

- RNases yeast cell internalization is observed at sublethal concentrations and short incubation times, before any significant decrease in cell viability.

- Tracking the cell population by a cell-sorting assay combining protein labelling with staining of dead cells, confirms the protein cell colocalization and the

absence of significant cell death at the assayed protein conditions selected to test the RNases action on cellular RNA.

- The designed catalytic and membrane binding defective mutants enabled the follow up of the protein mechanism of action.

- Ablation of catalytic activity is achieved by RNase H15A mutants, as confirmed by zymogram and degradation of oligocytidylic acid.

- The modified forms lacking the catalytic H15 do not decrease their membrane binding and cell internalization abilities. Analysis of cellular RNA supports their lack of catalytic activity.

- W35 is an important residue required for cell binding and membrane lysis. The results confirm an impaired membrane-depolarization and permeation activity on *Candida albicans* for the corresponding RNase 3-W35A mutant. Also, the mutants display an impaired yeast cell entrance.

- The results support the putative physiological role of the secreted RNases 3 and 7 against *Candida albicans*. Human secreted RNases, targeting pathogen cellular, are therefore promising antimicrobial tools.

Exploring RNase 8 structure-function. Design of a new expression protocol and functional characterization

- The designed prokaryote expression protocol for human RNase 8 using a His-tag and affinity-chelate chromatography, obtains a final purification yield of 4-5 mg of the protein per liter of culture.

- Prediction of the protein 3D structure using RNase 7 as a model suggests the formation of only three of the four potential disulphide bonds characteristic of the RNase A family. Cysteine 23 and 66 will remain as non-paired residues.

Indeed, evolutive studies suggest a disulphide bond reshuffling process in the RNase 8 linage.

- Non-paired cysteines are confirmed by quantitative determination of free sulfhydryl groups.

- A high aggregation tendency is observed at protein concentration over 1 mg/mL.

- Enzymatic characterization of RNase 8 reveals a predilection for poly(C) substrate and no activity for poly(A) corroborating that it is a pyrimidine specific ribonuclease. Cytidine containing substrates are preferred in comparison to uridine. Also, a moderate preference for exonucleolytic activity is observed, with formation of small size oligonucleotides.

- RNase 8 displays no membrane-aggregation activity and poor leakage capacity in comparison to its closest relative RNase 7.

- RNase 8 shows a high antimicrobial activity, with minimum bactericidal concentrations of 1 and 2 μM against Gram-negative and Gram-positive bacteria, respectively.

- We conclude that RNase 8, displaying a high bactericidal activity, can also be regarded as a component of innate immunity.

ACKNOWLEDGEMENTS

7. ACKNOWLEDGMENTS

I desire write my acknowledgements to all the people who have contributed to this work in my maternal tongue for better expression.

"Gracias a la vida que me ha dado tanto, me ha dado dos luceros que cuando los abro…"

A la Dra. M. Victòria Nogués, Dra Ester Boix, Dr Mohammed Moussaoui y Dr. Marc Torrent por permitirme desarrollar parte de mi carrera investigativa y académica en su grupo de investigación. El aprendizaje no ha sido únicamente académico, a nivel personal he aprendido mucho y es aún más enriquecedor.

A personas muy especiales en los servicios de soporte de la universidad de la UAB, los cuales siempre están dsponibles a enseñar. A mis comprañeros de laboratorio Javier, David y Jose Antonio.

A mi familia, mi mamá y mi hermana que son el soporte vital en todo mi desarrollo personal, gracias por siempre estar ahi, soy la más afortunada por tenerlos a todos a nuestro lado ya que nunca nos han dejado sin su apoyo. Gracias por las buenas canciones, los buenos momentos, los regalos, el tiempo y el amor que han dado a mi hijo Santiago y a mi, durante toda mi vida.

A gente maravillosa que conocí en la UAB y que conservaré para mi vida: Lynay, Luz y Yuria con ustedes tengo la certeza de la amistad. A mis compañeros de piso por cada uno de los buenos momentos que pasamos y las miles de aventuras.

A mis compañeras de universidad Carolina, Marthica, Gina, Natalia….a todas, por ser parte de nuestras vidas.

A lo más amado a mi hijo Santiago y Diego, son ejemplo e incentivo de amor, alegria paz y felicidad. Por los muchos años más juntos, por los números minutos que voy a recompensarles después de haber terminado esta época academica en mi vida. Los amo.

Gracias por la comprensión y por la espera infinita.

"*Si* dejas salir tus *miedos*, *tendrás más espacio para* vivir *tus sueños"*

REFERENCES

8. REFERENCES

Abtin, A., Eckhart, L., Mildner, M., Ghannadan, M., Harder, J., Schröder, J.-M. & Tschachler, E., 2009. Degradation by stratum corneum proteases prevents endogenous RNase inhibitor from blocking antimicrobial activities of RNase 5 and RNase 7. *The Journal of investigative dermatology*, 129(9), pp.2193–2201.

Acharya, K.R. & Ackerman, S.J., 2014. Eosinophil Granule Proteins: Form and Function. *The Journal of biological chemistry*, 289, pp.17406-17415.

Ardelt, B., Juan, G., Burfeind, P., Salomon, T., Wu, J.M., Hsieh, T.C., Li, X., et al., 2007. Onconase, an anti-tumor ribonuclease suppresses intracellular oxidative stress. *International Journal of Oncology*, 31(3), pp.663–669.

Becknell, B., Eichler, T.E., Beceiro, S., Li, B., Easterling, R.S., Carpenter, A.R., James, C.L., et al., 2014. Ribonucleases 6 and 7 have antimicrobial function in the human and murine urinary tract. *Kidney international*, 87 pp.1–11.

Beintema, J.J., Blank, A., Schieven, G.L., Dekker, C.A., Sorrentino, S. & Libonati, M., 1988. Differences in glycosylation pattern of human secretory ribonucleases. *The Biochemical journal*, 255(2), pp.501–505.

Benito, A., Vilanova, M. & Ribó, M., 2008. Intracellular routing of cytotoxic pancreatic-type ribonucleases. *Current pharmaceutical biotechnology*, 9(3), pp.169–79.

Boix, E., Nogués, M. V, Schein, C.H., Benner, S. a & Cuchillo, C.M., 1994. Reverse transphosphorylation by ribonuclease A needs an intact p2-binding site. Point mutations at Lys-7 and Arg-10 alter the catalytic properties of the enzyme. *The Journal of biological chemistry*, 269(4), pp.2529–2534.

Boix, E., Nikolovski, Z., Moiseyev, G.P., Rosenberg, H.F., Cuchillo, C.M., Nogués, M. V & Nogues, M. V, 1999. Kinetic and product distribution analysis of human eosinophil cationic protein indicates a subsite arrangement that favors exonuclease-type activity. *The Journal of biological chemistry*, 274(22), pp.15605–15614.

Boix, E. & Nogués, M.V., 2007. Mammalian antimicrobial proteins and peptides: overview on the RNase A superfamily members involved in innate host defence. *Molecular bioSystems*, 3(5), pp.317–335.

Boix, E., Torrent, M., Sánchez, D. & Nogués, M.V., 2008. The antipathogen activities of eosinophil cationic protein. *Current pharmaceutical biotechnology*, 9(3), pp.141–152.

Boix, E., Salazar, V.A., Torrent, M., Pulido, D., Noguès, M.V. & Moussaoui, M., 2012. Structural determinants of the eosinophil cationic protein antimicrobial activity. *Biological Chemistry*, 393(8), pp.801–815.

Boix, E., Blanco, J. a, Nogués, M.V. & Moussaoui, M., 2013. Nucleotide binding architecture for secreted cytotoxic endoribonucleases. *Biochimie*, 95(6), pp.1087–97.

Bondos, S.E. & Bicknell, A., 2003. Detection and prevention of protein aggregation before, during, and after purification. *Analytical Biochemistry*, 316(2), pp.223–231.

Bravo, J., Fernández, E., Ribó, M., Dellorens, R. & Cuchillo, C.M., 1994. A versatile negative-staining ribonuclease zymogram. *Analytical Biochemistry*, 219(1), pp.82–86.

Carreras, E., Boix, E., Rosenberg, H.F., Cuchillo, C.M. & Nogues, M. V, 2003. Both aromatic and cationic residues contribute to the membrane-lytic and bactericidal activity of eosinophil cationic protein. *Biochemistry*, 42(22), pp.6636–6644.

Carreras, E., Boix, E., Navarro, S., Rosenberg, H.F., Cuchillo, C.M. & Nogués, M.V., 2005. Surface-exposed amino acids of eosinophil cationic protein play a critical role in the inhibition of mammalian cell proliferation. *Molecular and cellular biochemistry*, 272(1-2), pp.1–7.

Castle, M., Nazarian, A., Yi, S.S. & Tempst, P., 1999. Lethal effects of apidaecin on Escherichia coli involve sequential molecular interactions with diverse targets. *The Journal of biological chemistry*, 274(46), pp.32555–32564.

Chan, C.C., Moser, J.M., Dyer, K.D., Percopo, C.M. & Rosenberg, H.F., 2012. Genetic diversity of human RNase 8. *BMC genomics*, 13(40), pp.1-10.

Chang, K.-C., Lo, C.-W., Fan, T.-C., Chang, M.D.-T., Shu, C.-W., Chang, C.-H., Chung, C.-T., et al., 2010. TNF-alpha mediates eosinophil cationic protein-induced apoptosis in BEAS-2B cells. *BMC cell biology*, 11(6), pp. e1471.2121.

Chao, T.Y. & Raines, R.T., 2011. Mechanism of ribonuclease a endocytosis: Analogies to cell-penetrating peptides. *Biochemistry*, 50(39), pp.8374–8382.

Conchillo-Solé, O., de Groot, N.S., Avilés, F.X., Vendrell, J., Daura, X. & Ventura, S., 2007. AGGRESCAN: a server for the prediction and evaluation of “hot spots” of aggregation in polypeptides. *BMC bioinformatics*, 8, p.(65), e1471.2105.

Cuchillo, C.M., Moussaoui, M., Barman, T., Travers, F. & Nogues, M. V, 2002. The exo- or endonucleolytic preference of bovine pancreatic ribonuclease A depends on its subsites structure and on the substrate size. *Protein science : a publication of the Protein Society*, 11(1), pp.117–128.

Cuchillo, C.M., Nogués, M.V. & Raines, R.T., 2011. Bovine pancreatic ribonuclease: fifty years of the first enzymatic reaction mechanism. *Biochemistry*, 50(37), pp.7835–7841.

Domachowske, J.B., Dyer, K.D., Bonville, C.A. & Rosenberg, H.F., 1998. Recombinant human eosinophil-derived neurotoxin/RNase 2 functions as an effective antiviral agent against respiratory syncytial virus. *The Journal of infectious diseases*, 177(6), pp.1458–1464.

Dyer, K.D. & Rosenberg, H.F., 2006. The RNase a superfamily: generation of diversity and innate host defense. *Molecular diversity*, 10(4), pp.585–597.

Eriksson, J., Woschnagg, C., Fernvik, E. & Venge, P., 2007a. A SELDI-TOF MS study of the genetic and post-translational molecular heterogeneity of eosinophil cationic protein. *Journal of leukocyte biology*, 82(6), pp.1491–1500.

Eriksson, J., Reimert, C.M., Kabatereine, N.B., Kazibwe, F., Ireri, E., Kadzo, H., Eltahir, H.B., et al., 2007b. The 434(G>C) polymorphism within the coding sequence of Eosinophil Cationic Protein (ECP) correlates with the natural course of Schistosoma mansoni infection. *International Journal for Parasitology*, 37(12), pp.1359–1366.

Fang, S., Fan, T., Fu, H.-W., Chen, C.-J., Hwang, C.-S., Hung, T.-J., Lin, L.-Y. & Chang, M.D.-T., 2013. A novel cell-penetrating peptide derived from human eosinophil cationic protein. *PloS one*, 8(3), pp.e57318.

Fisher, B.M., Grilley, J.E. & Raines, R.T., 1998. A new remote subsite in ribonuclease A. *Journal of Biological Chemistry*, 273(51), pp.34134–34138.

Fontecilla-Camps, J.C., de Llorens, R., le Du, M.H. & Cuchillo, C.M., 1994. Crystal structure of ribonuclease A.d(ApTpApApG) complex. Direct evidence for extended substrate recognition. *The Journal of biological chemistry*, 269(34), pp.21526–21531.

Fritz, P., Beck-Jendroschek, V. & Brasch, J., 2012. Inhibition of dermatophytes by the antimicrobial peptides human β-defensin-2, ribonuclease 7 and psoriasin. *Medical mycology : official publication of the International Society for Human and Animal Mycology*, 50(6), pp.579–84.

Fu, H., Feng, J., Liu, Q., Sun, F., Tie, Y., Zhu, J., Xing, R., Sun, Z. & Zheng, X., 2009. Stress induces tRNA cleavage by angiogenin in mammalian cells. *FEBS Letters*, 583(2), pp.437–442.

Gleich, G.J., Adolphson, C.R. & Leiferman, K.M., 1993. The biology of the eosinophilic leukocyte. *Annual review of medicine*, 44, pp.85–101.

Gupta, S.K., Haigh, B.J., Griffin, F.J. & Wheeler, T.T., 2013. The mammalian secreted RNases: mechanisms of action in host defence. *Innate immunity*, 19(1), pp.86–97.

Hamann, K.J., Barker, R.L., Ten, R.M. & Gleich, G.J., 1991. The molecular biology of eosinophil granule proteins. *International archives of allergy and applied immunology*, 94(1-4), pp.202–209.

Han, T.L., Cannon, R.D. & Villas-Bôas, S.G., 2011. The metabolic basis of Candida albicans morphogenesis and quorum sensing. *Fungal Genetics and Biology*, 48(8), pp.747–763.

Hancock, R.E.W. & Sahl, H.-G., 2006. Antimicrobial and host-defense peptides as new anti-infective therapeutic strategies. *Nature biotechnology*, 24(12), pp.1551–7.

Hansen, M., Kilk, K. & Langel, U., 2008. Predicting cell-penetrating peptides. *Advanced Drug Delivery Reviews*, 60(4-5), pp.572–579.

Harder, J. & Schroder, J.M., 2002. RNase 7, a novel innate immune defense antimicrobial protein of healthy human skin. *The Journal of biological chemistry*, 277(48), pp.46779–46784.

Harris, P., Johannessen, K.M., Smolenski, G., Callaghan, M., Broadhurst, M.K., Kim, K. & Wheeler, T.T., 2010. Characterisation of the anti-microbial activity of bovine milk ribonuclease4 and ribonuclease5 (angiogenin). *International Dairy Journal*, 20(6), pp.400–407.

Hofsteenge, J., Vicentini, A & Zelenko, O., 1998. Ribonuclease 4, an evolutionarily highly conserved member of the superfamily. *Cellular and molecular life sciences : CMLS*, 54(8), pp.804–10.

Hogan, S.P., Rosenberg, H.F., Moqbel, R., Phipps, S., Foster, P.S., Lacy, P., Kay, a B. & Rothenberg, M.E., 2008. Eosinophils: biological properties and role in health and disease. *Clinical and experimental allergy : journal of the British Society for Allergy and Clinical Immunology*, 38(5), pp.709–50.

Holm, T., Netzereab, S., Hansen, M., Langel, U. & Hällbrink, M., 2005. Uptake of cell-penetrating peptides in yeasts. *FEBS letters*, 579(23), pp.5217–22.

Hooper, L. V, Stappenbeck, T.S., Hong, C. V & Gordon, J.I., 2003. Angiogenins: a new class of microbicidal proteins involved in innate immunity. *Nature immunology*, 4(3), pp.269–73.

Huang, Y.C., Lin, Y.M., Chang, T.W., Wu, S.J., Lee, Y.S., Chang, M.D., Chen, C., Wu, S.H. & Liao, Y.D., 2007. The flexible and clustered lysine residues of human ribonuclease 7 are critical for membrane permeability and antimicrobial activity. *The Journal of biological chemistry*, 282(7), pp.4626–4633.

Jönsson, U.B., Byström, J., Stälenheim, G. & Venge, P., 2002. Polymorphism of the eosinophil cationic protein-gene is related to the expression of allergic symptoms. *Clinical and Experimental Allergy*, 32(7), pp.1092–1095.

Jang, W.S., Bajwa, J.S., Sun, J.N. & Edgerton, M., 2010. Salivary histatin 5 internalization by translocation, but not endocytosis, is required for fungicidal activity in Candida albicans. *Molecular Microbiology*, 77(2), pp.354–370.

Jones, D.T., Taylor, W.R. & Thornton, J.M., 1992. The rapid generation of mutation data matrices from protein sequences. *Computer applications in the biosciences : CABIOS*, 8(3), pp.275–282.

Kagan, S., Jabbour, A., Sionov, E., Alquntar, A. a, Steinberg, D., Srebnik, M., Nir-Paz, R., Weiss, A. & Polacheck, I., 2013. Anti-Candida albicans biofilm effect of novel heterocyclic compounds. *The Journal of antimicrobial chemotherapy*, pp.1–12.

Kierszenbaum, F., Villalta, F. & Tai, P.C., 1986. Role of inflammatory cells in Chagas' disease. III. Kinetics of human eosinophil activation upon interaction with parasites (Trypanosoma cruzi). *Journal of immunology (Baltimore, Md. : 1950)*, 136(2), pp.662–666.

Kim, J.S., Souček, J., Matoušek, J. & Raines, R.T., 1995. Mechanism of ribonuclease cytotoxicity. *Journal of Biological Chemistry*, 270(52), pp.31097–31102.

Kita, H., 2013. Eosinophils: multifunctional and distinctive properties. *International archives of allergy and immunology*, 161 Suppl (suppl 2), pp.3–9.

Köten, B., Simanski, M., Gläser, R., Podschun, R., Schröder, J.M. & Harder, J., 2009. RNase 7 contributes to the cutaneous defense against *Enterococcus faecium*. *PLoS ONE*, 4(7), pp. 1-9.

Kragol, G., Hoffmann, R., Chattergoon, M.A., Lovas, S., Cudic, M., Bulet, P., Condie, B.A., et al., 2002. Identification of crucial residues for the antibacterial activity of the proline-rich peptide, pyrrhocoricin. *European Journal of Biochemistry*, 269(17), pp.4226–4237.

Kruppa, M., 2009. Quorum sensing and Candida albicans. *Mycoses*, 52(1), pp.1–10.

Kruse, T. & Kristensen, H.-H., 2008. Using antimicrobial host defense peptides as anti-infective and immunomodulatory agents. *Expert review of anti-infective therapy*, 6(6), pp.887–895.

Lan, Y., Ye, Y., Kozlowska, J., Lam, J.K.W., Drake, A.F. & Mason, A.J., 2010. Structural contributions to the intracellular targeting strategies of antimicrobial peptides. *Biochimica et Biophysica Acta - Biomembranes*, 1798(10), pp.1934–1943.

Larsson, R., Trulson, A., Bystrom, J., Engstrom, A. & Venge, P., 2007. The functional heterogeneity of eosinophil cationic protein is determined by a gene polymorphism and post-translational modifications. *Clinical and Experimental Allergy*, 37(2), pp.208–218.

Lee-Huang, S., Huang, P.L., Sun, Y., Kung, H.F., Blithe, D.L. & Chen, H.C., 1999. Lysozyme and RNases as anti-HIV components in beta-core preparations of human chorionic gonadotropin. *Proceedings of the National Academy of Sciences of the United States of America*, 96(6), pp.2678–2681.

Lehrer, R.I., Szklarek, D., Barton, A., Ganz, T., Hamann, K.J. & Gleich, G.J., 1989. Antibacterial properties of eosinophil major basic protein and eosinophil cationic protein. *Journal of immunology (Baltimore, Md. : 1950)*, 142(12), pp.4428–4434.

Leland, P.A., Staniszewski, K.E., Park, C., Kelemen, B.R. & Raines, R.T., 2002. The ribonucleolytic activity of angiogenin. *Biochemistry*, 41(4), pp.1343–1350.

Luca, V., Olivi, M., Di Grazia, A., Palleschi, C., Uccelletti, D. & Mangoni, M.L., 2013. Anti-Candida activity of 1-18 fragment of the frog skin peptide esculentin-1b: in vitro and in vivo studies in a Caenorhabditis elegans infection model. *Cellular and molecular life sciences*, 71(13), pp.2535-2546.

MacPherson, J.C., Comhair, S., Erzurum, S.C., Klein, D.F., Lipscomb, M.F., Kavuru, M.S., Samoszuk, M.K. & Hazen, S.L., 2001. Eosinophils Are a Major Source of Nitric Oxide-Derived Oxidants in Severe Asthma: Characterization of Pathways Available to Eosinophils for Generating Reactive Nitrogen Species. *The Journal of Immunology*, 166(9), pp.5763–5772.

Maeda, T., Kitazoe, M., Tada, H., de Llorens, R., Salomon, D.S., Ueda, M., Yamada, H. & Seno, M., 2002. Growth inhibition of mammalian cells by eosinophil cationic protein. *European journal of biochemistry / FEBS*, 269(1), pp.307–316.

Malik, A. & Batra, J.K., 2012. Antimicrobial activity of human eosinophil granule proteins: involvement in host defence against pathogens. *Critical reviews in microbiology*, 38(2), pp.168–181.

Marchione, R., Daydé, D., Lenormand, J.-L. & Cornet, M., 2014. ZEBRA cell-penetrating peptide as an efficient delivery system in Candida albicans. *Biotechnology journal*, 9(8), pp.1088–1094.

Mayer, F.L., Wilson, D. & Hube, B., 2013. Candida albicans pathogenicity mechanisms. *Virulence*, 4(2), pp.119–128.

Meiller, T.F., Hube, B., Schild, L., Shirtliff, M.E., Scheper, M.A., Winkler, R., Ton, A. & Jabra-Rizk, M.A., 2009. A novel immune evasion strategy of Candida albicans: Proteolytic cleavage of a salivary antimicrobial peptide. *PLoS ONE*, 4(4), pp.1-9.

Melo, R.C.N. & Weller, P.F., 2010. Piecemeal degranulation in human eosinophils: a distinct secretion mechanism underlying inflammatory responses. *Histology and histopathology*, 25(10), pp.1341–1354.

Mochon, A.B. & Liu, H., 2008. The antimicrobial peptide histatin-5 causes a spatially restricted disruption on the Candida albicans surface, allowing rapid entry of the peptide into the cytoplasm. *PLoS Pathogens*, 4(10), pp1-12.

Moenner, M., Gusse, M., Hatzi, E. & Badet, J., 1994. The widespread expression of angiogenin in different human cells suggests a biological function not only related to angiogenesis. *European Journal of Biochemistry*, 226(2), pp.483–490.

Mohammed, I., Yeung, A., Abedin, A., Hopkinson, A. & Dua, H.S., 2011. Signalling pathways involved in ribonuclease-7 expression. *Cellular and Molecular Life Sciences*, 68(11), pp.1941–1952.

Molero, G., Díez-Orejas, R., Navarro-García, F., Monteoliva, L., Pla, J., Gil, C., Sánchez-Pérez, M. & Nombela, C., 1998. Candida albicans: genetics, dimorphism and pathogenicity. *International microbiology : the official journal of the Spanish Society for Microbiology*, 1(2), pp.95–106.

Moussaoui, M., Guasch, A., Boix, E., Cuchillo, C. & Nogues, M., 1996. The role of non-catalytic binding subsites in the endonuclease activity of bovine pancreatic ribonuclease A. *The Journal of biological chemistry*, 271(9), pp.4687–4692.

Navarro, S., Aleu, J., Jiménez, M., Boix, E., Cuchillo, C.M. & Nogués, M. V, 2008. The cytotoxicity of eosinophil cationic protein/ribonuclease 3 on eukaryotic cell lines takes place through its aggregation on the cell membrane. *Cellular and molecular life sciences : CMLS*, 65(2), pp.324–37.

Navarro, S., Boix, E., Cuchillo, C.M. & Nogués, M.V., 2010. Eosinophil-induced neurotoxicity: the role of eosinophil cationic protein/RNase 3. *Journal of neuroimmunology*, 227(1-2), pp.60–70.

Nicolas, P., 2009. Multifunctional host defense peptides: intracellular-targeting antimicrobial peptides. *The FEBS journal*, 276(22), pp.6483–6496.

Noguès, M. V & Cuchillo, C.M., 2001. Analysis by HPLC of distributive activities and the synthetic (back) reaction of pancreatic-type ribonucleases. *Methods in molecular biology (Clifton, N.J.)*, 160, pp.15–24.

Oxvig, C., Gleich, G.J. & Sottrup-Jensen, L., 1994. Localization of disulfide bridges and free sulfhydryl groups in human eosinophil granule major basic protein. *FEBS letters*, 341(2-3), pp.213–7.

Parés, X., Nogués, M. V, de Llorens, R. & Cuchillo, C.M., 1991. Structure and function of ribonuclease A binding subsites. *Essays in biochemistry*, 26, pp.89-103.

Park, C.B., Yi, K.S., Matsuzaki, K., Kim, M.S. & Kim, S.C., 2000. Structure-activity analysis of buforin II, a histone H2A-derived antimicrobial peptide: the proline hinge is responsible for the cell-penetrating ability of buforin II. *Proceedings of the National Academy of Sciences of the United States of America*, 97(15), pp.8245–8250.

Patel, L.N., Zaro, J.L. & Shen, W.-C., 2007. Cell penetrating peptides: intracellular pathways and pharmaceutical perspectives. *Pharmaceutical research*, 24(11), pp.1977–1992.

Pavia, K.E., Spinella, S.A. & Elmore, D.E., 2012. Novel histone-derived antimicrobial peptides use different antimicrobial mechanisms. *Biochimica et Biophysica Acta - Biomembranes*, 1818(3), pp.869–876.

Plager, D. a, Adolphson, C.R. & Gleich, G.J., 2001. A novel human homolog of eosinophil major basic protein. *Immunological reviews*, 179(4), pp.192–202.

Pulido, D., Moussaoui, M., Andreu, D., Nogués, M.V., Torrent, M. & Boix, E., 2012. Antimicrobial Action and Cell Agglutination By Eosinophil Cationic Protein Is Modulated By the Cell Wall Lipopolysaccharide Structure. *Antimicrobial agents and chemotherapy*, 56(5):2378-85

Pulido, D., Moussaoui, M., Nogués, M.V., Torrent, M. & Boix, E., 2013. Towards the rational design of antimicrobial proteins: single point mutations can switch on bactericidal and agglutinating activities on the RNase A superfamily lineage. *The FEBS journal*, pp.1–12.

Pulido, D., Torrent, M., Andreu, D., Nogués, M.V. & Boix, E., 2013. Two human host defense ribonucleases against mycobacteria, the eosinophil cationic protein (RNase 3) and RNase 7. *Antimicrobial agents and chemotherapy*, 57(8), pp.3797–3805.

Pushpanathan, M., Gunasekaran, P. & Rajendhran, J., 2013. Antimicrobial peptides: Versatile biological properties. *International Journal of Peptides*, 675391, pp. 1-24

Rahnamaeian, M., 2011. Antimicrobial peptides: Modes of mechanism, modulation of defense responses. *Plant Signaling & Behavior*, 6(9), pp.1325–1332.

Raines, R.T., Peptide, B.P. & Isomerization, B., 1998. Ribonuclease A. , 98(3), pp. 1045-1066.

Rausch, J.M., Marks, J.R., Rathinakumar, R. & Wimley, W.C., 2007. b-Sheet Pore-Forming Peptides Selected from a Rational Combinatorial Library: Mech Pore Formation in Lipid Vesicles & Activity in Membranes. *Biochemistry*, 46(43), pp.12124–12139.

Rooney, P.J. & Klein, B.S., 2002. Linking fungal morphogenesis with virulence. *Cellular Microbiology*, 4(3), pp.127–137.

Rosenberg, H.F., Ackerman, S.J. & Tenen, D.G., 1989. Human eosinophil cationic protein. Molecular cloning of a cytotoxin and helminthotoxin with ribonuclease activity. *The Journal of experimental medicine*, 170(1), pp.163–76.

Rosenberg, H.F. & Dyer, K.D., 1995a. Eosinophil cationic protein and eosinophil-derived neurotoxin. Evolution of novel function in a primate ribonuclease gene family. *The Journal of biological chemistry*, 270(37), pp.21539–21544.

Rosenberg, H.F. & Dyer, K.D., 1995b. Human ribonuclease 4 (RNase 4): coding sequence, chromosomal localization and identification of two distinct transcripts in human somatic tissues. *Nucleic acids research*, 23(21), pp.4290–4295.

Rosenberg, H.F. & Dyer, K.D., 1996. Molecular cloning and characterization of a novel human ribonuclease (RNase k6): increasing diversity in the enlarging ribonuclease gene family. *Nucleic acids research*, 24(18), pp.3507–3513.

Rosenberg, H.F. & Domachowske, J.B., 2001. Eosinophils, eosinophil ribonucleases, and their role in host defense against respiratory virus pathogens. *Journal of leukocyte biology*, 70(5), pp.691–698.

Rosenberg, H.F., 2008a. Eosinophil-derived neurotoxin / RNase 2: connecting the past, the present and the future. *Current pharmaceutical biotechnology*, 9(3), pp.135–140.

Rosenberg, H.F., 2008b. RNase A ribonucleases and host defense: an evolving story. *Journal of leukocyte biology*, 83(5), pp.1079–1087.

Rosenberg, H.F., Dyer, K.D. & Foster, P.S., 2013. Eosinophils: changing perspectives in health and disease. *Nature reviews. Immunology*, 13(1), pp.9–22.

Rubin, J., Zagai, U., Blom, K., Trulson, A., Engström, A. & Venge, P., 2009. The coding ECP 434(G>C) gene polymorphism determines the cytotoxicity of ECP but has minor effects on fibroblast-mediated gel contraction and no effect on RNase activity. *Journal of immunology (Baltimore, Md. : 1950)*, 183(1), pp.445–51.

Rubin, J. & Venge, P., 2013. Asparagine-linked glycans determine the cytotoxic capacity of eosinophil cationic protein (ECP). *Molecular Immunology*, 55(3-4), pp.372–380.

Rudolph, B., Podschun, R., Sahly, H., Schubert, S., Schröder, J.M., Harder, J., Schroder, J.M. & Harder, J., 2006. Identification of RNase 8 as a novel human antimicrobial protein. *Antimicrobial agents and chemotherapy*, 50(9), pp.3194–3196.

Rugeles, M.T., Trubey, C.M., Bedoya, V.I., Pinto, L.A., Oppenheim, J.J., Rybak, S.M. & Shearer, G.M., 2003. Ribonuclease is partly responsible for the HIV-1 inhibitory effect activated by HLA alloantigen recognition. *AIDS (London, England)*, 17(4), pp.481–486.

Russo, N., Shapiro, R., Acharya, K.R., Riordan, J.F. & Vallee, B.L., 1994. Role of glutamine-117 in the ribonucleolytic activity of human angiogenin. *Proceedings of*

the National Academy of Sciences of the United States of America, 91(8), pp.2920–2924.

Salazar, V.A., Rubin, J., Moussaoui, M., Pulido, D., Victòria Nogués, M., Venge, P., Boix, E., et al., 2014. Protein post-translational modification in host defense. The antimicrobial mechanism of action of human eosinophil cationic protein native forms. *FEBS Journal*, 281(24), pp.5432-5446.

Sánchez, D., Moussaoui, M., Carreras, E., Torrent, M., Nogués, V. & Boix, E., 2011. Mapping the eosinophil cationic protein antimicrobial activity by chemical and enzymatic cleavage. *Biochimie*, 93(2), pp.331–338.

Scheraga, H.A., Konishi, Y., Rothwarf, D.M. & Mui, P.W., 1987. Toward an understanding of the folding of ribonuclease A. *Proceedings of the National Academy of Sciences of the United States of America*, 84(16), pp.5740–5744.

Schmidt, N., Mishra, A., Lai, G.H. & Wong, G.C.L., 2010. Arginine-rich cell-penetrating peptides. *FEBS letters*, 584(9), pp.1806–13.

Shamri, R., Xenakis, J.J. & Spencer, L.A., 2011. Eosinophils in innate immunity: An evolving story. *Cell and Tissue Research*, 343(1), pp.57–83.

Sikriwal, D., Seth, D. & Batra, J.K., 2009. Role of catalytic and non-catalytic subsite residues in ribonuclease activity of human eosinophil-derived neurotoxin. *Biological Chemistry*, 390(3), pp.225–234.

Sinatra, F., Callari, D., Viola, M., Longombardo, M.T., Patania, M., Litrico, L., Emmanuele, G., et al., 2000. Bovine seminal RNase induces apoptosis in normal proliferating lymphocytes. *International Journal of Clinical and Laboratory Research*, 30(4), pp.191–196.

Singh, A. & Batra, J.K., 2011. Role of unique basic residues in cytotoxic, antibacterial and antiparasitic activities of human eosinophil cationic protein. *Biological chemistry*, 392(4), pp.337–46.

Sorrentino, S. & Libonati, M., 1994. Human pancreatic-type and nonpancreatic-type ribonucleases: a direct side-by-side comparison of their catalytic properties. *Archives of biochemistry and biophysics*, 312(2), pp.340–348.

Sorrentino, S. & Libonati, M., 1997. Structure-function relationships in human ribonucleases: Main distinctive features of the major RNase types. *FEBS Letters*, 404(1), pp.1–5.

Sorrentino, S., 1998. Human extracellular ribonucleases: multiplicity, molecular diversity and catalytic properties of the major RNase types. *Cellular and molecular life sciences : CMLS*, 54(8), pp.785–94.

Sorrentino, S., Naddeo, M., Russo, A. & D'Alessio, G., 2003. Degradation of double-stranded RNA by human pancreatic ribonuclease: Crucial role of noncatalytic basic amino acid residues. *Biochemistry*, 42(34), pp.10182–10190.

Sorrentino, S., 2010. The eight human "canonical" ribonucleases: molecular diversity, catalytic properties, and special biological actions of the enzyme proteins. *FEBS letters*, 584(11), pp.2194–200.

Strydom, D.J., Fett, J.W., Lobb, R.R., Alderman, E.M., Bethune, J.L., Riordan, J.F. & Vallee, B.L., 1985. Amino acid sequence of human tumor derived angiogenin. *Biochemistry*, 24(20), pp.5486–5494.

Sudbery, P., Gow, N. & Berman, J., 2004. The distinct morphogenic states of Candida albicans. *Trends in Microbiology*, 12(7), pp.317–324.

Tello-Montoliu, a, Patel, J. V & Lip, G.Y.H., 2006. Angiogenin: a review of the pathophysiology and potential clinical applications. *Journal of thrombosis and haemostasis : JTH*, 4(9), pp.1864–74.

Thornton, J.M., 1981. Disulphide bridges in globular proteins. *Journal of molecular biology*, 151(2), pp.261–287.

Torrent, M., Cuyás, E., Carreras, E., Navarro, S., López, O., de la Maza, A., Nogués, M.V., Reshetnyak, Y.K. & Boix, E., 2007. Topography studies on the membrane

interaction mechanism of the eosinophil cationic protein. *Biochemistry*, 46(3), pp.720–733.

Torrent, M., Navarro, S., Moussaoui, M., Nogues, M. V & Boix, E., 2008. Eosinophil cationic protein high-affinity binding to bacteria-wall lipopolysaccharides and peptidoglycans. *Biochemistry*, 47(11), pp.3544–3555.

Torrent, M., de la Torre, B.G., Nogues, V.M., Andreu, D. & Boix, E., 2009a. Bactericidal and membrane disruption activities of the eosinophil cationic protein are largely retained in an N-terminal fragment. *The Biochemical journal*, 421(3), pp.425–434.

Torrent, M., Sánchez, D., Buzón, V., Nogués, M.V., Cladera, J., Boix, E., Sanchez, D., et al., 2009b. Comparison of the membrane interaction mechanism of two antimicrobial RNases: RNase 3/ECP and RNase 7. *Biochimica et biophysica acta*, 1788(5), pp.1116–1125.

Torrent, M., Badia, M., Moussaoui, M., Sanchez, D., Nogues, M. V & Boix, E., 2010a. Comparison of human RNase 3 and RNase 7 bactericidal action at the Gram-negative and Gram-positive bacterial cell wall. *The FEBS journal*, 277(7), pp.1713–1725.

Torrent, M., Odorizzi, F., Nogues, M. V & Boix, E., 2010b. Eosinophil cationic protein aggregation: identification of an N-terminus amyloid prone region. *Biomacromolecules*, 11(8), pp.1983–1990.

Torrent, M., Pulido, D., de la Torre, B.G., García-Mayoral, M.F., Nogués, M.V., Bruix, M., Andreu, D. & Boix, E., 2011. Refining the eosinophil cationic protein antibacterial pharmacophore by rational structure minimization. *Journal of medicinal chemistry*, 54(14), pp.5237–5244.

Torrent, M., Pulido, D., Nogués, M.V. & Boix, E., 2012. Exploring new biological functions of amyloids: bacteria cell agglutination mediated by host protein aggregation. *PLoS pathogens*, 8(11), pp.e1003005.

Tsai, P.-W., Yang, C.-Y., Chang, H.-T. & Lan, C.-Y., 2011. Human antimicrobial peptide LL-37 inhibits adhesion of Candida albicans by interacting with yeast cell-wall carbohydrates. *PloS one*, 6(3), p.e17755.

Tsai, P.-W., Cheng, Y.-L., Hsieh, W.-P. & Lan, C.-Y., 2014. Responses of Candida albicans to the human antimicrobial peptide LL-37. *Journal of microbiology (Seoul, Korea)*, 52(7), pp.581–589.

Tschesche, H., Kopp, C., Hörl, W.H. & Hempelmann, U., 1994. Inhibition of degranulation of polymorphonuclear leukocytes by angiogenin and its tryptic fragment. *The Journal of biological chemistry*, 269(48), pp.30274–30280.

Turvey, S.E. & Broide, D.H., 2010. Innate immunity. *The Journal of allergy and clinical immunology*, 125(2 Suppl 2), pp.S24–S32.

Ulrich, M., Petre, A., Youhnovski, N., Prömm, F., Schirle, M., Schumm, M., Pero, R.S., et al., 2008. Post-translational tyrosine nitration of eosinophil granule toxins mediated by eosinophil peroxidase. *The Journal of biological chemistry*, 283(42), pp.28629–40.

Venge, P., Bystrom, J., Carlson, M., Hakansson, L., Karawacjzyk, M., Peterson, C., Seveus, L. & Trulson, A., 1999. Eosinophil cationic protein (ECP): molecular and biological properties and the use of ECP as a marker of eosinophil activation in disease. *Clinical and experimental allergy : journal of the British Society for Allergy and Clinical Immunology*, 29(9), pp.1172–1186.

Wagner, L. a, Ohnuki, L.E., Parsawar, K., Gleich, G.J. & Nelson, C.C., 2007. Human eosinophil major basic protein 2: location of disulfide bonds and free sulfhydryl groups. *The protein journal*, 26(1), pp.13–18.

Waters, L.S., Taverne, J., Tai, P.C., Spry, C.J., Targett, G. a & Playfair, J.H., 1987. Killing of Plasmodium falciparum by eosinophil secretory products. *Infection and immunity*, 55(4), pp.877–881.

Woschnagg, C., Rubin, J. & Venge, P., 2009. Eosinophil cationic protein (ECP) is processed during secretion. *Journal of immunology (Baltimore, Md. : 1950)*, 183(6), pp.3949–3954.

Wu, Y., Mikulski, S.M., Ardelt, W., Rybak, S.M. & Youle, R.J., 1993. A cytotoxic ribonuclease: Study of the mechanism of onconase cytotoxicity. *Journal of Biological Chemistry*, 268(14), pp.10686–10693.

Yang, D., Chen, Q., Rosenberg, H.F., Rybak, S.M., Newton, D.L., Wang, Z.Y., Fu, Q., et al., 2004. Human ribonuclease A superfamily members, eosinophil-derived neurotoxin and pancreatic ribonuclease, induce dendritic cell maturation and activation. *Journal of immunology (Baltimore, Md. : 1950)*, 173(10), pp.6134–6142.

Zhang, J., Dyer, K.D. & Rosenberg, H.F., 2000. Evolution of the rodent eosinophil-associated RNase gene family by rapid gene sorting and positive selection. *Proceedings of the National Academy of Sciences of the United States of America*, 97(9), pp.4701–4706.

Zhang, J., Dyer, K.D. & Rosenberg, H.F., 2002. RNase 8, a novel RNase A superfamily ribonuclease expressed uniquely in placenta. *Nucleic acids research*, 30(5), pp.1169–1175.

Zhang, J., Dyer, K.D. & Rosenberg, H.F., 2003. Human RNase 7: a new cationic ribonuclease of the RNase A superfamily. *Nucleic Acids Research*, 31(2), pp.602–607.

PAPERS INCLUDED IN THE THESIS

the FEBS Journal

Protein post-translational modification in host defense: the antimicrobial mechanism of action of human eosinophil cationic protein native forms

Vivian A. Salazar[1], Jenny Rubin[2], Mohammed Moussaoui[1], David Pulido[1], Maria Victoria Nogues[1], Per Venge[2] and Ester Boix[1]

1 Department of Biochemistry and Molecular Biology, Faculty of Biosciences, Universitat Autonoma de Barcelona, Spain
2 Department of Medical Sciences, Clinical Chemistry, Uppsala University, Sweden

Keywords

agglutination; antimicrobial proteins; glycosylation; immunity; membrane

Correspondence

E. Boix, Department of Biochemistry and Molecular Biology, Faculty of Biosciences, Universitat Autonoma_ de Barcelona, 08193 Cerdanyola del Valles,_ Spain

Fax: +34-935811264

Tel: +34-935814147 E-mail: Ester.Boix@uab.cat

Website: http://tinyurl.com/hRNasesUAB

(Received 7 March 2014, revised 17 September 2014, accepted 26 September 2014)

doi:10.1111/febs.13082

Knowledge on the contribution of protein glycosylation in host defense antimicrobial peptides is still scarce. We have studied here how the post-translational modification pattern modulates the antimicrobial activity of one of the best characterized leukocyte granule proteins. The human eosin-ophil cationic protein (ECP), an eosinophil specific granule protein secreted during inflammation and infection, can target a wide variety of pathogens. Previous work in human eosinophil extracts identified several ECP native forms and glycosylation heterogeneity was found to contribute to the pro-tein biological properties. In this study we analyze for the first time the antimicrobial activity of the distinct native proteins purified from healthy donor blood. Low and heavy molecular weight forms were tested on Esc-herichia coli cell cultures and compared with the recombinant non-glycosy-lated protein. Further analysis on model membranes provided an insight towards an understanding of the protein behavior at the cytoplasmic mem-brane level. The results highlight the significant reduction in protein toxic-ity and bacteria agglutination activity for heavy glycosylated fractions. Notwithstanding, the lower glycosylated fraction mostly retains the lipo-polysaccharide binding affinity together with the cytoplasmic membrane depolarization and membrane leakage activities. From structural analysis we propose that heavy glycosylation interferes with the protein self-aggre-gation, hindering the cell agglutination and membrane disruption processes. The results suggest the contribution of post-translational modifi-cations to the antimicrobial role of ECP in host defense.

Introduction

Eosinophils are key effectors in immune defense [1–4]. The eosinophil cationic protein (ECP) is one of the main proteins secreted by eosinophils during infection and inflammation [5,6]. It is a small cationic protein displaying toxicity towards a wide range of pathogens, such as bacteria, protozoa and helminths [7–9], the protein toxicity also being potentially harmful for host tissues during inflammation [10,11]. ECP, also named RNase 3, belongs to the vertebrate secreted RNase A superfamily [12]. Three sites for putative N-linked

Abbreviations

ANTS, 8-aminonaphthalene-1,3,6-trisulfonic acid disodium salt; BC, BODIPY-TR cadaverine; CFU, colony forming unit; DOPC, dioleoyl phosphatidylcholine; DOPG, dioleoyl phosphatidylglycerol; DPA, dipicolinic acid; DPX, p-xylenebispyridinium bromide; ECP, eosinophil cationic protein; EDN, eosinophil derived neurotoxin; HMW, high molecular weight; LMW, low molecular weight; LPS, lipopolysaccharide; LUV, large unilamellar vesicle; MBC, minimal bactericidal concentration; SELDI-TOF, surface-enhanced laser desorption/ionization time of flight.

glycosylation are found in the ECP sequence and two major glycosylated fractions were first isolated from eosinophils [13]. The protein molecular heterogeneity due to post-translational modifications varies between 15 and 18 kDa and up to five major molecular species have been identified [14,15]. Analysis of the purified native forms revealed the presence of N-linked oligo-saccharides containing sialic acid, galactose and N-ace-tyl glucosamine [14]. Further genomic studies revealed a polymorphism at the coding sequence Arg97Thr [16,17] that introduced an additional putative Asn-X-Thr glycosylation site and could contribute to the native form heterogeneity [14,18]. Interestingly, the polymorphism at the coding sequence was found to correlate with asthma predisposition and parasitic infection prevalence [19,20] and population studies revealed an uneven geographical distribution of the two genotypes [17,20]. Arg to Thr substitution at posi-tion 97 was found to drastically reduce the protein cytotoxicity but had no effect on the protein catalytic activity [18,21]. The loss of toxicity was attributed to the new putative glycosylation branch at the Thr97 site, which was suggested to cover one of the main protein active regions. Recent genotyping data on Hodgkin lymphoma patients linked the Arg97 poly-morphism with a higher tumor eosinophilia, suggesting that a higher protein toxicity further triggered the eosinophil recruitment at the tumor [22]. On the other hand, ECP glycosylation level was correlated to the protein cytotoxicity on several cancer cell lines [15,21– 23], where partial carbohydrate removal increased the protein activity [15,23]. Glycosylation, however, did not alter other protein properties such as skin lesions [24] or RNase catalytic activities [21].

The physiological role of glycosylation variability was considered based on the distinct biological proper-ties of the native forms [18]. While resting eosinophils contain a mixture of low and high glycosylated forms, upon stimulation secretion of low molecular weight forms is observed [15]. Glycosylation branches are processed during eosinophil activation and degranula-tion and heavy glycosylation was attributed a protec-tive role for the granule stored protein [15,23]. Complementary characterization of native form heter-ogeneity was undergone by in vitro enzymatic degly-cosylation [23].

Glycosylation has also been studied for other members of the RNase A superfamily, showing a non-conserved pattern [25,26]. The eosinophil derived neu-rotoxin (EDN) or RNase 2, sharing a 67% identity with ECP, includes five potential Asn N-glycosylation sites [27]. Glycosylation variability was correlated in EDN with distinct physiological conditions. In particu-lar, a protein glycosylated form was found to be ele-vated in some cancer patients [28].

Other post-translational modifications were also identified within the RNase A family members. In par-ticular, Tyr-nitration specific for eosinophil granule proteins was reported [29], where exposed Tyr residues are targeted by the eosinophil peroxidase during eosin-ophil maturation. It is also worth mentioning a partic-ular C-mannosylation reported for EDN at a specific Trp-XX-Trp site [30], which represents a rather unu-sual protein modification [31].

In any case, the role of protein glycosylation is still under study both within the RNase A family and, in a wider proteomics and glycomics context, within the immune system [32–34]. Although the key role of gly-cosylation in the host–pathogen recognition step is widely discussed [35,36], literature on the mechanism of action of glycosylated antimicrobial proteins is still scarce. A reduced toxicity on Staphylococcus aureus is reported for glycosylated lysostaphin [37], but the underlying molecular mechanism is unknown. Indeed, while a great deal has been studied on the role of glycoside derivates as alternative antibiotics [38], no literature is available on the direct influence of glyco-sylation on protein antimicrobial action.

In the present study we analyze the activity of native ECP variants on Escherichia coli cell cultures and model membranes. The results suggest that post-trans-lational modification modulates the antimicrobial mechanism of action by defining the protein mem-brane interaction mode.

Results

Identification of native eosinophil cationic protein forms

Native ECP was purified from pooled buffy coats from healthy blood donors. ECP was purified and fraction-ated by means of gel filtration and ion exchange chro-matographies as previously described [14]. The protein samples eluted from the cation exchange chromatogra-phy were analyzed by SDS/PAGE as previously [18]. The native ECP pools were further characterized by surface-enhanced laser desorption/ionization time of flight (SELDI-TOF) MS analysis using an anti-ECP monoclonal antibody and classified as previously described [14,21]. The nature and heterogeneity of the post-translational modifications were previously char-acterized by in vitro enzymatic deglycosylation treat-ment [23]. Figure 1 displays the SELDI spectra of nECP1–7, labeled from high to low molecular weight, according to chromatography elution order. Most

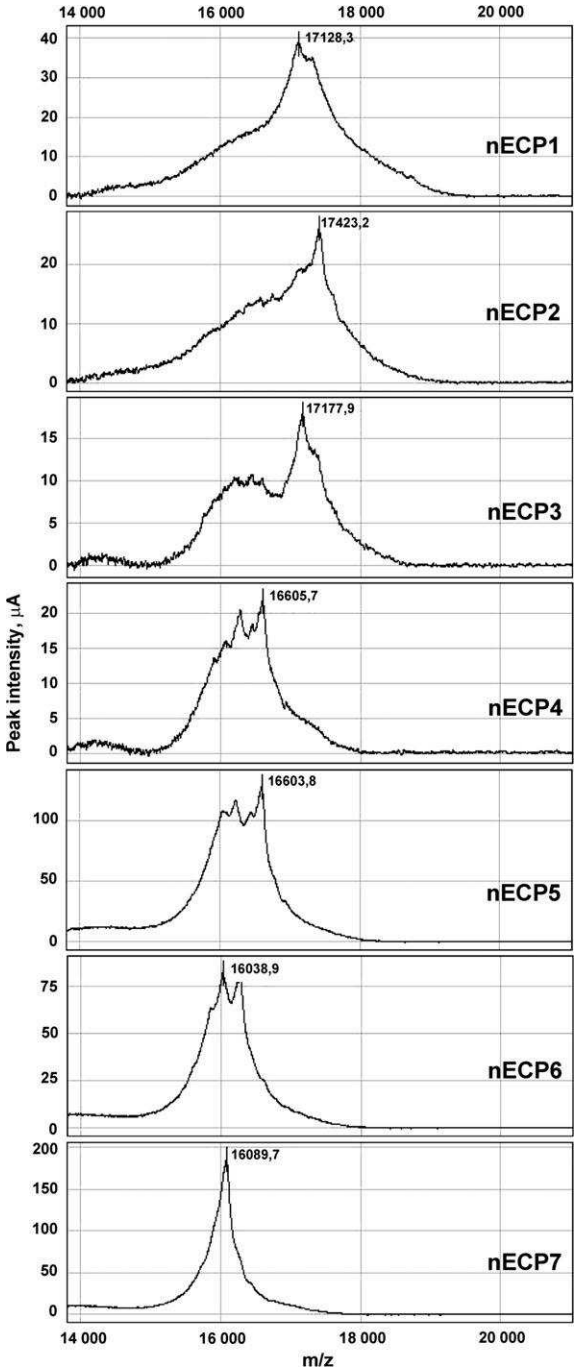

Fig. 1. SELDI-TOF MS analysis of nECP1–7 with the monoclonal anti-ECP antibody 614. The molecular weight of the peak of highest intensity is labeled in each spectrum. Note that the scale of peak intensity (y-axis) differs in the spectra. Number of peaks and molecular weight range for each fraction are as follows: nECP1, two peaks (17.1–17.3 kDa); nECP2, five peaks (16.6–17.6 kDa); nECP3, six peaks (15.8–17.4 kDa); nECP4, six peaks (15.9– 16.6 kDa); nECP5, four peaks (16.04–16.6 kDa); nECP6, three peaks (15.9–16.3 kDa); nECP7, one peak (16.1 kDa).

ECP pools were quite heterogeneous with several molecular species present. A mass label at the peak of highest intensity is included for each spectrum. Several molecular variants of ECP were detected, ranging in mass from ~ 15.8 to 17.6 kDa. The number of peaks in each ECP pool varied from one to six. Some molec-ular variants were present in several pools. The cap-tion to Fig. 1 includes detailed information on the number of peaks and the molecular weight range. For comparison purposes, in some assays the highest (HMW) and lowest (LMW) molecular weight frac-tions, according to their major highest intensity refer-ence peak, were selected. Native forms were compared with the non-glycosylated recombinant protein [39], which shows a molecular weight of 15.7 kDa as deter-mined by MALDI-TOF analysis.

Antimicrobial activity of native ECP forms

The antimicrobial activity of recombinant and native ECP forms purified from eosinophils was assayed on E. coli cultures. The results indicated that an increase in the overall molecular weight correlated with a reduc-tion of the protein antimicrobial activity (Table 1), where the heavily glycosylated forms showed higher minimal bactericidal concentration (MBC) values. Bac-teria viability was then tested using the BacTiter-Glo assay based on the quantification of ATP levels, as an estimate of viable cell number, confirming an inverse correlation between glycosylation and cytotoxicity (Fig. 2). Interestingly, the lowest glycosylated form displayed a comparable or even slightly higher bacteri-cidal activity than the non-glycosylated protein.

Action at the bacterial envelope

Following this, we compared the cell agglutination activity of native and recombinant proteins. Previous work on recombinant ECP highlighted the protein cell agglutination activity on Gram negative species [40,41]. The present studies show how glycosylated forms mostly lose the bacteria agglutination ability dis-played by the recombinant protein (Table 1). Next, we assessed the protein binding affinity to the outer mem-brane lipopolysaccharides (LPSs) (Table 2), which was previously found to correlate with the protein cell agglutination activity for the recombinant protein [40]. Protein interaction with the LPSs was estimated by BODIPY-TR cadaverine (BC) probe displacement after sequential protein addition. Comparison of the calculated occupancy displacement factor (ED_{50}) val-ues for recombinant and native fractions revealed a reduction of LPS affinity for the highest molecular

Table 1. Comparison of recombinant and native ECP forms. Antimicrobial and agglutination activities were tested on E. coli cell cultures. The MBC was estimated by calculating the protein concentration that reduced by 99.9% the starting CFU per milliliter; MBC_T was the protein concentration that rendered the assay mixture essentially sterile and the minimal agglutination concentration (MAC) was calculated as described in Materials and methods. All values are averaged from three replicates of two independent experiments.

Protein	MBC (lM)	MBC_T (lM)	MAC (lM)
nECP1	0.70	2–3	> 2
nECP2	0.80	2–2.5	> 2
nECP3	0.65	1.5	> 2
nECP4	0.60	1.5	> 2
nECP5	0.55	1.0	> 2
nECP6	0.50	1.0	2
nECP7	0.20	0.5	2
rECP	0.30	0.6	0.4

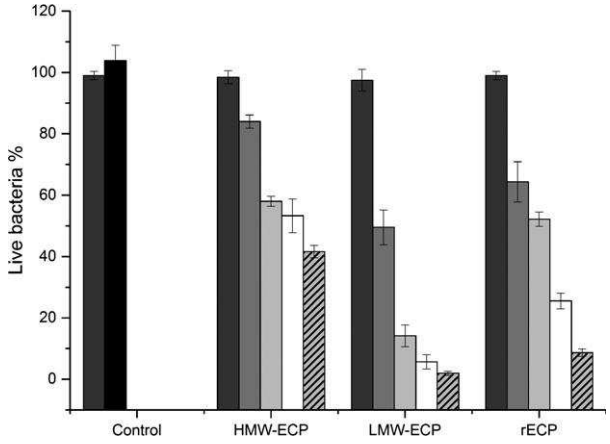

Fig. 2. Effect of recombinant and native ECP forms on bacteria viability. Escherichia coli cell survival percentage was registered after 4 h of exposure at increasing protein concentrations. Bacteria viability was assessed using the BactTiter-Glo assay, as described in Materials and methods. Values are given as mean SD. Dark grey bar corresponds to initial time and black bar corresponds to control untreated cell survival after 4 h of incubation. Assayed protein concentrations were as follows: grey bar, 0.1 lM; light grey bar, 0.3 lM; white bar, 0.5 lM; striped bar, 1 lM. HMW-ECP and LMW-ECP refer to nECP forms showing the highest and lowest major molecular weight peaks respectively.

weight fractions, although no major differences were registered and a higher dispersion was detected for the in between, more heterogeneous, fractions.

Action at the bacterial cytoplasmic membrane

To further interpret the distinct behavior of the stud-ied native forms on bacteria cultures, we decided to analyze their action on the bacteria cytoplasmic membrane. Our previous work on the recombinant protein illustrated how actions at both bacterial envelope and membrane levels were complementing each other [7,42]. To analyze the protein direct effect on the bac-terial cytoplasmic membrane we applied the SYTOX Green assay, where the fluorescence increase is regis-tered to monitor the cell dye uptake. The assay is sen-sitive to any membrane local disturbance that would allow access of the LMW dye (600 molecular weight) to the intracellular compartment and subsequent stain-ing of cell nucleic acids. Comparison of the bacteria cell leakage induced by recombinant and native proteins indicated a moderate reduction as a function of the protein glycosylation degree, where the HMW forms exhibit a reduced activity (Table 3). In particu-lar, significant differences were observed on comparing the IC_{50} leakage activities of high and low representa-tive glycosylated forms (Table 4). Interestingly, the lowest molecular weight native form, which did not induce cell agglutination, destabilized the membrane in

Table 2. Comparison of LPS binding by recombinant and native ECP forms. The occupancy displacement factor (ED_{50}) was calculated as described in Materials and methods. ED_{50} is given as the mean SD. t test significance is indicated for n = 3: *P < 0.05.

Protein	ED_{50} (lM)
nECP1	0.42 0.13*
nECP2	0.46 0.10*
nECP3	0.17 0.09
nECP4	0.48 0.05*
nECP5	0.29 0.05
nECP6	0.28 0.04
nECP7	0.30 0.09
rECP	0.23 0.07

Table 3. Bacteria cell leakage by recombinant and native ECP forms. Leakage activity was estimated by the SYTOX Green uptake assay as described in Materials and methods. Arbitrary fluorescence units are used for maximum disruption. 10% Triton X-100 was used as a positive reference control, giving a fluorescence value of 250 units. Values are given as mean SD. t test significance is indicated for n = 3: ***P < 0.001.

Protein	t_{50} (s)	Maximum disruption
nECP1	74329	130.40 0.37***
nECP2	63020	141.19 0.25***
nECP3	140295	136.48 2.11***
nECP4	90137	146.81 0.67***
nECP5	82419	148.35 0.40***
nECP6	80946	153.29 1.06***
nECP7	52237	170.20 1.20
rECP	117443	176.90 2.06

Table 4. Comparison of membrane destabilization activities of recombinant and native ECP forms. E. coli bacteria cell leakage was estimated by the SYTOX Green uptake assay as detailed in Materials and methods. Depolarization activity on E. coli cytoplasmic membrane was monitored by the $DiSC_3(5)$ dye assay as described. Half time to achieve maximum depolarization (t_{50}) at 50 nM protein concentration is estimated. The membrane leakage activity on DOPC/DOPG liposomes was analyzed using encapsulated Tb^{3+}. Values are calculated as mean SD. HMW-ECP and LMW-ECP refer to nECP forms showing the highest and lowest major molecular weight peaks respectively, as detailed in Materials and methods.

	Bacteria cell leakage		Depolarization activity	Liposome leakage
Protein	(%)[a]	IC_{50} (lM)	t_{50} (s)	IC_{50} (lM)
HMW-ECP	56.5 0.2	> 1	330 50	1.24 0.09
LMW-ECP	68.1 1.2	0.63 0.14	54 0.05	0.17 0.02
rECP	70.8 2.1	0.84 0.10	85 0.01	0.15 0.03

[a] Percentage values calculated at 1 lM protein concentration in relation to the positive reference control (10% Triton X-100). Percentage mean values are determined from two independent experiments performed in triplicate.

a shorter period of time than the recombinant protein (Table 3).

Following this we evaluated the depolarization activ-ity of the recombinant and native forms. Assays were performed at a protein concentration of 50 nM, well below the bacteria leakage IC_{50} values. Comparable maximum depolarization activities were observed for the assayed samples (data not shown). However, a sig-nificant reduction was registered in the t_{50} depolariza-tion time for the highest molecular weight form (Table 4), which could be attributed to its diminished affinity towards the bacteria outer membrane LPSs. The effective protein concentration for depolarization activity was well below that required for lipid vesicles and cell agglutination activities, suggesting that ECPs can depolarize the cytoplasmic membrane without undergoing any local self-aggregation process. On the other hand, time course monitoring showed similar depolarization profiles for recombinant and LMW ECPs, indicating that the protein lowest post-transla-tional modification did not hinder protein access and subsequent action at the cytoplasmic membrane.

Mechanism of action on model membranes

Finally, with the aim of better understanding the pro-tein behavior at the bacteria cell membrane we ana-lyzed both the protein membrane lysis and vesicle aggregation activities using synthetic lipid bilayers. Mixed neutral/anionic phospholipid liposomes entrap-ping fluorescent markers of distinct molecular weight were prepared. Previous work on the recombinant pro-tein action using a variety of phospholipids [43,44] showed the protein preference for anionic type lipids. Here, the degree of membrane disturbance by native ECP forms was evaluated following the release of the vesicle inner content. Three assays were chosen that could provide direct information on the magnitude of the local membrane disturbance [45]. The Tb^{3+}/DPA assay monitors the release of encapsulated Tb^{3+}, which upon interaction with the DPA present at the outer compartment emits fluorescence. Tb^{3+} was cho-sen to detect small local membrane disturbance. Results were complemented with the ANTS/DPX assay, where ANTS (450 molecular weight) is encapsu-lated together with its quencher, DPX, and the fluores-cence of free unquenched ANTS correlates with the liposome inner content release. Additionally, labeled dextran of about 3 kDa was chosen to assess massive vesicle lysis. The release of each marker was monitored as a function of time and protein concentration (Tables 4 and 5). For each marker, lysis percentage of native LMW and HMW was compared with the recombinant protein. Lastly, time courses were ana-lyzed at a protein concentration below the MBC and minimal agglutination concentration values to check whether the dye release was taking place well before any vesicle aggregation process (Fig. 3). Significant but moderate differences between samples were observed for Tb^{3+} and ANTS release, while dextran release was mostly reduced for the heavy glycosylated fraction. Of note, the HMW sample could hardly induce the release of the entrapped dextran, even after a long exposure

Table 5. Membrane leakage activity was assayed using DOPC/DOPG liposome encapsulated markers of distinct molecular weight (Tb^{3+}, ANTS and 3 kDa dextran). Leakage percentages were calculated as described in Materials and methods taking the recombinant protein as a reference. All assays were performed at 0.4 lM of protein and final fluorescence values were calculated after 1 h of incubation. Percentage mean values are determined from two independent experiments performed in triplicate. Values are indicated as mean SD. HMW-ECP and LMW-ECP refer to the nECP forms showing the highest and lowest major molecular weight peaks respectively, as detailed in Materials and methods.

	Liposome leakage (%)		
Protein	Tb^{3+}	ANTS	Dextran
HMW-ECP	59 5	69 10	22 5
LMW-ECP	74 10	94 7	92 8
rECP	100	100	100

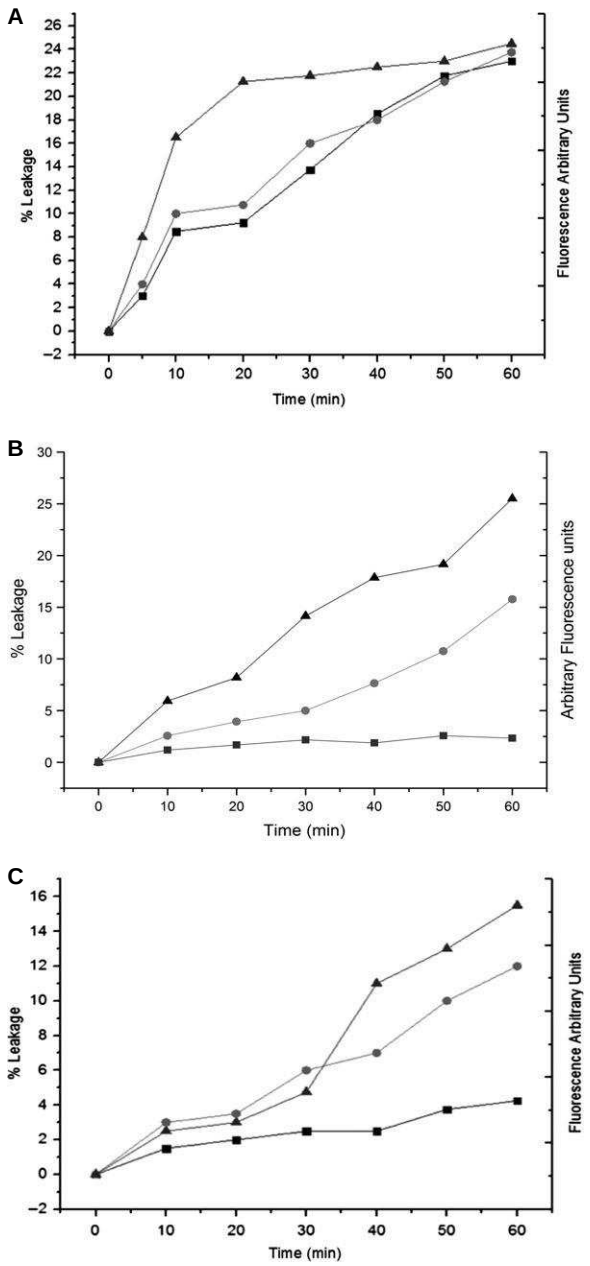

Fig. 3. Profile comparison of DOPC/DOPG liposome leakage process as a function of time for encapsulated molecular weight markers. (A) Tb^{3+}, (B) ANTS and (C) 3 kDa dextran. Each data point was analyzed after addition of 0.1 lM of HMW-ECP (■), LMW-ECP (●) and rECP (▲), as described in Materials and methods. Percentage values were calculated in relation to 10% Triton X-100. HMW-ECP and LMW-ECP refer to representative nECP forms showing the highest and lowest major molecular weight peaks respectively, as detailed in Materials and methods.

time. The data indicated that the massive membrane disruption required for dextran release is mostly hin-dered by heavy glycosylation. Moreover, about a 10-fold protein concentration is required for the HMW sample to induce liposome leakage, even for the Tb^{3+} entrapped marker (Table 4). On the other hand, a close follow-up of the time course release of the Tb^{3+} dye marker (Fig. 3) suggested a local mem-brane transient disturbance mechanism rather than the formation of a defined local pore.

The protein action on lipid bilayers was also assessed by following the vesicle aggregation activity. Aggregation was monitored by registering the mean size of the liposome population by static and dynamic light scattering. Liposome aggregation activity observed for recombinant ECP (rECP) [43] was mostly lost for all native forms, and fully abolished for the heaviest glycosylated forms (Fig. 4). Noteworthy, for all the studied native forms no lipid aggregation is observed at the protein concentrations where liposome leakage is taking place. On the contrary, the side by side comparative profiles for rECP liposome lysis and aggregation activities, where vesicle aggregation pre-cedes the dye release, indicate that the recombinant protein triggers the leakage process by its lipid aggre-gation activity (Fig. 5).

Discussion

There is a growing bulk of evidence of the key role of eosinophil granule proteins in innate immunity [4,5]. Early work by Lehrer et al. [9] reported the bacterici-dal activity of native ECP on both E. coli and S. aureus species. Native ECP heterogeneity was subsequently further characterized thanks to the availability of an optimized protocol for protein extraction from eosinophil granules [21,23]. The pres-ent study is the first comparative report on the antimi-

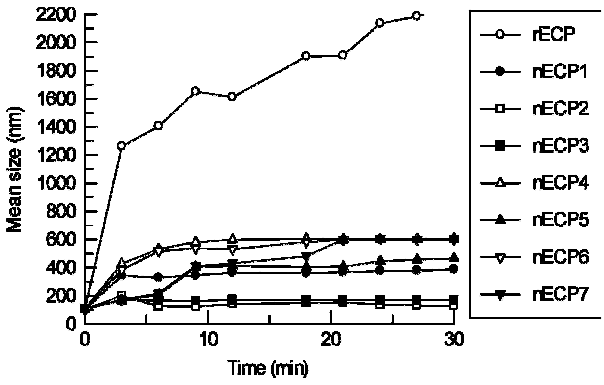

Fig. 4. Liposome agglutination by recombinant and native ECP forms. Vesicle aggregation was followed by dynamic light scattering as described in Materials and methods. Protein at 0.4 lM final concentration was added to DOPC/DOPG liposomes.

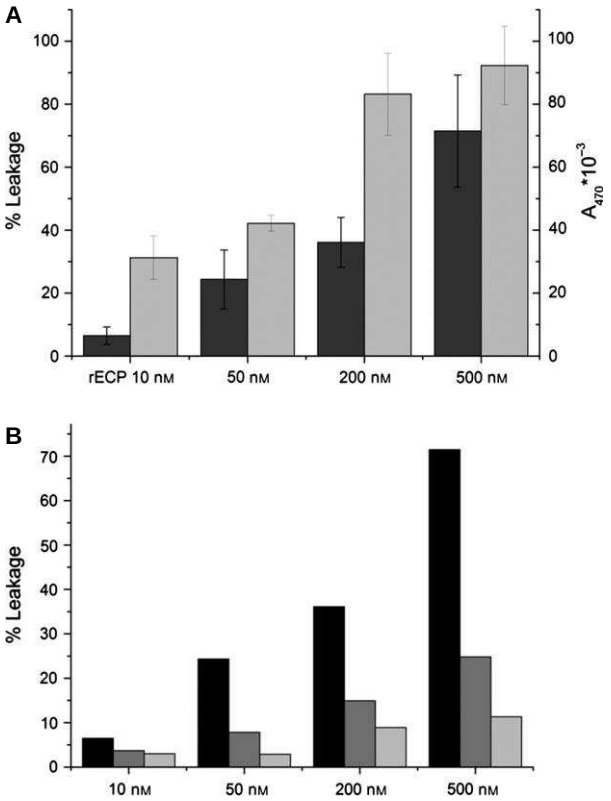

Fig. 5. Comparison of liposome leakage and aggregation activities of recombinant and native ECP forms. Liposome leakage was assayed following the release of vesicle entrapped ANTS/DPX and liposome aggregation was registered by static light scattering at 470 nm. Liposomes were prepared at 100 lM and proteins were added from 10 to 500 nM. Activities were assayed after 1 h of incubation. (A) Liposome leakage (in black) and aggregation (in grey) for rECP. (B) Comparison of liposome leakage for rECP (in black), LMW-ECP (in dark grey) and HMW-ECP (in light grey). No aggregation at the assayed protein concentrations was detected for native ECP forms. HMW-ECP and LMW-ECP refer to nECP fractions showing the highest and lowest major molecular weight peaks respectively.

crobial properties of ECP native forms purified from eosinophils. The results indicate that the protein antimicrobial action is modulated by post-translational modifications and highlight the importance of analyz-ing, whenever available, the native protein. We observe here how LMW and HMW native forms display a dis-tinct antimicrobial profile, where heavy glycosylation significantly reduces the protein toxicity (Table 1, Fig. 2). This pattern is similar to the profile reported for native ECP activity on mammalian cell lines [22,23], where in vitro deglycosylation unmasked the protein cytotoxicity [23]. Interestingly, intracellular and secreted ECPs have a distinct molecular weight profile, where intracellular forms range from 16.1 to 17.7 kDa while the secreted protein is much less glycosylated, showing values between 16.1 and 16.3 kDa [15]. Indeed, heavy glycosylation was suggested to protect the eosinophil granule from the toxicity of the stored protein, where subsequent partial deglycosyla-tion would take place during the eosinophil activation and degranulation process [15,23]. We can hypothesize that eosinophil degranulation at the infectious focus would free the protein to act on the targeted patho-gens.

Our previous work on bactericidal action of rECP indicated that the protein binds first to the bacteria surface through electrostatic interactions, triggering a subsequent membrane destabilization process [41,42]. We have analyzed here the action of the purified native forms on E. coli cultures, observing that heavy glycosylation reduces the protein binding affinity to the outer membrane LPSs (Table 2) and hinders the protein cytoplasm membrane leakage activity (Table 4). In order to fully assess the membrane dam-age extent, we have compared the native and recom-binant protein action on lipid vesicles containing dye markers of variable size (Table 5, Fig. 3), observing vesicle content release profile characteristics of a local membrane disturbance event. Previous work using encapsulated Tb^{3+} and ANTS estimated that a minimum 'pore' size of around 10 Å is required for the vesicle content release [45,46]. On its side, the 3 kDa labeled dextran is estimated to adopt in solution an effective hydrodynamic radius of about 20 Å [45,47]. Additionally, the protein assessment on membrane models has been complemented with functional assays. Results indicate that bacteria cytoplasmic membrane depolarization precedes cell leakage (Tables 3 and 4), suggesting that an incubation time is required for the protein to 'organize itself' in an active disruption species. Besides, the gradual lipo-some leakage process is directly dependent on the lipid/protein ratio (Table 4) and the total vesicle con-tent release for HMW entrapped dextran is only accomplished for the recombinant and LMW fraction after a long incubation time, pointing to an overall 'carpet like' mechanism (Table 5). A similar behavior is observed for other antimicrobial peptides that destabilize the lipid bilayer by inducing local transient disturbances but do not form a proper transmembrane pore [45].

On the other hand, rECP vesicle aggregation activity was found to correlate with bacteria agglutina-tion in previous work [41,42]. Interestingly, the lipid aggregation and bacteria agglutination activities are mostly lost in the studied glycosylated forms, where heavy glycosylation totally impairs the protein aggluti-

nation action (Table 1, Fig. 4). However, bacteria agglutination is not mandatory for bactericidal action. Even the lowest molecular weight form shows an equivalent or slightly higher cytotoxicity than the recombinant protein. We can hypothesize that the native forms, lacking agglutination activity, would work as single molecule entities when encountering the cytoplasm membrane. Moreover, the data suggest that some particular post-translational modification present in the LMW fraction can contribute to the final protein bactericidal properties. Indeed, recent results on the cytotoxic properties of ECP on a cancer cell line indicate that a high toxicity can be achieved by the lowest molecular weight fractions, whose post-translational modification cannot be fully removed by N-glycosidase treatment [23].

Besides, our results represent the first comparative analysis of the protein activity on lipid bilayers. Interestingly, formation of defined local membrane pores was reported for ECP purified from eosinophils [48], whereas a 'carpet-like' mechanism was ascribed to the recombinant protein [43,44]. The new data may shed light on the earlier observed discrepancies between recombinant and native proteins. Recombinant protein aggregation and subsequent cell agglutination processes were previously proved to be driven by an exposed hydrophobic patch located at the ECP N-terminus [41,49,50]. We demonstrate here how heavy glycosyla-tion interferes with the protein agglutination and mem-brane destabilization activities. A three-dimensional representation model for a putative N-glycosylated ECP molecule (Fig. 6) suggests that the glycosylation branch at Asn65 is covering the aggregation-prone stretch and hence is interfering with the protein mem-brane interaction mode. In the structure model, glyco-sylation would cover both the hydrophobic and cationic surfaces and block not only the protein-self interaction site but also the protein –membrane binding region. In particular, the putative attached glycosyla-tion at Asn65 would mask residues, such as Arg1, Trp35 and Lys38, that are reported to contribute to interactions with phospholipids and the outer mem-brane LPSs [40,51]. We cannot discard the potential contribution of other additional post-translational modifications either, such as the nitration of Tyr33 identified by Ulrich et al. [29]. The presence of a bulky anionic group at the exposed N-terminus region might also block the protein self-aggregation and/or modify its membrane binding activity. On the other hand, lack of any major differences in the LPS binding affinity data suggests that glycosylation would hinder the protein cell agglutination activity mostly by blocking the protein self-aggregation activity rather than by reducing the binding towards the bacteria wall surface.

The present results highlight the contribution of the native post-translational modification in the protein cytotoxic mechanism of action. ECP glycosylation pattern is indeed one of the best characterized within the vertebrate secreted RNase superfamily. Aside from the pioneering studies on pancreatic RNases [25,52], little is known

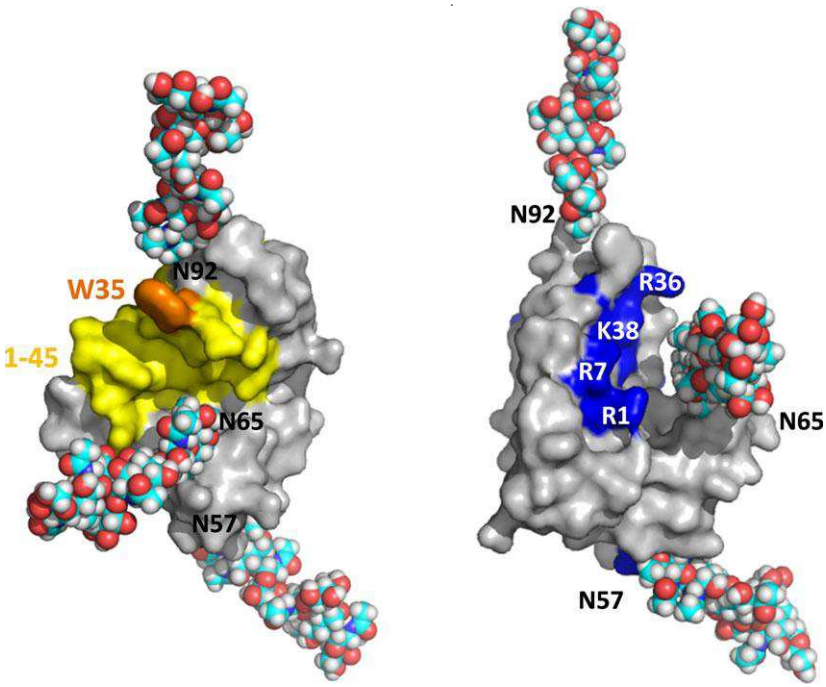

Fig. 6. Model showing the location of putative N-glycosylation for ECP native forms. A reference glycan structure (2K33 pdb) was attached to Asn residues at potential glycosylation sites. (A) The main ECP region involved in the protein antimicrobial activity is colored in yellow and key residue for membrane interaction in orange. (B) Cationic residues involved in the bactericidal activity are colored in blue. Potential residues located at the vicinity of the modeled oligosaccharide chain are labeled in white.

about the role of post-translational modifications within the family. Early studies by X-ray crystallography revealed no significant structural changes for RNase B, the glycosylated form of bovine pancreatic RNase A, showing how the oligosaccharide portion extended towards the solvent [53]. RNase B enzymatic activity did not differ significantly from the non-glycosylated form [54,55], while NMR studies highlighted the glycosylation contribution to the protein stability [56,57] and folding rate [54,58]. Some complementary examples are avail-able, as EDN or onconase, a family related RNase with antitumoral activity, where glycosylation also contributes to the protein cytotoxicity [28,59].

In a wider context, glycosylation contributes to pro-tein pharmacokinetics, intracellular trafficking and final biological properties. In particular, glycosylation can enhance the protein solubility and thermal stabil-ity, favoring the folding pathway and providing pro-tection against proteolysis [60,61]. Interestingly, the prevention of protein aggregation by glycosylation might also be a key mechanism to ensure cell viability, where deglycosylation of aged proteins is among the processes involved in the loss of cell vital functions. Unfortunately, the large scale production of properly glycosylated therapeutic proteins is still a pending challenge in the biotechnology field [62–64].

Conclusions

ECP native forms purified from eosinophils differ in their antimicrobial properties. In particular, bacteria and liposome agglutination activities displayed by the recombinant protein are hindered by post-translational modifications. We conclude that heavy glycosylation drastically reduces the protein toxicity by interfering with the protein anchoring to the bacteria wall, protein self-aggregation and further membrane destabilization action. The results highlight the contribution of glyco-sylation to ECP's biological properties, suggesting a role for post-translational modifications in the protein physiological function. Further work is in progress to elucidate the mechanism of action at the molecular level of each post-translational native form.

Materials and methods

Materials

Escherichia coli BL21(DE3) cells and the pET11 expression vector were from Novagen (Madison,WI, USA). The BacTiter-Glo assay kit was from Promega (Madison, WI, USA). SYTOX Green, $DiSC_3(5)$ (3,3-dipropylthiacarbocya-nine) and BC [BODIPY-TR cadaverine, where BODIPY is boron dipyrromethane (4,4-difluoro-4-bora-3a,4a-diaza-s-indacene)], were purchased from Invitrogen (Groeningen, The Netherlands). Dioleoyl phosphatidylcholine (DOPC) and dioleoyl phosphatidylglycerol (DOPG) were from Avanti Polar Lipids (Alabaster, AL, USA). ANTS (8-amino-naphthalene-1,3,6-trisulfonic acid disodium salt), DPX (p-xylenebispyridinium bromide), DPA (dipicolinic acid) and terbium chloride ($TbCl_3$) were obtained from Molecular Probes (Eugene, OR, USA). 3 kDa dextran labeled with rho-damine green and LPSs from E. coli serotype 0111:B4 were purchased from Sigma-Aldrich (St Louis, MO, USA). Monoclonal anti-ECP antibody 614 was from Diagnostics Development (Uppsala, Sweden). AKTA prime system, G-75 Superfine and Mono-S columns were from GE Healthcare Bio-sciences (Uppsala, Sweden). Bownlee Bu300 column was from Perkin Elmer (Waltham, MA, USA). NuPAGE⁻ Bis-Tris gels were from Invitrogen. The UniCAP system was from Phadia (Uppsala, Sweden). ProteinChip⁻ arrays were from Bio-Rad Laboratories (Hercules, CA, USA).

Native ECP form purification

Native forms of the ECP (nECP1–nECP7) were purified by a modification of the previously described protocol [18]. ECP was extracted and purified from about 200 buffy coats of healthy blood donors. Eosinophil granules were prepared by nitrogen cavitation of buffy coat leuko-cytes and were separated from other organelles by ultra-centrifugation. Following this, the granules were extracted in 0.2 M NaAc pH 4.0 and subjected to gel filtration chro-matography on a G-75 Superfine column. The eluted frac-tions were divided into nine pools of which two contained ECP as detailed [18]. The first ECP-containing pool included HMW ECP and the second contained LMW ECP.

Ion exchange chromatography was performed using the AKTA prime system and a Mono-S column, equilibrated with 50 mM 4-morpholino ethane sulfonic acid, 2% betain, 0.1 M LiCl, pH 6.0. The proteins were eluted using a linear gradient from 0.1 M to 1.0 M LiCl. Four peaks were selected from the ion exchange chromatography of the gel filtration HMW ECP pool; hence eluted fractions were pooled in samples nECP1–nECP4. Ion exchange chroma-tography of the LMW ECP pool resulted in other addi-tional chromatographic peaks, pooled in samples nECP5– nECP7. Fractions showing the lowest and highest molecu-lar weight peaks were also pooled as LMW and HMW samples, namely nECP7 with a single main peak at 16 kDa as LMW-ECP and nECP1–2 with a single major peak above 17 kDa as HMW-ECP. Further reversed-phase chro-matography was performed on a Bownlee Bu300 column. The proteins were eluted using a gradient from 0% to 60% acetonitrile in 0.1% trifluoroacetic acid. All purification steps were performed in the presence of the protease inhibi-tor PMSF at a concentration of 100 lg mL^{1}.

Purification of recombinant ECP

Non-glycosylated rECP was expressed in E. coli BL21 (DE3) strain using a human synthetic gene cloned in pET11c and purified from inclusion bodies as previously described [39]. The recombinant protein includes a Met res-idue at its N-terminus and has no post-translational modifi-cations, showing a calculated molecular weight of 15.7 kDa.

Protein determination and concentration

Recombinant protein purity was confirmed by SDS/15% PAGE gels and the protein molecular weight, 15.7 kDa, was checked by MALDI-TOF methodology. The purity of native ECP fractions was assessed by analysis on Nu-PAGE⁻ 10% Bis-Tris gels and radioimmunoassay as previ-ously [18], showing values over 95%. The concentration of ECP was determined by the absorbance at 280 nm using the extinction coefficient ($E^{1\%.1\ cm}$) of ECP of 15.45 [65,66] and by immunoassay in the UniCAP system (Phadia). ECP-containing fractions were concentrated using Amicon YM-10 filters and buffer exchanged using the ÄKTA prime system. Purified ECP samples were stored in 0.2 M NaAc buffer (pH 5.5) at 70 °C.

Affinity capture of ECP by SELDI-TOF MS

The native ECP pools were analyzed by the affinity capture assay as described previously [14]. In short, 0.6 lg mono-clonal anti-ECP antibody 614 (Diagnostics Development) diluted in 10 lL of PBS was added to each spot of PS20 ProteinChip⁻ arrays. After 2.5 h incubation at room tem-perature and blocking of unspecific binding to the surface by incubation with 25 lL of 0.5 M ethanolamine in PBS, the arrays were washed three times for 5 min with 0.5% Triton in PBS and three times for 5 min with PBS. ECP (0.2–0.7 lg) was added to each spot and the arrays were incubated overnight at 4 °C. The following morning the arrays were washed three times for 5 min with 0.5% Triton in PBS and three times for 5 min with PBS. Afterwards, the arrays were washed with 1 mM HEPES buffer before the addition of saturated sinapinic acid in 0.5% trifluoro-acetic acid and 50% acetonitrile.

The arrays were then analyzed in a PCS4000 Enterprise Edition instrument and a total of 106 transients were col-lected from each spot.

Bactericidal activity assay

The proteins' antimicrobial activity was assayed by calcu-lating the MBC, which is defined conventionally as the low-est concentration of protein that reduces the starting colony forming units (CFU) per milliliter (~ 1×10^5 CFU mL^{-1}) by 99.9%. We also estimated the MBC_T, which we defined as the protein concentration that ren-dered the assay mixtures essentially sterile (< 1 CFU mL^{-1}). The assay was performed as previously described [67]. E. coli BL21(DE3) cells were incubated at 37 °C overnight in LB broth and diluted in the broth med-ium to give ~ 5×10^5 CFU mL^{-1}. Bacteria cells were pel-leted for 2 min at 5000 g and resuspended in 10 mM sodium phosphate, pH 7.5. Proteins (from 0.06 to 3 lM final concentration) were added to the bacterial suspension and samples were incubated for 4 h at 37 °C, plated onto Petri dishes and incubated at 37 °C overnight. Remaining CFUs after 4 h incubation were counted.

Minimal agglutination concentration (MAC)

Escherichia coli cells were grown at 37 °C to A_{600} ~ 0.2, centrifuged at 5000 g for 2 min and resuspended in Tris/ HCl buffer, 0.1 M NaCl, pH 7.5, to an absorbance of 10 at 600 nm (~ $1–2 \times 10^9$ CFU mL^{-1}). Aliquots of 100 lL of the bacteria suspension were treated with increasing protein concentrations (from 0.06 to 2 lM) and incubated at 25 °C for 1 h. The aggregation was checked by macroscopic visual inspection and the activity was expressed as the minimum agglutinating concentration, as previously described [41].

Bacteria viability assay

Bacterial viability was assayed using the BacTiter-Glo microbial cell viability kit, which estimates the percentage of metabolically active cells by ATP quantification using a coupled luminescence assay [40]. Briefly, overnight E. coli BL21(DE3) bacteria cultures grown in LB at 37 °C were used to inoculate 100 lL of fresh LB and cultures were grown to A_{600} ~ 0.2. Pelleted cells were resuspended in PBS buffer and incubated for 4 h at 37 °C with the proteins, serially diluted from 2 to 0.1 lM final concentration. An aliquot of 50 lL of culture was mixed with 50 lL of BacT-iter-Glo reagent in a microtiter plate and incubated at 25 °C for 15 min. Luminescence was read on a Victor3 plate reader (Perkin Elmer) with a 1-s integration time and the percentage of viable bacteria cells was calculated as pre-viously [40].

Liposome preparation

The liposomes used in our studies were large unilamellar vesicles (LUVs), ~ 100 nm in diameter, that were prepared as previously described [43]. A 1-mM stock solution of lipo-some containing DOPC and DOPG (3 : 2 molar ratio) in 10 mM Tris/HCl, 0.1 M NaCl, pH 7.4, was prepared. The lipid suspension was frozen and thawed several times before extrusion through polycarbonate membranes. Lipo-some population mean size was checked by dynamic light scattering as previously [43].

Liposome leakage assay

Liposome leakage assay was performed using a range of encapsulated markers of distinct molecular weight (Tb^{3+}, ANTS and dextran) as previously described [45]. Lipo-somes with encapsulated markers were diluted to 30 lM before addition of protein samples at distinct lipid/protein ratios. Encapsulated marker release was followed for up to 1 h at 25 °C after adding a protein concentration ranging from 0.05 to 1 lM. Leakage percentage (%L) was calcu-lated as follows: %L = 100 9 (F_p F_0)/(F_{100} F_0), where F_p is the final fluorescence intensity 1 h after the addition of the protein, F_0 is the fluorescence intensity before adding the protein and F_{100} is the maximum reference fluorescence after the addition of Triton X-100 at 10%. Fluorescence measurements were performed on a Cary Eclipse spectro-fluorimeter.

The Tb^{3+}/DPA leakage assay was performed as described previously [45]. Dried lipid films were resus-pended to a concentration of 1 mM lipid to maximize encapsulation. For LUVs encapsulating Tb^{3+}, a buffer of 50 mM $TbCl_3$, 100 mM sodium citrate and 10 mM TES, pH 7.2, was used. After extrusion, liposomes were separated from external terbium via gel filtration chromatography using a buffer containing 300 mM NaCl to balance the ionic strength of $TbCl_3$. Entrapped Tb^{3+} liposomes were diluted to 30 lM in 100 mM sodium citrate, 10 mM TES, 300 mM NaCl, pH 7.2, and before leakage measurement 75 lM of DPA was added to the buffer. Fluorescence emit-ted when Tb^{3+} interacts with DPA was recorded using excitation and emission wavelengths of 270 nm and 490 nm.

The ANTS/DPX leakage assay was performed as previ-ously described [68]. LUVs of DOPC/DOPG (3 : 2 molar ratio) lipids were obtained containing 12.5 mM ANTS, 45 mM DPX, 20 mM NaCl and 10 mM Tris/HCl, pH 7.5. The ANTS/DPX liposome suspension was diluted to 30 lM in 10 mM Tris/HCl, 0.1 M NaCl, pH 7.4, and was incubated at 25 °C in the presence of protein samples. The leakage activity was assayed at different protein concentrations by monitoring the release of the liposome content. Fluores-cence was measured using a 386 nm excitation wavelength and a 535 nm emission wavelength.

The dextran leakage assay was performed as described previously [45]. Rhodamine labeled dextran (3 kDa) was encapsulated in DOPC/DOPG LUVs. Liposomes were pre-pared in 10 mM potassium phosphate, pH 7.5, buffer con-taining 10 mg mL^{-1} of labeled dextran. To ensure maximal encapsulation, 20 cycles of freeze–thaw were applied during preparation of dextran LUVs. Following extrusion, LUV samples were run over a gel filtration column of Sephadex G-200 equilibrated with elution buffer. Unlabeled dextrans were added to the buffer at 10 mg mL^{-1} to eliminate osmo-tic pressure on the vesicles. Proteins were added to 30 lM of liposome suspension in 10 mM potassium phosphate, pH 7.5. After incubation, fluorescence of samples was recorded using excitation and emission wavelengths of 545 and 600 nm.

Liposome aggregation

Liposome aggregation was assessed both by dynamic light scattering and by static light scattering signal at 470 nm. LUVs of DOPC/DOPG (3 : 2 molar ratio) lipids were obtained as described previously [43]. For dynamic light scattering assays, a liposome stock of 1 mM was diluted to 200 lM in 10 mM Tris/HCl, 0.1 M NaCl, pH 7.4, and was tested in the presence of recombinant and native ECP (from 10 to 500 nM). The liposome aggregation was mea-sured by monitoring the sample size changes during 1 h using a Malvern Zetasizer Nano instrument. For static light scattering experiments the scattering signal at 470 nm was collected at 90L from the beam source using a Cary Eclipse spectrofluorimeter.

Bacteria cell leakage assay

Bacteria cell leakage was assessed using the SYTOX Green nucleic acid dye as described previously [69]. Escherichia coli cells were grown at 37 °C to A_{600} ~ 0.2, centrifuged at 5000 g for 2 min, resuspended in PBS and diluted to A_{600} ~ 0.05. Aliquots of 100 lL of the bacteria suspension were treated with 5 lM of SYTOX Green nucleic acid dye for 1 h. Afterwards, proteins ranging from 0.05 to 2 lM final concentration were added. Fluorescence was measured during 45 min using a 485 nm excitation wavelength and a 520 nm emission wavelength. The cell disruption percent-age was calculated as percent disruption = 100 9 (F_p F_0)/(F_{100} F_0), where F_p is the final fluorescence intensity after adding the protein, and F_0 and F_{100} are the fluores-cence intensities before the addition of the protein and after the addition of 10% Triton X-100. IC_{50} values were calculated by fitting the data to a nonlinear regression curve.

Bacteria cytoplasmic membrane depolarization assay

Membrane depolarization was followed using the sensitive membrane potential $DiSC_3(5)$ fluorescent probe as described previously [42]. After interaction with intact cyto-plasmic membrane, the fluorescent probe $DiSC_3(5)$ is quenched. Following incubation with the protein, the mem-brane potential is lost and the probe release to the medium can be monitored as a function of time. Bacteria cultures were grown at 37 °C to A_{600} ~ 0.2, centrifuged at 5000 g for 7 min, washed with 5 mM HEPES/KOH, 20 mM glu-cose, pH 7.2, and resuspended in 5 mM HEPES/KOH, 20 mM glucose and 100 mM KCl, pH 7.2, to A_{600} ~ 0.05.

$DiSC_3(5)$ was added to a final concentration of 0.4 lM. When the dye uptake was maximal, as observed by a stable reduction in the fluorescence because of quenching of the accumulated dye at the membrane inner side, the protein was added to a final concentration of 50 nM. Fluorescence increase was continuously recorded after addition of pro-tein and the time required to achieve half of total mem-brane depolarization was estimated from nonlinear regression analysis.

LPS binding assay

LPS binding was assessed using the fluorescent probe BC that binds to the LPS lipid A portion, as described previously [70]. Briefly, the displacement assay was per-formed by the addition of 1 lL aliquots of protein solution to 1 mL of a continuously stirred mixture of LPS (10 lg mL^{1}) and BC (10 lM) in 5 mM HEPES buffer at pH 7.5. Fluorescence was recorded on a Cary Eclipse spec-trofluorimeter. The BC excitation wavelength was 580 nm and the emission wavelength was 620 nm. Final values correspond to an average of four replicates and were the mean of a 0.3 s continuous measurement. The BC probe displacement by sequential protein addition was registered and the occupancy displacement factor (ED_{50}) was calcu-lated as previously described [70].

Statistical analysis

Results are reported as mean SD. Each native form was compared with the recombinant protein, where n is the number of repeated experiments. Statistical analysis was performed by the paired Student's t test using STATA 11 software and IBM SPS 19 software. One-way analysis of vari-ance (ANOVA) was applied. A P value < 0.05 was consid-ered significant.

Acknowledgements

Spectrofluorescence assays were performed at the Laboratori d'An_alisi i Fotodocumentacio,_ Universitat Autonoma_ de Barcelona. We thank Ms Lena Moberg for her technical assistance. The work was supported by the Ministerio de Econom_ıa y Competitividad (BFU2012-38965), co-financed by FEDER funds and by the Generalitat de Catalunya (2009 SGR 795). VAS is a recipient of a 'Francisco Jos_e de Caldas' predoctoral fellowship, Colciencias. DP was a recipient of an FPU predoctoral fellowship (Ministerio de Educacion_ y Cultura).

Author contributions

VAS, DP, MM and JR performed the experimental work; EB, MM and VAS planned the experiments, analyzed the data and drafted the manuscript; VAS, JR and EB prepared the corresponding artwork; EB wrote the final manuscript; JR, VN and PV partici-pated in discussion of the paper and correction.

References

1 Hewitson JP, Grainger JR & Maizels RM (2009) Helminth immunoregulation: the role of parasite secreted proteins in modulating host immunity. Mol Biochem Parasitol 167, 1–11.

2 Shamri R, Xenakis JJ & Spencer LA (2011) Eosinophils in innate immunity: an evolving story. Cell Tissue Res 343, 57–83.

3 Rosenberg HF, Dyer KD & Foster PS (2013) Eosinophils: changing perspectives in health and disease. Nat Rev Immunol 13, 9–22.

4 Simon D, Simon HU & Yousefi S (2013) Extracellular DNA traps in allergic, infectious, and autoimmune diseases. Allergy 68, 409–416.

5 Akuthota P, Xenakis JJ & Weller PF (2011) Eosinophils: offenders or general bystanders in allergic airway disease and pulmonary immunity? J Innate Immun 3, 113–119.

6 Ackerman SJ, Gleich GJ, Loegering DA, Richardson BA & Butterworth AE (1985) Comparative toxicity of purified human eosinophil granule cationic proteins for schistosomula of schistosoma mansoni. Am J Trop Med Hyg 34, 735–745.

7 Boix E, Salazar VA, Torrent M, Pulido D, Nogu_es MV & Moussaoui M (2012) Structural determinants of the eosinophil cationic protein antimicrobial activity. Biol Chem 393, 801–815.

8 Malik A & Batra JK (2012) Antimicrobial activity of human eosinophil granule proteins: involvement in host defence against pathogens. Crit Rev Microbiol 38, 168–181.

9 Lehrer RI, Szklarek D, Barton A, Ganz T, Hamann KJ & Gleich GJ (1989) Antibacterial properties of eosinophil major basic protein and eosinophil cationic protein. J Immunol 142, 4428–4434.

10 Venge P, Bystrom J, Carlson M, Hakansson L, Karawacjzyk M, Peterson C, Seveus L & Trulson A (1999) Eosinophil cationic protein (ECP): molecular and biological properties and the use of ECP as a marker of eosinophil activation in disease. Clin Exp Allergy 29, 1172–1186.

11 Bystrom J, Amin K & Bishop-Bailey D (2011) Analysing the eosinophil cationic protein - a clue to the function of the eosinophil granulocyte. Respir Res 12, 10.

12 Beintema JJ & Kleineidam RG (1998) The ribonuclease a superfamily: general discussion. Cell Mol Life Sci 54, 825–832.

13 Gleich GJ, Loegering DA, Bell MP, Checkel JL, Ackerman SJ & McKean DJ (1986) Biochemical and

functional similarities between human eosinophil-derived neurotoxin and eosinophil cationic protein: homology with ribonuclease. Proc Natl Acad Sci U S A 83, 3146–3150.

14 Eriksson J, Woschnagg C, Fernvik E & Venge P (2007) A SELDI-TOF MS study of the genetic and post-translational molecular heterogeneity of eosinophil cationic protein. J Leukoc Biol 82, 1491–1500.

15 Woschnagg C, Rubin J & Venge P (2009) Eosinophil cationic protein (ECP) is processed during secretion. J Immunol 183, 3949–3954.

16 Zhang J & Rosenberg HF (2000) Sequence variation at two eosinophil-associated ribonuclease loci in humans. Genetics 156, 1949–1958.

17 Jonsson UB, Bystrom J, Stalenheim G & Venge P (2002) Polymorphism of the eosinophil cationic protein-gene is related to the expression of allergic symptoms. Clin Exp Allergy 32, 1092–1095.

18 Trulson A, Bystrom J, Engstrom A, Larsson R & Venge P (2007) The functional heterogeneity of eosinophil cationic protein is determined by a gene polymorphism and post-translational modifications. Clin Exp Allergy 37, 208–218.

19 Munthe-Kaas MC, Gerritsen J, Carlsen KH, Undlien D, Egeland T, Skinningsrud B, Torres T & Carlsen KL (2007) Eosinophil cationic protein (ECP) polymorphisms and association with asthma, s-ECP levels and related phenotypes. Allergy 62, 429–436.

20 Eriksson J, Reimert CM, Kabatereine NB, Kazibwe F, Ireri E, Kadzo H, Eltahir HB, Mohamed AO, Vennervald BJ & Venge P (2007) The 434(G>C) polymorphism within the coding sequence of Eosinophil Cationic Protein (ECP) correlates with the natural course of Schistosoma mansoni infection. Int J Parasitol 37, 1359–1366.

21 Rubin J, Zagai U, Blom K, Trulson A, Engstrom A & Venge P (2009) The coding ECP 434(G>C) gene polymorphism determines the cytotoxicity of ECP but has minor effects on fibroblast-mediated gel contraction and no effect on RNase activity. J Immunol 183, 445–451.

22 Glimelius I, Rubin J, Fischer M, Molin D, Amini RM, Venge P & Enblad G (2011) Effect of eosinophil cationic protein (ECP) on Hodgkin lymphoma cell lines. Exp Hematol 39, 850–858.

23 Rubin J & Venge P (2013) Asparagine-linked glycans determine the cytotoxic capacity of eosinophil cationic protein (ECP). Mol Immunol 55, 372–380.

24 Plager DA, Davis MDP, Andrews AG, Coenen MJ, George TJ, Gleich GJ & Leiferman KM (2009) Eosinophil ribonucleases and their cutaneous lesion-forming activity. J Immunol 183, 4013–4020.

25 Beintema JJ, Blank A, Schieven GL, Dekker CA, Sorrentino S & Libonati M (1988) Differences in glycosylation pattern of human secretory ribonucleases. Biochem J 255, 501–505.

26 Sorrentino S (2010) The eight human 'canonical' ribonucleases: molecular diversity, catalytic properties, and special biological actions of the enzyme proteins. FEBS Lett 584, 2194–2200.

27 Rosenberg HF (2008) Eosinophil-derived neurotoxin/RNase 2: connecting the Past, the Present and the Future. Curr Pharm Biotechnol 9, 135–140.

28 Ye B, Skates S, Mok SC, Horick NK, Rosenberg HF, Vitonis A, Edwards D, Sluss P, Han WK, Berkowitz RS et al. (2006) Proteomic-based discovery and characterization of glycosylated eosinophil-derived neurotoxin and COOH-terminal osteopontin fragments for ovarian cancer in urine. Clin Cancer Res 12, 432–441.

29 Ulrich M, Petre A, Youhnovski N, Promm F, Schirle M, Schumm M, Pero RS, Doyle A, Checkel J, Kita H et al. (2008) Post-translational tyrosine nitration of eosinophil granule toxins mediated by eosinophil peroxidase. J Biol Chem 283, 28629–28640.

30 Hofsteenge J, Muller DR, Debeer T, Loffler A, Richter WJ & Vliegenthart JFG (1994) New-type of linkage between a carbohydrate and a protein - C-glycosylation of a specific tryptophan residue in human Rnase U-S. Biochemistry 33, 13524–13530.

31 Julenius K (2007) NetCGlyc 1.0: prediction of mammalian C-mannosylation sites. Glycobiology 17, 868–876.

32 Marth JD & Grewal PK (2008) Mammalian glycosylation in immunity. Nat Rev Immunol 8, 874–887.

33 Kolarich D, Lepenies B & Seeberger PH (2012) Glycomics, glycoproteomics and the immune system. Curr Opin Chem Biol 16, 214–220.

34 North SJ, von Gunten S, Antonopoulos A, Trollope A, MacGlashan DW, Jang-Lee J, Dell A, Metcalfe DD, Kirshenbaum AS, Bochner BS et al. (2012) Glycomic analysis of human mast cells, eosinophils and basophils. Glycobiology 22, 12–22.

35 Barboza M, Pinzon J, Wickramasinghe S, Froehlich JW, Moeller I, Smilowitz JT, Ruhaak LR, Huang JC, Lonnerdal B, German JB et al. (2012) Glycosylation of human milk lactoferrin exhibits dynamic changes during early lactation enhancing its role in pathogenic bacteria-host interactions. Mol Cell Proteomics 11, 1–28.

36 Krachler AM & Orth K (2013) Targeting the bacteria-host interface: strategies in anti-adhesion therapy. Virulence 4, 284–294.

37 Huang CY, Hsu JT, Chung PH, Cheng WTK, Jiang YN & Ju YT (2013) Site-specific N-Glycosylation of caprine lysostaphin restricts its bacteriolytic activity toward staphylococcus aureus. Anim Biotechnol 24, 129–147.

38 Kren V & Rezanka T (2008) Sweet antibiotics - the role of glycosidic residues in antibiotic and antitumor activity and their randomization. FEMS Microbiol Rev 32, 858–889.

39 Boix E, Nikolovski Z, Moiseyev GP, Rosenberg HF, Cuchillo CM & Nogues MV (1999) Kinetic and product distribution analysis of human eosinophil cationic protein indicates a subsite arrangement that favors exonuclease-type activity. J Biol Chem 274, 15605–15614.

40 Pulido D, Moussaoui M, Andreu D, Nogues MV, Torrent M & Boix E (2012) Antimicrobial action and cell agglutination by the eosinophil cationic protein are modulated by the cell wall lipopolysaccharide structure. Antimicrob Agents Chemother 56, 2378–2385.

41 Torrent M, Pulido D, Nogu_es MV & Boix E (2012) Exploring new biological functions of amyloids: bacteria cell agglutination mediated by host protein aggregation. PLoS Pathog 8, e1003005.

42 Torrent M, Badia M, Moussaoui M, Sanchez D, Nogues MV & Boix E (2010) Comparison of human RNase 3 and RNase 7 bactericidal action at the Gram-negative and Gram-positive bacterial cell wall. FEBS J 277, 1713–1725.

43 Torrent M, Cuyas E, Carreras E, Navarro S, Lopez O, de la Maza A, Nogues MV, Reshetnyak YK & Boix E (2007) Topography studies on the membrane interaction mechanism of the eosinophil cationic protein. Biochemistry 46, 720–733.

44 Torrent M, de la Torre BG, Nogues VM, Andreu D & Boix E (2009) Bactericidal and membrane disruption activities of the eosinophil cationic protein are largely retained in an N-terminal fragment. Biochem J 421, 425–434.

45 Rausch JM, Marks JR, Rathinakumar R & Wimley WC (2007) beta-Sheet pore-forming peptides selected from a rational combinatorial library: mechanism of pore formation in lipid vesicles and activity in biological membranes. Biochemistry 46, 12124–12139.

46 Krauson AJ, He J & Wimley WC (2012) Gain-of-function analogues of the pore-forming peptide melittin selected by orthogonal high-throughput screening. J Am Chem Soc 134, 12732–12741.

47 Wimley WC, Selsted ME & White SH (1994) Interactions between human defensins and lipid bilayers: evidence for formation of multimeric pores. Protein Sci 3, 1362–1373.

48 Young JD, Peterson CG, Venge P & Cohn ZA (1986) Mechanism of membrane damage mediated by human eosinophil cationic protein. Nature 321, 613–616.

49 Torrent M, Odorizzi F, Nogues MV & Boix E (2010) Eosinophil cationic protein aggregation: identification of an N-terminus amyloid prone region. Biomacromolecules 11, 1983–1990.

50 Pulido D, Moussaoui M, Nogu_es MV, Torrent M & Boix E (2013) Towards the rational design of antimicrobial proteins: single point mutations can switch on bactericidal and agglutinating activities on the RNase A superfamily lineage. FEBS J 280, 5841–5852.

51 Garc_ıa-Mayoral MF, Moussaoui M, de la Torre BG, Andreu D, Boix E, Nogu_es MV, Rico M, Laurents DV & Bruix M (2010) NMR structural determinants of eosinophil cationic protein binding to membrane and heparin mimetics. Biophys J 98, 2702–2711.

52 Joao HC & Dwek RA (1993) Effects of glycosylation on protein-structure and dynamics in ribonuclease-B and some of its individual glycoforms. Eur J Biochem 218, 239–244.

53 Williams RL, Greene SM & Mcpherson A (1987) The crystal-structure of ribonuclease-B at 2.5-a resolution. J Biol Chem 262, 16020–16031.

54 Wang FFC & Hirs CHW (1977) Influence of heterosaccharides in porcine pancreatic ribonuclease on conformation and stability of protein. J Biol Chem 252, 8358–8364.

55 Carsana A, Furia A, Gallo A, Beintema JJ & Libonati M (1981) Nucleic acid-protein interactions - degradation of double-stranded-Rna by glycosylated ribonucleases. Biochim Biophys Acta 654, 77–85.

56 Joao HC, Scragg IG & Dwek RA (1992) Effects of glycosylation on protein conformation and amide proton-exchange rates in Rnase-B. FEBS Lett 307, 343–346.

57 Rudd PM, Joao HC, Coghill E, Fiten P, Saunders MR, Opdenakker G & Dwek RA (1994) Glycoforms modify the dynamic stability and functional-activity of an enzyme. Biochemistry 33, 17–22.

58 Puett D (1973) Conformational studies on a glycosylated bovine pancreatic ribonuclease. J Biol Chem 248, 3566–3572.

59 Kim BM, Kim H, Raines RT & Lee Y (2004) Glycosylation of onconase increases its conformational stability and toxicity for cancer cells. Biochem Biophys Res Commun 315, 976–983.

60 Helenius A & Aebi M (2001) Intracellular functions of N-linked glycans. Science 291, 2364–2369.

61 Hart GW & Copeland RJ (2010) Glycomics hits the big time. Cell 143, 672–676.

62 Jefferis R (2009) Glycosylation as a strategy to improve antibody-based therapeutics. Nat Rev Drug Discovery 8, 226–234.

63 Sethuraman N & Stadheim TA (2006) Challenges in therapeutic glycoprotein production. Curr Opin Biotechnol 17, 341–346.

64 Wang LX & Lomino JV (2012) Emerging technologies for making glycan-defined glycoproteins. ACS Chem Biol 7, 110–122.

65 Peterson CG, Jornvall H & Venge P (1988) Purification and characterization of eosinophil cationic protein from normal human eosinophils. Eur J Haematol 40, 415–423.

66 Peterson CG, Eklund E, Taha Y, Raab Y & Carlson M (2002) A new method for the quantification of neutrophil and eosinophil cationic proteins in feces:

establishment of normal levels and clinical application in patients with inflammatory bowel disease. Am J Gastroenterol 97, 1755–1762.

67 Carreras E, Boix E, Rosenberg HF, Cuchillo CM & Nogues MV (2003) Both aromatic and cationic residues contribute to the membrane-lytic and bactericidal activity of eosinophil cationic protein. Biochemistry 42, 6636–6644.

68 Torrent M, S_anchez D, Buzon_ V, Nogu_es MV, Cladera J & Boix E (2009) Comparison of the membrane interaction mechanism of two antimicrobial RNases: RNase 3/ECP and RNase 7. Biochim Biophys Acta 1788, 1116–1125.

69 Pulido D, Torrent M, Andreu D, Nogues MV & Boix E (2013) Two human host defense ribonucleases against mycobacteria, the eosinophil cationic protein (RNase 3) and RNase 7. Antimicrob Agents Chemother 57, 3797–3805.

70 Torrent M, Navarro S, Moussaoui M, Nogues MV & Boix E (2008) Eosinophil cationic protein high-affinity binding to bacteria-wall lipopolysaccharides and peptidoglycans. Biochemistry 47, 3544–3555.

molecular microbiology

Human secretory RNases as multifaceted antimicrobial proteins. Exploring RNase 3 and RNase 7 mechanism of action against Candida albicans.

Journal:	*Molecular Microbiology*
Manuscript ID:	Draft
Manuscript Type:	Research Article
Date Submitted by the Author:	n/a

Complete List of Authors:	Salazar, Vivian; Universitat Autònoma de Barcelona, Biochemistry and Molecular Biology Arranz-Trullen, Javier; Universitat Autònoma de Barcelona, Biochemistry and Molecular Biology Navarro, Susanna; Universitat Autonoma de Barcelona, Institut de Biotecnologia i Biomedicina; Universitat Autònoma de Barcelona, Biochemistry and Molecular Biology Blanco, Jose; Universitat Autònoma de Barcelona, Biochemistry and Molecular Biology Sanchez, Daniel; Universitat Autònoma de Barcelona, Biochemistry and Molecular Biology Nogués, Victoria; Universitat Autònoma de Barcelona, Biochemistry and Molecular Biology Moussaoui, Mohammed; Universitat Autònoma de Barcelona, Biochemistry and Molecular Biology Boix, Ester; Universitat Autònoma de Barcelona, Biochemistry and Molecular Biology

Key Words:	infectious diseases, innate immunity, cytotoxicity, host-pathogen interactions

TITLE PAGE

Human secretory RNases as multifaceted antimicrobial proteins. Exploring RNase 3 and RNase 7 mechanism of action against *Candida albicans*.

Vivian A. Salazar[1]; Javier Arranz-Trullen[1]; Susanna Navarro[1,2]; Jose A. Blanco[1]; Daniel Sánchez[1]; M.Victòria Nogués[1]; Mohammed Moussaoui[1]; and Ester Boix[1]

[1] From the Department of Biochemistry and Molecular Biology, Faculty of Biosciences, Universitat Autònoma de Barcelona, E-08193 Cerdanyola del Vallès, Spain and [2]Institut de Biotecnologia i Biomedicina, Universitat Autònoma de Barcelona, E-08193 Cerdanyola del Vallès, Spain

Address correspondence to: Ester Boix, Department of Biochemistry and Molecular Biology, Biosciences Faculty, Universitat Autònoma de Barcelona, 08193 Cerdanyola del Vallès, Spain; +34-93-5814147; Fax: +34-93-5811264; E –mail: Ester.Boix@uab.cat

Running title: *Antifungal activity of human RNases*

Keywords: infectious diseases, innate immunity, cytotoxicity, host-pathogen interactions

SUMMARY

Human antimicrobial RNases, belonging to the vertebrate RNase A superfamily and secreted upon infection by innate cells, display a wide spectrum of antipathogen activities. In this work we have studied the antifungal activity of the eosinophil RNase 3 and the skin derived RNase 7. *Candida albicans* was chosen as a reference eukaryote pathogen model. By applying a wide range of methodologies and assaying defective point mutants, that ablate either the protein cell binding or its catalytic activity, we were able to explore the distinct levels of action on yeast cells. Results highlighted the multifaceted mechanism of action of both host defence RNases. Together with an overall unspecific membrane destabilization process, the RNases are able to internalize and target the cellular RNA at sublethal concentrations. The data would support the putative contribution of the enzymatic activity in the antipathogen action of both antimicrobial proteins. Moreover, we also evaluate here for the first time the antifungal activity of RNase 3, which can be envisaged as a suitable template for the development of alternative antifungal drugs. We suggest that both human RNases work as multitask antimicrobial proteins providing a first line immune barrier.

INTRODUCTION

Fungal infections are a threat to hospitalized and immunocompromised patients. *Candida albicans* is a major common fungal pathogen in humans that colonizes the skin and mucosal surfaces of most healthy individuals. Together with superficial infections, like oral or vaginal candidiasis, life-threatening systemic infection eventually occur (Mayer *et al.*, 2013). *Candida albicans* is the causative agent of most candidiasis; although other emerging species, as *C. glabrata* and *C. krusei*, are also not negligible threats to patient populations. *Candida* infections have increased dramatically over the last two decades. Considering the increment in *Candida* pathogenesis, mostly in inmunocompromised patients but also in healthy individuals, active research is focused in new therapies and treatments. Several factors and activities have been identified which contribute to the pathogenic potential of this fungus. As first consideration, *Candida albicans* displays a complex cell wall organization that plays a role in maintaining structural integrity and mediating adherence. Its specific composition, with a carbohydrates predominance (Chitin, β-1,3 glucan and β-1,6 glucan) offers resistance to host molecules defence and impermeability to most potential antifungal drugs (Mayer *et al.*, 2013)
(Molero *et al.*, 1998).

Knowledge of pathogenicity mechanisms, from cell wall complexity to the adhesion and host cell invasion mechanism (Chaffin, 2008), is crucial towards the rational design of novel antifungal drugs (Mayer *et al.*, 2013)(Molero *et al.*, 1998). Antimicrobial peptides (AMPs), and in particular the secreted peptides at the human skin first natural barrier against infections, are regarded as appealing candidates for applied antifungal therapy (den Hertog *et al.*, 2005)(Vylkova *et al.*, 2007)(Andrès, 2012). Indeed, AMPs offer a chemical defense system that protects the skin from potential pathogenic microorganisms threatening to colonize the host tissues(Bardan *et al.*, 2004)(Gläser *et al.*, 2005)(Harder *et al.*, 2002). Among skin AMPs, we find peptides with reported antifungal activity, as cathelicidins (López-García *et al.*, 2005) and defensins (De Smet and Contreras, 2005)*;* both rapidly released at high local concentrations when needed in response to infection or epidermal injury (Dorschner *et al.*, 2001)(Sørensen *et al.*, 2006)(Niyonsaba and Ogawa, 2005). Besides, the constant level of some constitutively produced antimicrobial peptides and proteins at skin surfaces, suggests that these AMPs have been optimized during evolution to protect the skin surface from infection (Schröder and Harder, 2006). In particular, human RNase 7 is one of the main constitutive product released by keratinocytes (Schröder and Harder, 2006), with not only well documented bactericidal activity (Harder *et al.*, 2002)(Torrent, Badia, *et al.*, 2010)(Pulido, Torrent, *et al.*, 2013), but also ability to inhibit the growth of dermatophytes (Fritz *et al.*, 2012).

Interestingly, RNase 7 is a member of the RNase A superfamily (Fig.1), which includes other secretory RNases with antimicrobial properties (Boix and Nogués, 2007); a protein family

suggested to have emerged with an ancestral host defense role (Rosenberg, 2008)(Pizzo and D'Alessio, 2007). Antimicrobial RNases are expressed by epithelial tissues and blood cell types and their expression can be induced by inflammatory agents and bacterial infection (Boix and Nogués, 2007)(Spencer *et al.*, 2013)(Becknell *et al.*, 2014)(Gupta *et al.*, 2012). In particular, RNase 3 and RNase 7 are the main representative members showing a high bactericidal activity (Torrent, Badia, *et al.*, 2010)(Pulido, Torrent, *et al.*, 2013)(Torrent *et al.*, 2012). RNase 7 is expressed in skin-derived stratum, gut and the respiratory and genitourinary tracts, and is particularly active against Gram negative strains as *Enterococcus faecium*, *Pseudomonas aeruginosa* and *Escherichia coli* (Torrent, Odorizzi, *et al.*, 2010)(Harder *et al.*, 2002)(Huang *et al.*, 2007).

The other main antimicrobial RNase within the RNase A superfamily (Fig.1), the RNase 3, also called the Eosinophil Cationic Protein (ECP), is involved in inflammatory processes mediated by eosinophils and is released by secondary granules upon infection (Acharya and Ackerman, 2014). A high antimicrobial activity has been reported for RNase 3 against both Gram negative *Escherichia coli*, *Acinetobacter baumannii*, *Pseudomonas sp.* (Torrent, Pulido, *et al.*, 2011) and Gram positive species *Staphylococcus aureus, Micrococcus luteus and Enterococcus faecium*, (Torrent, Pulido, *et al.*, 2011) and *Mycobacteria* (Pulido, Torrent, *et al.*, 2013).

In this work we committed ourselves to explore the antifungal properties of both RNase 3 and 7. *C. albicans* was chosen as an eukaryote pathogen model, which has proven most appropriate as a first approach to understand the distinct levels of action of antimicrobial RNases. Complementary, site directed single mutants were designed to ablate either the protein active site or the key anchoring region for cell membrane binding.

RESULTS

Human RNases against Candida albicans

RNase 3 and RNase 7 antifungal mechanism of action on *Candida albicans* was characterized by applying a variety of methodological approaches. The protein toxicity on yeast cells was first analyzed by registering the colony forming unit (CFU) reduction as a function of protein concentration. Both RNases showed an effective protein concentration in the low micromolar range (Table 1), achieving Minimal Fungicidal Concentrations (MFC_{100}) around 3 to 4 μM, with slight better results for RNase 7. Calculated antifungal activity was comparable to the previously reported bactericidal activity for the tested Gram negative and Gram positive species (Torrent *et al.*, 2012). The antifungal activity was also assessed by a cell viability assay based on ATP levels quantification. Following, percentage of cell survival was estimated at final

incubation time by the Live/Dead® assay kit, where the number of live and dead cells is estimated using the cell nonperrmeant and permeant nucleic acids dyes respectively (Table 1). Next, the proteins action at the cell plasma membrane was evaluated by assessing their ability to trigger the cell membrane permeation, where the release of the cellular content was monitored by using a membrane impermeable dye (Table 2). Again, RNase 7 showed a better performance, requiring less concentration for effective cell leakage. Also, the proteins depolarization activities were compared using a fluorescent probe, indicating a higher activity for RNase 7. Registered maximum membrane depolarization and permeation activities were also compared at final incubation time (Table 2). Complementary, the activity profile as a function of time was recorded and the respective time to achieve 50 % of membrane depolarization and permeation activities were compared (Table 3).

Following, the protein toxicity on the yeast cell population was visualized by confocal microscopy using the Live/Dead® staining kit. We observed a gradual increase of dead cells during the incubation time course. Kinetic of time course reduction of cell survival percentage was followed for up to 180 min (Fig. S1). Next we labeled the recombinant proteins with fluorescent marker and tracked the protein location in cell cultures, where cell nuclei were stained with Hoechst (Fig. 2). Protein location was registered by tracking the fluorescent signal distribution, where an increase of the Alexa Fluor fluorescence colocalized with the Hoechst signal intracellular compartment (Fig. 3). The protein internalization process was also visualized at sublethal concentrations and short incubation times, after removal of any remaining free protein (Fig. 4).

A dual mode for RNases antifungal activity

Mechanism of action against *Candida albicans* was then analyzed by ablating either the protein enzymatic activity or cell binding ability. To assess the potential contribution of the RNases catalytic activity on their antimicrobial action we prepared mutant variants of both RNases with defective active sites. Active site mutants were designed by substitution of His 15 at the active site catalytic triad (Huang *et al.*, 2007)(Boix *et al.*, 1999), where His 15 is the counterpart of His 12 in RNase A (Fig. 1), working as a base catalyst in RNA cleavage (Cuchillo *et al.*, 2011). Histidine for alanine substitution mostly abolished the protein enzymatic activity for both RNases. Comparative catalytic activity values by a spectrophotometric assay using oligocytidylic acid as a substrate (Table 4) confirmed close to total removal of both RNases catalytic activity. Also, maintenance of the protein overall three dimensional structure and active site architecture was confirmed by solving the RNase 3- H15A mutant X-ray crystal structure (PDB ID: 4OWZ) (Fig.1 and Table S1). Functional characterization of both RNases active site mutants confirmed that the proteins conserved their membrane lytic activity, showing equivalent leakage activity on ANTS/DPX containing lipid vesicles (Table 4). Besides, the

potential contribution of the H15 positive net charge on the protein membrane association was discarded, being the residue not exposed to the protein surface, as confirmed by calculating the solvent accessible surface area using the *Areaimol* software utility from the CCP4 integrate Program package (The CCP4 suite: programs for protein crystallography., 1994) (SASA for His 15 ~ 14Å; 4A2Y.pdb (Boix, Pulido, *et al.*, 2012)). Therefore the chosen active site mutants proved to serve as adequate catalytic defective forms.

Following we compared the recombinant variants with ablated active sites with the wild type proteins in yeast cell cultures (Table 1). Interestingly, a significant decrease in their respective fungicidal action was observed. Also, an increase in the percentage of viable cells was registered for both H15A mutants (Table 1). Differences between wild type and active site mutants' cytotoxicity were mostly patent at sublethal concentrations (see Table 2 and Table 3). Time course kinetic of yeast cell viability indicated that catalytically defective proteins showed a significant delay in their t_{50} values together with a lower rate of cell killing (Table 3). On the other hand, comparison of the depolarization time course profile revealed no significant differences between the samples (Table 3). Similar t_{50} values indicated that the active site mutation did not interfere with the protein access to the cellular membrane. Indeed, no difference in the protein binding to the yeast cells was observed for the H15A variant as quantified by fluorescence assisted cell sorting (FACS) assay (Fig. 5), and visualized by confocal microscopy (Figs. 2 and 4). On the other hand, the FACS methodology combined with the propidium iodide (PI) staining assay provided us useful tools to quantify simultaneously the protein- cell interaction process and the cell population survival rates (Fig. 5 and Fig. S2). We observed how RNase H15A mutants displayed an increase in the survival rates, mostly significant at long incubation times.

Finally, the RNases potential effect on the yeast intracellular RNA was assessed. Total cellular RNA was extracted from treated cultures and analyzed by capillary electrophoresis (Fig. 6A). The corresponding time course decrease in rRNA subunits was also evaluated by densitometry as a function of time (Fig. 6B). Results confirmed the drastic reduction of the cellular RNA degradation rate for the active site mutants. All assays were carried out at sublethal concentrations and at short incubation times. By a time course monitoring of the cell culture population by optical density at 600 nm and CFUs counting, we confirmed that no reduction on the cell viability was significant at the assayed conditions. Cell viability was also followed by quantification of ATP levels, observing no reduction during the first 15 min an even a slight increase in ATP concentration (Fig. S3) at the very beginning of the incubation time, a fact that might be attributed to a blockage of the cell protein synthesis machinery, which could be induced by the RNase binding to cellular nucleic acids.

Additionally, an RNase 3 mutant defective at the protein membrane interaction (W35A) was assayed to analyze the protein action at the fungal cell surface. Previous work using both

synthetic membrane models and bacteria cells already indicated that the W35 is key for the protein interaction and membrane disruption activities in bacteria (Pulido, Torrent, *et al.*, 2013)(Torrent *et al.*, 2007)(Carreras *et al.*, 2003), while not interfering in the enzyme catalytic activity (Carreras *et al.*, 2003). Residue 35 is an unusual highly solvent exposed Trp (Torrent *et al.*, 2007) and no changes in the overall structural conformation were observed for the Ala substitution variant (Nikolovski *et al.*, 2006). Extensive work using lipid vesicles enabled the characterization of the protein membrane binding, partial insertion into the lipid bilayer and subsequent membrane lysis by a carpet-like mechanism (Torrent *et al.*, 2007)(Torrent *et al.*, 2009). Also, Trp35 was found directly involved in the protein toxicity on a tumor cell line (Carreras *et al.*, 2005) and to contribute to RNase 3 anchoring to heterosaccharides, as heparin derivates (Fan *et al.*, 2008) (García-Mayoral *et al.*, 2013). The present results confirm the key role of surface exposed Trp (Fig.1B) in the protein toxicity to yeast cells. The W35A mutant displays a two-three fold reduction in its fungicidal (Table 1) and membrane destabilizing (Table 2) activities. Mostly, the RNase 3 membrane depolarization and disruption abilities are severely impaired (Table 2). Indeed, by confocal microscopy we can visualize how the labeled W35A mutant does not associate to the cell surface (Figs. 2 and 4). Also, the mutant is not internalized into the yeast cells, as revealed by the fluorescence profile of culture cells stained with Hoechst and treated with Alexa labeled proteins (Fig. 3). The RNase 3-W35A mutant definitely remains outside the cells, and no protein signal is registered at the intracellular compartment. Also, no significant rate of intracellular RNA cleavage corroborates the protein defective internalization mechanism (Fig. 6).

Therefore, the combined time course analysis of wild type RNases with their protein variants, defective at either the active site or the cell binding region, revealed the contribution of distinct processes that target the yeast cells, as discussed below.

DISCUSSION

There is an urgent need to develop alternative antibiotics. Exploring the mechanism of action of our own self defense machinery is a promising strategy towards the design of new drugs. Human antimicrobial RNases, secreted upon infection and displaying a variety of cytotoxic activities, provide a suitable working model. In particular, several members of the vertebrate RNase A family were previously reported to display toxicity against fungal pathogens, as RNase 5 (Hooper *et al.*, 2003), RNase 7 (Harder *et al.*, 2002) (Huang *et al.*, 2007) or RNase 8 (Rudolph *et al.*, 2006).

Here we have chosen two main human antimicrobial RNases, RNase 3 and RNase 7, expressed by eosinophils and keratinocytes, two cellular types involved in innate immunity, and directly implicated in the host defense against fungal infections (Rosenberg *et al.*, 2013)(Rothenberg

and Hogan, 2006). Increase in both the eosinophil RNase 3 and the skin derived RNase 7 expression has already been reported in infection processes (Becknell *et al.*, 2014)(Boix, Salazar, *et al.*, 2012)(Glaser *et al.*, 2009)(Mohammed *et al.*, 2011). We have analyzed in previous works both RNases bactericidal activity, identifying their mechanism of action at the bacteria envelope (Torrent, Badia, *et al.*, 2010)(Pulido, Torrent, *et al.*, 2013)(Torrent *et al.*, 2012)(Torrent *et al.*, 2007). *Candida albicans* was chosen here as a simple eukaryote pathogen, providing a suitable model to analyze the distinct protein targets at the cellular level. High fungicidal activities are achieved for both RNases at the low micromolar scale (Table 1). Moreover, the present results highlight the proteins dual mode of action. Indeed, antimicrobial RNases would represent an interesting example of a multifunctional protein, combining an enzymatic activity with a mechanical action at membrane level.

Therefore we can regard the studied RNases as multifaceted AMPs, where the unspecific lytic action at the pathogen cell surface is combined with a selective catalytic activity towards the intracellular ribonucleic acids. Similar examples of multitargeted antimicrobial proteins are available in the literature, where a specific enzymatic activity tackles one of the main cellular functions, as DNases or proteases (Peschel and Sahl, 2006)(Hancock and Sahl, 2006)(Nicolas, 2009). Complementary, the enzymatic cleavage of the peptidoglycan glycosydic bond is observed together with lysozyme membrane lytic action (Düring *et al.*, 1999). Likewise, many AMPs combine a bactericidal action with a variety of immunomodulating properties (Haney and Hancock, 2013). However, methodological limitations and disparity of experimental conditions have mostly delayed the understanding of AMPs mechanism (Stalmans *et al.*, 2013). In particular, an accurate monitoring of the effective working concentrations and the assay timing is required for proper results interpretation (Nicolas, 2009)(Spindler *et al.*, 2011). As an example, some AMPs proposed roles, such as immunomodulation, are only observed when working below the cytotoxic concentration threshold (Haney and Hancock, 2013). Likewise, the protein intracellular action can only be visualized at sublethal assay conditions (Holm *et al.*, 2005).

In this context, the results presented here highlight once again the key contribution of the chosen working conditions. RNases internalization into yeast cells was visualized here by confocal microscopy. Results indicated that the fluorescent labeled protein is associated to the yeast cells already after two minutes of incubation and is subsequently internalized (Figs. 2-4). Complementary, by tracking the cell population by a cell sorting assay combined with staining of membrane compromised cells, we confirmed that in the assayed conditions no significant cell death is registered (Fig. 5 and Fig. S2). Timing of events illustrated how the cell membrane leakage is delayed respect to the first membrane depolarization event, following protein cell binding. Membrane destabilization and cell leakage were also achieved when increasing the protein concentration above the threshold value. Therefore, a combined dual mode strategy is

proposed for the antimicrobial RNases mechanism of action on the studied eukaryote pathogen. Notwithstanding, the present results may apparently seem contradictory in light of some previously reported data. However, we must bear in mind that most RNase 3 studies were carried out in bacteria cells and at higher protein concentration. This would explain why the eosinophil protein toxicity was mainly attributed to a cell lysis action (Torrent *et al.*, 2007)(Carreras *et al.*, 2003)(Singh and Batra, 2011). Also, the protein cytotoxicity not dependant on its enzymatic activity does not discard other complementary intracellular processes, such as nucleic acid binding and subsequent inhibition of the cell protein translation machinery. Indeed, previous report on RNase 7 bactericidal activity already suggested the putative protein internalization and interaction with cellular nucleic acids (Lin *et al.*, 2010). Also, the observed differences in RNases action at membrane level (Torrent, Badia, *et al.*, 2010)(Young *et al.*, 1986)(Salazar *et al.*, 2014) could explain the divergence in the results interpretation. In other words, a local membrane disturbance can induce either transient pore formation or end up in a massive cell lysis by a carpet –like mechanism. In this line, the RNase 3 promoted aggregation at membrane level, when the protein concentration reaches a critical threshold, would trigger the pathogen cell agglutination and subsequent cell lysis (Torrent, Badia, *et al.*, 2010) (Torrent *et al.*, 2012). Likewise, the recently observed significant differences between the mechanism of action of the native glycosylated and the nonglycosylated recombinant protein (Salazar *et al.*, 2014) can also explain the disparity of earlier reports on the protein mechanism on lipid bilayers (Torrent *et al.*, 2007)(Carreras *et al.*, 2003)(Young *et al.*, 1986). Apparently contradictory reports on the eosinophil RNase on mammalian cell lines could also be attributed to experimental conditions (Maeda *et al.*, 2002)(Navarro *et al.*, 2008)(Navarro *et al.*, 2010).

In a wider context, controversy on the contribution of the RNase catalytic activity on the protein cytotoxicity remains unsolved within the RNase A superfamily. We find examples where the antimicrobial activity of family members, as RNase 5 and RNase 7, are inhibited by either diethyl pyrocarbonate (DEPC) treatment or by the proteinaceous RNase inhibitor (RI) (Abtin *et al.*, 2009). However, experiments using RI should be interpreted with caution, considering the horseshoe-like shape of the inhibitor structure and its RNase binding mode, engulfing the protein inside its internal cavity. We cannot discard that the RI inhibitor may block the RNase antimicrobial activity merely by covering the cationic surface exposed residues. Similarly, the DEPC treatment would modify not only the catalytic His but other protein surface exposed His residues. Indeed, both RNase 3 and RNase 7 were found to be dependent on cationic surface exposed patches (Huang *et al.*, 2007)(Carreras *et al.*, 2003). Interestingly, cationic RNases may work as other cationic AMPs by strongly associating to the cellular nucleic acids (Nicolas, 2009)(Brogden, 2005) thereby blocking the protein expression process, as suggested for RNase 7 by Lin and co-workers (Lin *et al.*, 2010).

In any case, our results confirm not only both RNase 3 and 7 internalization in yeast cells (Figs. 3 and 4) but also the contribution of the enzymatic activity in the final cell killing process, as revealed by the characterization of mutant variants devoid of catalytic activity. Site directed mutagenesis at one of the two catalytic His residue provided direct evidence of the involvement of the RNase activity in the protein cytotoxic mechanism. His 15 to ala mutant was selected as the most effective way to ablate the protein catalytic activity. Kinetic characterization of mutant variants confirmed the drastic reduction of RNase activity, as previously reported by Raines and coworkers for RNase A H12A mutant counterpart (Park *et al.*, 2001). Both RNases H15A variants showed an impaired catalytic activity, while retaining their desestabilization action on lipid bilayers (Table 4). Besides, both RNase 3 and 7 active site mutants retained their cell binding and internalization ability (Figs. 2-5). On the contrary, reduction of their fungicidal activity was significant (Table 1) and cellular RNA degradation rates were mostly reduced for active site mutants (Fig. 6).

Complementary, contribution of the protein association to the cell surface was also assessed by site- directed mutagenesis. RNase 3 mutant W35A allowed the direct assessment of the impaired protein at the main cell binding region. Trp 35 lies at the protein 33-38 patch reported to be involved in membrane interaction, lipopolysaccharides at Gram negative outer membrane (Torrent, Nogués, *et al.*, 2011)(García-Mayoral *et al.*, 2010) and heterosaccharide binding in general (Boix, Salazar, *et al.*, 2012)(Lien *et al.*, 2013). Recently, this region has been used as a cell penetrating peptide (CPP) and proposed to serve as a vehicle for drug delivery (Fang *et al.*, 2013). Previous work on W35A variant already confirmed that the exposed Trp is not required for the catalytic activity, but is essential for the membrane lysis (Torrent *et al.*, 2007), (Carreras *et al.*, 2003). Also, Trp was reported directly involved in RNase 3 recognition of LPS (Fan *et al.*, 2008)(Pulido, Moussaoui, *et al.*, 2013) and glycosaminoglycans' binding (García-Mayoral *et al.*, 2013). We can hypothesize that this residue may also contribute to the protein association to *Candida* cell wall predominant glucan components. Indeed, common binding motives are found for beta glucan pattern recognition proteins and other carbohydrate binding proteins, as LPS and heparan sulphate. In particular, a shared binding motif for LPS and 1,3 beta glucans would participate in invertebrate innate immunity (Iwanaga and Lee, 2005).

Our studies on *Candida* highlighted the requirement of Trp residue for the protein internalization, where labeled W35A remains outside the cells (Figs. 2-4) and no significant cellular RNA degradation is visualized (Fig. 6). Moreover, the results confirmed that the W35 mutant displayed significantly impaired membrane depolarization and permeation activities (Table 2), as previously reported for bacteria cells and synthetic lipid vesicles (Carreras *et al.*, 2003)(Torrent *et al.*, 2007).

Interestingly, a high membrane binding affinity and tendency for cell entrance is achieved by other vertebrate RNases members (Chao and Raines, 2011)(Benito *et al.*, 2008)(Haigis and

Raines, 2003)(Sundlass *et al.*, 2013). In particular, the interaction of RNases cationic domains with exposed anionic components at the extracellular matrix would mediate an unspecific cell entrance (Haigis and Raines, 2003)(Ribo *et al.*, 2011). Also, the high RNase 3 affinity for heparan sulfate was related to cell internalization and toxicity for eukaryote cells (Fan *et al.*, 2007), where a specific sugar binding tag sequence would promote the protein intracellular translocation (Fang *et al.*, 2013). The antimicrobial RNases might also be regarded as "cell penetrating proteins", as was proposed for RNase A by analyzing its internalization process into human cell lines (Chao and Raines, 2011). Indeed, secretory RNases intracellular routing and access to nucleic acids could have key physiological roles, that can be regulated by the presence of the abundant ribonuclease inhibitor (RI) ubiquous in mammalian cells (Lomax *et al.*, 2014). As an example, cellular trafficking and ribonucleolytic activity of human RNase 5 are essential for its angiogenic action (Thiyagarajan *et al.*, 2012).

Understanding the determinants that can assist protein translocation without inducing any cell damage is desired for the design of alternative targeted drugs. Indeed, many cationic and amphipathic AMPs that are easily structured in lipid bilayers can be classified as Cell Penetrating Peptides (CPP) (Nicolas, 2009)(Stalmans *et al.*, 2013)(Brogden, 2005). However, most CPP behavior has been analyzed towards mammalian cells (Last *et al.*, 2013) but few peptides have been described against putative eukaryote pathogens (Do *et al.*, 2014). Notwithstanding, the study of CPP in yeast is an emerging field offering promising biotechnological applications (Holm *et al.*, 2005)(Nekhotiaeva *et al.*, 2004)(Mochon and Liu, 2008)(Marchione *et al.*, 2014).

In conclusion, the observed antimicrobial effective doses for both RNases in the low micromolar range are promising in the design of antifungal agents. In particular, a high antifungal activity is found for RNase 7, which might be related to its putative function as a skin protector against infections. Secretory cytotoxic proteins from blood and epithelial cells would work as first line sentinels for the organism safeguard. Human secretory RNases, combining membrane lytic and enzymatic RNase activities could work as protectors of epithelium surfaces. In a wider context, the vertebrate secreted RNases would contribute to the protection of a variety of body fluids, from seminal to placental fluids, tears or even milk (D'Alessio *et al.*, 1991)(Leonardi *et al.*, 1995)(Harris *et al.*, 2010). Indeed, an unspecific cellular RNA degradation would represent one of the quickest, unspecific and more effective ways to target the cell viability. Also, we can speculate that secreted RNases may exert a direct host defense role by the removal of pathogenic RNA both within infected cells and resident at the extracellular matrix (Gupta *et al.*, 2012). Therefore, human RNases as innate immunity effectors are providing an ideal system for the design of non antigenic nanodelivery tools to fight invading pathogens. AMPs offer us the opportunity to find new antifungal agents, as still few

374 effective antifungal peptides are currently available (Swidergall and Ernst, 2014)(Tsai *et al.*,
375 2014). The studied human antimicrobial RNases provide thus a promising model towards the
376 design of new applied therapies against fungal infections.

EXPERIMENTAL PROCEDURES

Protein expression and purification

Recombinant RNase 3 and RNase 7 were expressed in *E. coli* BL21 (DE3) using the pET11c plasmid vector as previously described (Torrent *et al.*, 2009). Protein expression, solubilization from inclusion bodies, refolding and purification steps were carried out as described (Boix *et al.*, 1999). RNase 3-H15A, RNase 3-W35A and RNase 7-H15A variants were constructed using the Quick Change Site-Directed Mutagenesis kit (Stratagene, La Jolla, CA). All constructs were confirmed by DNA sequencing and the purified protein was analyzed by MALDI-TOF MS and N-terminal sequencing.

Crystal structure determination

RNase 3-H15A mutant was crystallized following the conditions for wild type RNase 3 modified from (Mallorquí-Fernández *et al.*, 2000). An additional reverse phase chromatography was applied as previously described before protein crystallization (Boix, Pulido, *et al.*, 2012). Protein sample was lyophilised and resuspended at 12 mg/mL in 20 mM sodium cacodylate pH 5.0 and equilibrated against 7% Jeffamine™ M-600, 0.1 M Na citrate, pH 5.2, 10mM $FeCl_3$. One microlitre of the sample was mixed with an equal volume of the reservoir solution and set to incubation at 20 °C. After 5 to 10 days, crystals appeared and were soaked using 30% methyl pentanediol (MPD) as cryofreezing agent. Data were captured at 100K using a λ_{XRD} = 0.9795 Å at the BL13(XALOC) beamline of the ALBA Synchrotron Light Facility (Spain). XDS (Kabsch, 2010) was used for data processing, scaling was performed with SCALA and molecular replacement with PHASER (McCoy et al., 2007) using the RNase 7 NMR structure (PDB coordinate file 2HKY (Huang et al., 2007)) as a model. Iterative cycles of refinement and manual structure fitting were performed with PHENIX (Adams et al., 2010) and COOT (Emsley and Cowtan, 2004) until R_{free} could not be further improved (Brunger, 1992). Finally, the stereochemistry of the structure was validated with SFCHECK (Vaguine et al., 1999). Table S1 shows all the data collection and structure refinement statistics.

Enzymatic activity analysis

To measure the RNases enzymatic activity of RNases 3 and 7 and the respective active site mutants the degradation of an oligocytidylic acid was continuously monitored by following the 286 nm absorption in a Cary Eclipse spectrophotometer. $(Cp)_4C>p$ acids, purified from poly(C), were used as a substrate, as previously described (Boix *et al.*, 1999). Assay conditions were 1 μM protein, 84 μM oligocytidylic acid in 0.2 M NaAcO, pH 5.0, incubation for 3 min at 25ºC. Alternatively, a zymogram analysis was performed using a 15% SDS-PAGE gel containing

polyuridylic acid, poly(U), as a substrate according to the method previously described (Bravo *et al.*, 1994).

Model membrane leakage activity

Membrane leakage activity was assessed by ANTS/DPX (8-aminonaphthalene-1,3,6-trisulfonic acid disodium salt/p-xylenebispyridinium bromide) as previously (Torrent *et al.*, 2007). Large unilamellar vesicles of dioleoyl-phosphatidyl choline: dioleoyl-phosphatidyl glycerol (3:2 molar ratio), containing 12.5 mM ANTS and 45 mM DPX in 20 mM NaCl, 10 mM Tris/HCl, pH 7.5, were diluted to 30 μM and incubated at 25 ºC with the proteins for 45 min. Leakage was monitored as the increase in fluorescence ($\lambda_{excitation}$= 386 nm; $\lambda_{emission}$= 535 nm).

Fluorescent labeling of RNases

RNase 3, RNase 3-H15A, RNase 3-W35A, RNase 7-H15A and RNase 7 were labeled with Alexa Fluor 488 Labeling kit (Molecular Probes, Invitrogen, Carlsbad, CA), following the manufacturer´s instruction as previously described (Torrent, Badia, *et al.*, 2010). To 0.5 mL of 2 mg/mL protein solution in phosphate saline buffer (PBS), 50 μl of 1M sodium bicarbonate, pH 8.3, was added. The protein was incubated for 1h at room temperature with the reactive dye, with stirring, and the labeled protein was separated from the free dye by PD-10 desalting column.

Candida albicans *growth conditions*

C. albicans (ATCC 90028) cells were maintained at -70ºC and incubated overnight with agitation at 37ºC in Sabouraud Dextrose broth (mycological peptone, glucose, pH 5.6) Fluka-Sigma S3306). Previous to each assay, cells were subcultured for ~ 2-3 h to yield a mid-logarithmic culture.

Minimum fungicidal concentration

C. albicans ATCC 90028 was culture overnight in Sabouraud Dextrose broth at 37ºC and subculture the next day in fresh Sabouraud and grow to an optical density of 0.4 at 600 nm (mid log-phase). Cells were washed twice with 10 mM sodium phosphate buffer, pH 7.5, and diluted to OD_{600}= 0.2 (~2 x 10^6 cells/ mL). Proteins serially diluted from 10 to 0.1 μM were added to 2 x 10^5 cells. *C. albicans* was incubated at 37ºC during 4 h with each protein solution, the samples were plated onto Sabouraud Petri dishes and incubated at 37 ºC overnight. Antifungal activity was expressed as the MFC, defined as the lowest protein concentration required for more than 99% of microorganism killing. MFC of each protein was determined from two independent experiments performed in triplicate for each concentration.

Cell viability assay

Antimicrobial activity was also assayed by following the cell viability of *C. albicans*, using the BacTiter-Glo™ Microbial Cell Viability kit (Promega), which measures the number of viable fungal cells, by ATP quantification. ATP, as an indicator of metabolically active cells, is indirectly measured by a coupled luminescence detection assay. The luminescent signal is proportional to the amount of ATP, required for the conversion of luciferin into oxyluciferin, in the presence of luciferase.

An overnight culture of *C.albicans* was used to inoculate fresh Sabouraud liquid culture, and logarithmic phase culture was grown to an OD_{600} of 0.2. RNase 3, RNase 7 and mutants were added to 0.1 mL of cell culture at a final concentration from 0.025 to 20 µM. The *C. albicans* viability was followed after 4h of incubation at 37 ºC. 50 µl of incubation culture were mixed with 50 µl of BacTiter-Glo™ reagent in a microtiter plate following the manufacturer instructions and incubated at room temperature for 10 min. Luminiscence was read on a Victor3 plate reader (PerkinElmer, Waltham, MA) with a 1-s integration time. IC_{50} values were calculated by fitting the data to a dose-response curve.

Cell survival assay

C.albicans viability assay was performed using the Live⁄Dead® microbial viability kit as previously described (Torrent, *et al.*, 2010). *Candida* strain was grown at 37ºC to OD_{600}=0.4 (~5 x 10^6 cells/mL), centrifuged at 5000xg for 5 min and resuspended in a 0.85% NaCl solution. *C. albicans* cell culture was stained using a SYTO®9/propidium iodide 1:1 mixture. SYTO®9 is a DNA green fluorescent dye that diffuses thorough intact cell membranes and propidium iodide comprises a DNA red fluorescent dye that can only access the nucleic acids of membrane damaged cells, displacing the DNA bound SYTO®9. The method allows the labeling of intact viable cells and membrane compromised cells, which are labeled in green and red respectively, referred to as live and dead cells. The viability kinetics was monitored using a Cary Eclipse Spectrofluorimeter (Varian Inc., Palo Alto, CA, USA). Cell viability profiles were registered after adding from 1 and 5 µM protein. To calculate cell viability, the signal in the range 510–540 nm was integrated to obtain the SYTO®9 signal (live cell) and from 620–650 nm to obtain the propidium iodide signal (dead cell). Then, the percentage of live bacteria was represented as a function of time.

Cell viability by confocal microscopy

The kinetics of *C. albicans* survival was followed by confocal microscopy for 180 min at 37ºC. Experiments were carried out in a plate-coverslide system. Two hundred and fifty microlitres of *C. albicans* OD_{600} = 0.4 (~5 x 10^6 cells/mL) were stained as described below and mixed with 5 µM final protein concentration. *C. albicans* cell cultures were pre-stained using the SYTO®9 /

propidium iodide 1 : 1 mixture provided in the Live /Dead® staining kit (Molecular Probes (Eugene, OR, USA). Confocal images of the yeast culture were captured using a laser scanning confocal microscope (Leica TCS SP2 AOBS equipped with a HCX PL APO 63, x1.4 oil immersion objective; Leica Microsystems, Wetzlar, Germany). SYTO®9 was excited using a 488 nm argon laser (515–540 nm emission collected) and propidium iodide was excited using a diode pumped solid state (DPSS) laser at 561 nm (588– 715 nm emission collected). To record the time-lapse experiment, Life Data Mode software (Leica) was used, obtaining an image every 1 min.

Alternatively, labeled protein distribution in cell cultures was followed by confocal microscopy. 300 µL of *Candida albicans* yeast (~3 x10^6 cell/mL) were incubated with Alexa-labeled proteins at 1 to 5 µM during 1 hour in PBS. Previously, cells were washed with PBS and labeled with Hoescht 33342 at 0.5 µg/mL for 10 min before observation of unfixed cells in Leica TCS SP5 AOBS equipped with a PL APO 63x1.4- 0.6 CS oil immersion objective (Leica Microsystems, Mannheim, Germany). Fluorochromes were excited by 405 nm (Hoechst 33342) and 488 nm (Alexa Fluor 488 nm) and both emissions collected with a HyD detector. Alexa Fluor 488- labeled proteins were added directly to the cultures and time lapse was recorded at intervals of 30 s for 1 h.

Cell plasma membrane depolarization assay

Membrane depolarization was assayed by monitoring the $DiSC_3(5)$ fluorescence intensity change in response to changes in transmembrane potential as described previously (Torrent *et al.*, 2008). *Candida albicans* cells were grown at 37 ºC to the mid-exponential phase and resuspended in 5 mM Hepes-KOH, 20 mM glucose and 100 mM KCl at pH 7.2 until OD_{600} of 0.05 was reached. DiSC3(5) was added to a final concentration of 0.4 µM. Changes in the fluorescence for alteration of the cell plasma membrane potential were continuously monitored at 20 ºC at an excitation wavelength of 620 nm and an emission wavelength of 670 nm. When the dye uptake was maximal, as indicated by a stable reduction in the fluorescence as a result of quenching of the accumulated dye in the membrane interior, protein in 5 mM Hepes-KOH buffer at pH 7.2 was added at a final protein concentration from 1 to 5 µM. All conditions were assayed in duplicate. The time required to reach a stabilized maximum fluorescence reading was recorded for each condition, and the time required to achieve half of total membrane depolarization was estimated from the nonlinear regression curve.

Cell leakage activity

Cell leakage was monitored by using a Sytox® *Green* uptake assay. *Sytox® Green* is a cationic cyanine dye (≈ 900 Da) that is not membrane permeable. When a cell's plasma membrane

integrity is compromised, influx of the dye, and subsequent binding to DNA causes a large increase in fluorescence. For *Sytox® Green* assays, *C. albicans* cells were grown to mid-exponential growth phase at 37ºC and then centrifuged, washed, and resuspended in PBS. Cell suspensions in PBS (OD_{600}=0.2) were incubated with 1 µM *Sytox® Green* for 15 min in the dark prior to the influx assay. At 2 to 4 min after initiating data collection, 1 and 5 µM concentrations of proteins were added to the cell suspension, and the increase in *Sytox® Green* fluorescence was measured (excitation wavelength at 485 nm and emission at 520 nm) for 50 min in a Cary Eclipse spectrofluorimeter. Bacterial cell lysis with 10% Triton X-100 gives the maximum fluorescence reference value.

Fluorescent assisted cell sorting (FACS) assay

Cell population evolution incubated with labeled proteins was followed by cell cytometry. *C. albicans* were grown at 37ºC to mid-exponential phase (OD_{600}= 0.2), centrifuged at 5000 xg for 2 min, resuspended in PBS. 500 µl aliquot of the yeast suspension was incubated with 1 to 5 µM of protein for 60 min. After incubation, 25000 cells were washed three times with PBS buffer and subjected to FACS analysis using a FACSCalibur cytometer (BD Biosciences) and excitation and emission wavelengths of 488 nm and 515–545 nm respectively. Internal fluorescence uptake was evaluated at 2, 5, 15 and 60 minutes in 10,000 cells. Dead cells were stained with PI at a concentration of 10 µg/mL.

Cellular RNA degradation

A *Candida albicans* 1 mL suspension (OD_{600}= 0.6) incubated in PBS with the proteins for 30, 60 and 120 min at 3 µM final concentration. After incubation, cells were sedimented and resuspended in lysis buffer, 10% SDS and Phenol:Chloroform: isoamyl alcohol (IAA) and mixed with zirconia beads. RNA isolation was done using the (Ribopure Yeast kit, Invitrogen) according to manufacturer's instructions. Samples were analyzed in a High Sensitivity nucleic acid microfluidic Chip using an *Experion* Automated electrophoresis system (Bio-Rad, Madrid, Spain). Cellular RNA populations were quantified by virtual gel densitometry.

ACKNOWLEDGMENTS

Spectrofluorescence assays were performed at the *Laboratori d'Anàlisi i Fotodocumentació*, Universitat Autònoma de Barcelona. The work was supported by the *Ministerio de Economía y Competitividad* (BFU2012-38965), co-financed by *FEDER* funds and by the *Generalitat de Catalunya* (2009SGR-795; 2014SGR-728). VAS was a recipient of a "Francisco José de Caldas" predoctoral fellowship, *Colciencias.* JA is a recipient of a predoctoral fellowship (*Personal Investigador en Formación*, Universitat Autònoma de Barcelona).

All authors declare no conflict of interests.

The three dimensional crystal structures of RNase 3-H15A was submitted to the Protein Data Bank (PD ID code: 4OWZ).

REFERENCES

Abtin, A., Eckhart, L., Mildner, M., Ghannadan, M., Harder, J., Schröder, J.-M., and Tschachler, E. (2009) Degradation by stratum corneum proteases prevents endogenous RNase inhibitor from blocking antimicrobial activities of RNase 5 and RNase 7. *J Invest Dermatol* **129**: 2193–2201.

Acharya, K.R., and Ackerman, S.J. (2014) Eosinophil Granule Proteins: Form and Function. *J Biol Chem* **289**: 17406–17415.

Andrès, E. (2012) Cationic antimicrobial peptides in clinical development, with special focus on thanatin and heliomicin. *Eur J Clin Microbiol Infect Dis* **31**: 881–8.

Bardan, A., Nizet, V., and Gallo, R.L. (2004) Antimicrobial peptides and the skin. **4**:543–549.

Becknell, B., Eichler, T.E., Beceiro, S., Li, B., Easterling, R.S., Carpenter, A.R., *et al.* (2014) Ribonucleases 6 and 7 have antimicrobial function in the human and murine urinary tract. *Kidney Int* **87**: 151–161.

Benito, A., Vilanova, M., and Ribó, M. (2008) Intracellular routing of cytotoxic pancreatic-type ribonucleases. *Curr Pharm Biotechnol* **9**: 169–179.

Boix, E., Nikolovski, Z., Moiseyev, G.P., Rosenberg, H.F., Cuchillo, C.M., and Nogues, M. V (1999) Kinetic and product distribution analysis of human eosinophil cationic protein indicates a subsite arrangement that favors exonuclease-type activity. *J Biol Chem* **274**: 15605–15614.

Boix, E., and Nogués, M.V. (2007) Mammalian antimicrobial proteins and peptides: overview on the RNase A superfamily members involved in innate host defence. *Mol Biosyst* **3**: 317–335.

Boix, E., Pulido, D., Moussaoui, M., Nogues, M. V, Russi, S., and Nogués, M.V. (2012) The sulfate-binding site structure of the human eosinophil cationic protein as revealed by a new crystal form. *J Struct Biol* **179**: 1–9.

Boix, E., Salazar, V. a., Torrent, M., Pulido, D., Nogués, M.V., and Moussaoui, M. (2012) Structural determinants of the eosinophil cationic protein antimicrobial activity. *Biol Chem* **393**: 801–815.

Bravo, J., Fernández, E., Ribó, M., Dellorens, R., and Cuchillo, C.M. (1994) A versatile negative-staining ribonuclease zymogram. *Anal Biochem* **219**: 82–86.

Brogden, K. a (2005) Antimicrobial peptides: pore formers or metabolic inhibitors in bacteria? *Nat Rev Microbiol* **3**: 238–250.

Carreras, E., Boix, E., Navarro, S., Rosenberg, H.F.F., Cuchillo, C.M.M., Nogués, M.V.V., *et al.* (2005) Surface-exposed amino acids of eosinophil cationic protein play a critical role in the inhibition of mammalian cell proliferation. *Mol Cell Biochem* **272**: 1–7 http://www.ncbi.nlm.nih.gov/pubmed/16010966.

Carreras, E., Boix, E., Rosenberg, H., Cuchillo, C.M., and Nogues, M. V (2003) Both aromatic and cationic residues contribute to the membrane-lytic and bactericidal activity of eosinophil cationic protein. *Biochemistry* **42**: 6636–6644.

Chaffin, W.L. (2008) Candida albicans cell wall proteins. *Microbiol Mol Biol Rev* **72**: 495–544.

Chao, T.Y., and Raines, R.T. (2011) Mechanism of ribonuclease a endocytosis: Analogies to cell-penetrating peptides. *Biochemistry* **50**: 8374–8382.

Cuchillo, C.M., Nogués, M.V., and Raines, R.T. (2011) Bovine pancreatic ribonuclease: Fifty years of the first enzymatic reaction mechanism. *Biochemistry* **50**: 7835–7841.

D'Alessio, G., Donato, A. Di, Parente, A., and Piccoli, R. (1991) Seminal RNase: a unique member of the ribonuclease superfamily. *Trends Biochem Sci* **16**: 104–106.

Do, N., Weindl, G., Grohmann, L., Salwiczek, M., Koksch, B., Korting, H.C., and Schäfer-Korting, M. (2014) Cationic membrane-active peptides - anticancer and antifungal activity as well as penetration into human skin. *Exp Dermatol* **23**: 326–331.

Dorschner, R.A., Pestonjamasp, V.K., Tamakuwala, S., Ohtake, T., Rudisill, J., Nizet, V., *et al.* (2001) Cutaneous injury induces the release of cathelicidin anti-microbial peptides active against group A streptococcus. *J Invest Dermatol* **117**: 91–97.

Düring, K., Porsch, P., Mahn, A., Brinkmann, O., and Gieffers, W. (1999) The non-enzymatic microbicidal activity of lysozymes. *FEBS Lett* **449**: 93–100.

Fan, T., Fang, S., Hwang, C., Hsu, C., Lu, X., Hung, S., *et al.* (2008) Characterization of molecular interactions between eosinophil cationic protein and heparin. *J Biol Chem* **283**: 25468–25474.

Fan, T.C., Chang, H.T., Chen, I.W., Wang, H.Y., and Chang, M.D.T. (2007) A heparan sulfate-facilitated and raft-dependent macropinocytosis of eosinophil cationic protein. *Traffic* **8**: 1778–1795.

Fang, S., Fan, T., Fu, H.-W., Chen, C.-J., Hwang, C.-S., Hung, T.-J., *et al.* (2013) A novel cell-penetrating peptide derived from human eosinophil cationic protein. *PLoS One* **8**: e57318.

Fritz, P., Beck-Jendroschek, V., and Brasch, J. (2012) Inhibition of dermatophytes by the antimicrobial peptides human β-defensin-2, ribonuclease 7 and psoriasin. *Med Mycol* **50**: 579–84.

García-Mayoral, M.F., Canales, Á., Díaz, D., López-Prados, J., Moussaoui, M., Paz, J.L. De, *et al.* (2013) Insights into the glycosaminoglycan-mediated cytotoxic mechanism of eosinophil cationic protein revealed by NMR. *ACS Chem Biol* **8**: 144–151.

García-Mayoral, M.F., Moussaoui, M., La Torre, B.G. De, Andreu, D., Boix, E., Nogués, M.V., *et al.* (2010) NMR structural determinants of eosinophil cationic protein binding to membrane and heparin mimetics. *Biophys J* **98**: 2702–2711.

Gläser, R., Harder, J., Lange, H., Bartels, J., Christophers, E., and Schröder, J.-M. (2005) Antimicrobial psoriasin (S100A7) protects human skin from Escherichia coli infection. *Nat Immunol* **6**: 57–64.

Glaser, R., Navid, F., Schuller, W., Jantschitsch, C., Harder, J., Schroder, J.M., *et al.* (2009) UV-B radiation induces the expression of antimicrobial peptides in human keratinocytes in vitro and in vivo. *J Allergy ClinImmunol* **123**: 1117–1123.

Gupta, S.K., Haigh, B.J., Griffin, F.J., and Wheeler, T.T. (2012) The mammalian secreted RNases: Mechanisms of action in host defence. *Innate Immun* **19**: 86–97.

Haigis, M.C., and Raines, R.T. (2003) Secretory ribonucleases are internalized by a dynamin-independent endocytic pathway. *J Cell Sci* **116**: 313–324.

Hancock, R.E.W., and Sahl, H.-G. (2006) Antimicrobial and host-defense peptides as new anti-infective therapeutic strategies. *Nat Biotechnol* **24**: 1551–1557.

Haney, E.F., and Hancock, R.E.W. (2013) Peptide design for antimicrobial and immunomodulatory applications. *Biopolymers* **100**: 572–583.

Harder, J.J., Schroder, J.-M. (2002) RNase 7, a novel innate immune defense antimicrobial protein of healthy human skin. *J Biol Chem* **277**: 46779–46784.

Harris, P., Johannessen, K.M., Smolenski, G., Callaghan, M., Broadhurst, M.K., Kim, K., and Wheeler, T.T. (2010) Characterisation of the anti-microbial activity of bovine milk ribonuclease4 and ribonuclease5 (angiogenin). *Int Dairy J* **20**: 400–407.

Hertog, A.L. den, Marle, J. van, Veen, H. a van, Van't Hof, W., Bolscher, J.G.M., Veerman, E.C.I., and Nieuw Amerongen, A. V (2005) Candidacidal effects of two antimicrobial peptides: histatin 5 causes small membrane defects, but LL-37 causes massive disruption of the cell membrane. *Biochem J* **388**: 689–95.

Holm, T., Netzereab, S., Hansen, M., Langel, Ü., and Hällbrink, M. (2005) Uptake of cell-penetrating peptides in yeasts. *FEBS Lett* **579**: 5217–5222.

Hooper, L. V, Stappenbeck, T.S., Hong, C. V, and Gordon, J.I. (2003) Angiogenins: a new class of microbicidal proteins involved in innate immunity. *Nat Immunol* **4**: 269–73.

Huang, Y.C., Lin, Y.M., Chang, T.W., Wu, S.H., Lee, Y.S., Chang, M.D., *et al.* (2007) The flexible and clustered lysine residues of human ribonuclease 7 are critical for membrane permeability and antimicrobial activity. *J Biol Chem* **282**: 4626–4633.

Iwanaga, S., and Lee, B.L. (2005) Recent advances in the innate immunity of invertebrate animals. *J Biochem Mol Biol* **38**: 128–150.

Last, N.B., Schlamadinger, D.E., and Miranker, A.D. (2013) A common landscape for membrane active peptides. *Protein Sci* **22**: 870–882.

Leonardi, A., Borghesan, F., Faggian, D., Secchi, A., and Plebani, M. (1995) Eosinophil cationic protein in tears of normal subjects and patients affected by vernal keratoconjunctivitis. *Allergy* **50**: 610–613.

Lien, P., Kuo, P., Chen, C., Chang, H., Fang, S., Wu, W., *et al.* (2013) In Silico Prediction and In Vitro Characterization of. *Biomed Res Int* **2013**: 170398.

Lin, Y.M., Wu, S.J., Chang, T.W., Wang, C.F., Suen, C.S., Hwang, M.J., *et al.* (2010) Outer membrane protein I of pseudomonas aeruginosa is a target of cationic antimicrobial peptide/protein. *J Biol Chem* **285**: 8985–8994.

Lomax, J.E., Bianchetti, C.M., Chang, A., Phillips, G.N., Fox, B.G., and Raines, R.T. (2014) Functional evolution of ribonuclease inhibitor: Insights from birds and reptiles. *J Mol Biol* **426**: 3041–3056 http://dx.doi.org/10.1016/j.jmb.2014.06.007.

López-García, B., Lee, P.H.A., Yamasaki, K., and Gallo, R.L. (2005) Anti-fungal activity of cathelicidins and their potential role in Candida albicans skin infection. *J Invest Dermatol* **125**: 108–115.

Maeda, T., Kitazoe, M., Tada, H., Llorens, R. de, Salomon, D.S., Ueda, M., *et al.* (2002) Growth inhibition of mammalian cells by eosinophil cationic protein. *Eur J Biochem* **269**: 307–316.

Mallorquí-Fernández, G., Pous, J., Peracaula, R., Aymamí, J., Maeda, T., Tada, H., *et al.* (2000) Three-dimensional crystal structure of human eosinophil cationic protein (RNase 3) at 1.75 A resolution. *J Mol Biol* **300**: 1297–1307.

Marchione, R., Daydé, D., Lenormand, J.L., and Cornet, M. (2014) ZEBRA cell-penetrating peptide as an efficient delivery system in Candida albicans. *Biotechnol J* **9**: 1088–1094.

Mayer, F.L.L., Wilson, D., and Hube, B. (2013) Candida albicans pathogenicity mechanisms. *Virulence* **4**: 119–28.

Mochon, A.B., and Liu, H. (2008) The antimicrobial peptide histatin-5 causes a spatially restricted disruption on the Candida albicans surface, allowing rapid entry of the peptide into the cytoplasm. *PLoS Pathog* **4:**e1000190.

Mohammed, I., Yeung, A., Abedin, A., Hopkinson, A., and Dua, H.S. (2011) Signalling pathways involved in ribonuclease-7 expression. *Cell Mol Life Sci* **68**: 1941–1952.

Molero, G., Díez-Orejas, R., Navarro-García, F., Monteoliva, L., Pla, J., Gil, C., and Sánchez-Pérez, M. (1998) Candida albicans: Genetics, dimorphism and pathogenicity. *Int Microbiol* **1**: 95–106.

Navarro, S., Aleu, J., Jiménez, M., Boix, E., Cuchillo, C.M., and Nogués, M. V. (2008) The cytotoxicity of eosinophil cationic protein/ribonuclease 3 on eukaryotic cell lines takes place through its aggregation on the cell membrane. *Cell Mol Life Sci* **65**: 324–337.

Navarro, S., Boix, E., Cuchillo, C.M., and Nogués, M.V. (2010) Eosinophil-induced neurotoxicity: The role of eosinophil cationic protein/RNase 3. *J Neuroimmunol* **227**: 60–70.

Nekhotiaeva, N., Elmquist, A., Rajarao, G.K., Hällbrink, M., Langel, U., and Good, L. (2004) Cell entry and antimicrobial properties of eukaryotic cell-penetrating peptides. *FASEB J* **18**: 394–6.

Nicolas, P. (2009) Multifunctional host defense peptides: Intracellular-targeting antimicrobial peptides. *FEBS J* **276**: 6483–6496.

Nikolovski, Z., Buzón, V., Ribó, M., Moussaoui, M., Vilanova, M., Cuchillo, C.M., *et al.* (2006) Thermal unfolding of eosinophil cationic protein/ribonuclease 3: a nonreversible process. *Protein Sci* **15**: 2816–2827.

Niyonsaba, F., and Ogawa, H. (2005) Protective roles of the skin against infection: Implication of naturally occurring human antimicrobial agents β-defensins, cathelicidin LL-37 and lysozyme. *J Dermatol Sci* **40**: 157–168.

Park, C., Schultz, L.W., and Raines, R.T. (2001) Contribution of the active site histidine residues of ribonuclease A to nucleic acid binding. *Biochemistry* **40**: 4949–4956.

Peschel, A., and Sahl, H.-G. (2006) The co-evolution of host cationic antimicrobial peptides and microbial resistance. *Nat Rev Microbiol* **4**: 529–536.

Pizzo, E., and D'Alessio, G. (2007) The success of the RNase scaffold in the advance of biosciences and in evolution. *Gene* **406**: 8–12.

Pulido, D., Moussaoui, M., Victòria Nogués, M., Torrent, M., and Boix, E. (2013) Towards the rational design of antimicrobial proteins: Single point mutations can switch on bactericidal and agglutinating activities on the RNase A superfamily lineage. *FEBS J* **280**: 5841–5852.

Pulido, D., Torrent, M., Andreu, D., Nogues, M.V., and Boix, E. (2013) Two human host defense ribonucleases against mycobacteria, the eosinophil cationic protein (RNase 3) and RNase 7. *Antimicrob Agents Chemother* **57**: 3797–3805.

Ribo, M., Benito, A., and Vilanova, M. (2011) Antitumor ribonucleases. In *Ribonucleases, Nucleic Acids and Molecular Biology*. Nicholson, A.W. (ed.). Springer-Verlag, Berlin. pp. 55–88.

Rosenberg, H.F. (2008) RNase A ribonucleases and host defense: an evolving story. *J Leukoc Biol* **83**: 1079–1087.

Rosenberg, H.F., Dyer, K.D., and Foster, P.S. (2013) Eosinophils: changing perspectives in health and disease. *Nat Rev Immunol* **13**: 9–22.

Rothenberg, M.E., and Hogan, S.P. (2006) The eosinophil. *Annu Rev Immunol* **24**: 147–174.

Rudolph, B., Podschun, R., Sahly, H., Schubert, S., Schröder, J.M., and Harder, J. (2006) Identification of RNase 8 as a novel human antimicrobial protein. *Antimicrob Agents Chemother* **50**: 3194–3196.

Salazar, V. a., Rubin, J., Moussaoui, M., Pulido, D., Nogués, M.V., Venge, P., and Boix, E. (2014) Protein post-translational modification in host defense: the antimicrobial mechanism of action of human eosinophil cationic protein native forms. *FEBS J* **281**: 5432–5446.

Schröder, J.-M., and Harder, J. (2006) Antimicrobial peptides in skin disease. *Drug Discov Today Ther Strateg* **3**: 93–100.

Singh, A., and Batra, J.K. (2011) Role of unique basic residues in cytotoxic, antibacterial and antiparasitic activities of human eosinophil cationic protein. *Biol Chem* **392**: 337–346.

Smet, K. De, and Contreras, R. (2005) Human antimicrobial peptides: Defensins, cathelicidins and histatins. *Biotechnol Lett* **27**: 1337–1347.

Sørensen, O.E., Thapa, D.R., Roupé, K.M., Valore, E. V, Sjöbring, U., Roberts, A.A., *et al.* (2006) Injury-induced innate immune response in human skin mediated by transactivation of the epidermal growth factor receptor. *J Clin Invest* **116**: 1878–1885.

Spencer, J.D., Schwaderer, a L., Wang, H., Bartz, J., Kline, J., Eichler, T., *et al.* (2013) Ribonuclease 7, an antimicrobial peptide upregulated during infection, contributes to microbial defense of the human urinary tract. *Kidney Int* **83**: 615–625.

Spindler, E.C., Hale, J.D.F., Giddings, T.H., Hancock, R.E.W., and Gill, R.T. (2011) Deciphering the mode of action of the synthetic antimicrobial peptide bac8c. *Antimicrob Agents Chemother* **55**: 1706–1716.

Stalmans, S., Wynendaele, E., Bracke, N., Gevaert, B., D'Hondt, M., Peremans, K., *et al.* (2013) Chemical-Functional Diversity in Cell-Penetrating Peptides. *PLoS One* **8**: e71752.

Sundlass, N.K., Eller, C.H., Cui, Q., and Raines, R.T. (2013) Contribution of electrostatics to the binding of pancreatic-type ribonucleases to membranes. *Biochemistry* **52**: 6304–6312.

Swidergall, M., and Ernst, J.F. (2014) Interplay between Candida albicans and the antimicrobial peptide armory. *Eukaryot Cell* **13**.

The CCP4 suite: programs for protein crystallography. (1994) *Acta Crystallogr D Biol Crystallogr* **50**: 760–3.

Thiyagarajan, N., Ferguson, R., Subramanian, V., and Acharya, R. (2012) Structural and molecular insights into the mechanism of action of human angiogenin-ALS variants in neurons. *Nat Commun* **3**: 1114–1121 http://dx.doi.org/10.1038/ncomms2126.

Torrent, M., Badia, M., Moussaoui, M., Sanchez, D., Nogués, M.V., and Boix, E. (2010) Comparison of human RNase 3 and RNase 7 bactericidal action at the Gram-negative and Gram-positive bacterial cell wall. *FEBS J* **277**: 1713–1725.

Torrent, M., Cuyás, E., Carreras, E., Navarro, S., López, O., la Maza, A. de, *et al.* (2007) Topography studies on the membrane interaction mechanism of the eosinophil cationic protein. *Biochemistry* **46**: 720–733.

Torrent, M., Navarro, S., Moussaoui, M., Nogués, M.V., and Boix, E. (2008) Eosinophil Cationic Protein High-Affinity Binding to Bacteria-Wall. *Scan Electron Microsc* 3544–3555.

Torrent, M., Nogués, M.V., and Boix, E. (2011) Eosinophil cationic protein (ECP) can bind heparin and other glycosaminoglycans through its RNase active site. *J Mol Recognit* **24**: 90–100.

Torrent, M., Odorizzi, F., Nogués, M.V., and Boix, E. (2010) Eosinophil cationic protein aggregation: Identification of an N-terminus amyloid prone region. *Biomacromolecules* **11**: 1983–1990.

Torrent, M., Pulido, D., La Torre, B.G. De, García-Mayoral, M.F., Nogués, M.V., Bruix, M., *et al.* (2011) Refining the eosinophil cationic protein antibacterial pharmacophore by rational structure minimization. *J Med Chem* **54**: 5237–5244.

Torrent, M., Pulido, D., Nogués, M.V., and Boix, E. (2012) Exploring New Biological Functions of Amyloids: Bacteria Cell Agglutination Mediated by Host Protein Aggregation. *PLoS Pathog* **8**: 2012–2014.

Torrent, M., Sanchez, D., Buzon, V., Nogues, M. V, Cladera, J., Boix, E., *et al.* (2009) Comparison of the membrane interaction mechanism of two antimicrobial RNases: RNase 3/ECP and RNase 7. *Biochim Biophys Acta - Biomembr* **1788**: 1116–1125.

Tsai, P.-W.W., Cheng, Y.-L.L., Hsieh, W.-P.P., and Lan, C.-Y.Y. (2014) Responses of Candida albicans to the human antimicrobial peptide LL-37. *J Microbiol* **52**: 581–589.

Vylkova, S., Sun, J.N., and Edgerton, M. (2007) The role of released ATP in killing Candida albicans and other extracellular microbial pathogens by cationic peptides. *Purinergic Signal* **3**: 91–7.

Young, J.D., Peterson, C.G., Venge, P., and Cohn, Z.A. (1986) Mechanism of membrane damage mediated by human eosinophil cationic protein. *Nature* **321**: 613–6.

TABLES

Table 1: Antifungal activity of RNase 7, RNase 7-H15A, RNase 3, RNase 3-H15A and RNase 3-W35A, on *Candida albicans*. IC_{50}, given as mean ± SD, were determined using the Bactiter-Glo™ kit as detailed in the Experimental Procedures. Minimal fungicidal concentration (MFC_{100}) values were calculated by CFU counting on plated Petri dishes. Cell survival percentage was calculated using the Live/Dead® kit at 5 µM protein concentration after 240 min of incubation time. All values are averaged from three replicates of two independent experiments. For the comparison of numerical variables between wild type and mutant, the Student's T test was used. Values of $p < 0.05^*$ and $p < 0.09^{**}$ were considered significant.

Protein	IC_{50} (µM)	MFC_{100} (µM)	Cell survival (%)
RNase 7	1.60 ± 0.09	3.75	7.74 ± 0.12
RNase 7-H15A	1.93 ± 0.07*	4.12	9.07 ± 0.09*
RNase 3	2.50 ± 0.01	4.70	9.72 ± 0.05
RNase 3-H15A	3.45 ± 0.08**	9.0**	14.08 ± 0.12**
RNase 3-W35A	9.03 ± 0.52**	> 20**	37.84 ± 0.36**

Table 2: Cell membrane depolarization and permeation activities of RNases on *Candida albicans*. Maximum membrane depolarization and permeation activities were determined after 50 min at 1 μM final protein concentration using the $DiSC_3(5)$ probe and *Sytox® Green*, respectively, as described in Experimental Procedures. All values, given as mean ±SD, are averaged from three replicates of two independent experiments.

Protein	Max. membrane depolarization (AU)[a]	Membrane depolarization (%)[b]	Max. membrane permeation (AU)[a]	Membrane permeation (%)[b]
RNase 7	165.77 ± 1.10	71.67 ± 0.1	134.56 ± 1.95	45.90 ± 0.5
RNase 7-H15A	153 [illegible] 1.65*	66.54 ± 0.9	93.05 ± 1.24*	31.52 ± 0.3
RNase 3	80.0[illegible] ± 0.90	34.62 ± 0.08	104.93 ± 2.80	35.55 ± 0.4
RNase 3-H15A	67.2[illegible] ± 1[illegible]3*	29.08 ± 1.0	61.32 ± 0.63**	20.77 ± 0.2
RNase 3-W35A	28.42 ± 0[illegible].2	12.28 ± 0.7	24.84 ± 0.25**	8.46 ± 0.6

[a]Arbitrary fluorescence unit (AU) values are indicated for maximum membrane depolarization and permeation. [b]For membrane permeation and membrane depolarization, the calculated percentages refer to the maximum values achieved at final incubation time, referred to the positive control (10 % of Triton X-100). The p value were calculated using as reference each wild type activity (* corresponds to $p < 0.05$ and ** to $p < 0.09$).

Table 3. Comparison of calculated time to achieve 50% activity (t_{50}) for depolarization, cell leakage and cell survival. All assays were carried out at 1 μM final protein concentration. Depolarization was assayed using DISC3(5) dye, cell leakage by the *Sytox Green* assay and survival percentage at final incubation time (120 min) was evaluated using the Live/dead® kit. T-student was applied for comparison of numerical variables using as reference each activity corresponding to wild type protein, where * corresponds to $p < 0.05$ and ** to $p < 0.09$.

Protein	Depolarization t_{50} (s)	Cell Leakage t_{50} (s)	Cell survival t_{50} (s)	Cell survival (%)
RNase 7	261.23	595.53	1397	38.2
RNase 7-H15A	288.53	698.15*	1763*	54.86**
RNase 3	251.36	490.84	2354	56.87
RNase 3-H15A	356.75*	975.5**	2965*	67.89**

Table 4: Relative enzymatic activity was determined by the spectrophotometric method using $(Cp)_4C>p$ substrate as described in the Experimental Procedures section. Leakage of large unilamellar vesicles (LUV) is expressed as 50% effective dose (ED_{50}), given as mean ±SD, averaged from three replicates of two independent experiments.

Protein	**RNase activity (%)**	**LUV Leakage ED_{50} (μ M)**
RNase 7	100	1.14 ± 0.03
RNase 7-H15A	9	1.24 ± 0.09
RNase 3	100	1.33 ± 0.71
RNase 3-H15A	0	1.44 ± 0.14

FIGURE LEGENDS

Figure 1: A) Sequence alignment of RNase 3 and RNase 7. Primary sequences (UniProt codes: P12724 and Q9H1E1) were used, respectively. RNase 3 three dimensional structure is indicated (PDB ID: 4OXF). Cationic residues are shown in both proteins in green and fuchsia boxes, respectively. The alignment was performed using the ESPript program (http://espript.ibcp.fr/EsPript/). B) Three dimensional representation of crystal structures of wild type RNase 3 (yellow; PDB ID: 4OXF) and active site mutant RNase 3-H15A (purple; PDB ID: 4OWZ). Mutated residues (His 15 and Trp 35) are depicted in baton sticks. C).Detail of active centre in both proteins. Picture was drawn with PYMOL (Schrödinger).

Figure 2: Effects of RNase 3, RNase 3-H15A and RNase 3-W35A (A-C) on C. *albicans* in mid-exponential growth phase (~3 x10^6 cell/mL) visualized by confocal microscopy. The yeast morphology is showing in the left-hand side. Second panel shows labeled cells with Hoechst 33342. The third and forth panels show the merged Hoechst and Alexa Fluor 488– labeled protein after 5 and 20 min of incubation respectively. The protein final concentration was 3 μM. *ImageJ* software was used for analysis. The magnification scale is indicated at the bottom of each micrograph. Images were taken using a Leica TCS SP5 AOBS microscope.

Figure 3: Distribution of Alexa Fluor 488-labeled protein in treated *C. albicans* cells visualized by confocal microscopy, following the assay incubation conditions detailed in the Materials and methods section. Analysis was made at 2 and 20 min after protein addition at 1 μM final concentration. A total of 20 *Candida* cells were analyzed by regions of interest (ROIs) using Leica TCS software. Bar graphs of total internal and external fluorescence intensity values (maximum peak) are shown. Yeast size mean was adjusted according to Hoescht labeled distribution and disc image. The cell mean size was around 4.5 μm and a distance >4.5 μm was ascribed to the cell environment. Black bar correspond to outer fluorescence and gray and light gray bar to inner fluorescence at 2 and 20 min respectively.

Figure 4: Confocal microscopy analysis of *Candida* cell culture (~3 x10^6 cells/mL) incubated with 1 μM of RNase 3, 7 and mutants labeled with alexa fluor 488. Fluorescent and Differential Interference Contrast (DIC) merge images are shown. A) Protein localization in yeast cells after 20 min of incubation at 37ºC with labeled proteins. B) Merged images after additional PBS washes to eliminate fluorescence background and free labeled proteins. The images were taken using a Leica TCS SP5 AOBS microscope.

Figure 5: Analysis of C. *albicans* cell culture (1x10^6 cells/mL) incubated with 1 μM of protein by FACS. Cells were gated by Forward scatter (FSC) / Side scatter (SSC). Additionally, the incubation mixture was treated with PI to identify the dead cell population. After addition of RNase 7 (A) and RNase 7-H15A (B) the samples were analyzed using a FACSCalibur cytometer at 2, 5, 15 and 60 min. Dot plot diagrams of Protein Alexa Fluor 488/ PI show cell population divided in: free live cells (blue), cells with uptake protein (green), free dead cell (red) and dead cells with protein uptake (orange).

Figure 6: Effect of RNase 3 and mutants on *C. albicans* cellular RNA. RNA was extracted as described in Materials and methods; 1 mL of yeast cell suspension (~ 1 x10^7 cells/mL) was treated with 3 μM of each protein. A) Samples were analyzed by Experion automated electrophoresis and RNA was visualized with the Experion software. Left lane contains molecular mass markers, where reference base pairs are indicated. Control lane corresponds to cellular RNA from untreated cells. The RNA extraction was made at different time intervals up

to 20 min. B) Peak area corresponding to 18/28s subunits of rRNA of treated cells for each incubation time are shown.

Figure 7: Illustrative graph of suggested timing of events after RNase 3 and RNase 7 addition at 1 μM to a yeast cell culture grown to ~3 x10^6 cells/mL and incubated at 37ºC. Membrane depolarization was analyzed by monitoring the $DiSC_3(5)$ fluorescence intensity change. Cell permeation analysis was monitored by using a *Sytox® green* uptake assay. Intracellular localization was observed by confocal microscopy for both labeled RNases and subsequent cellular RNA degradation was analyzed. Cell death was estimated by the Live/dead® kit.

FIGURES

Figure 1

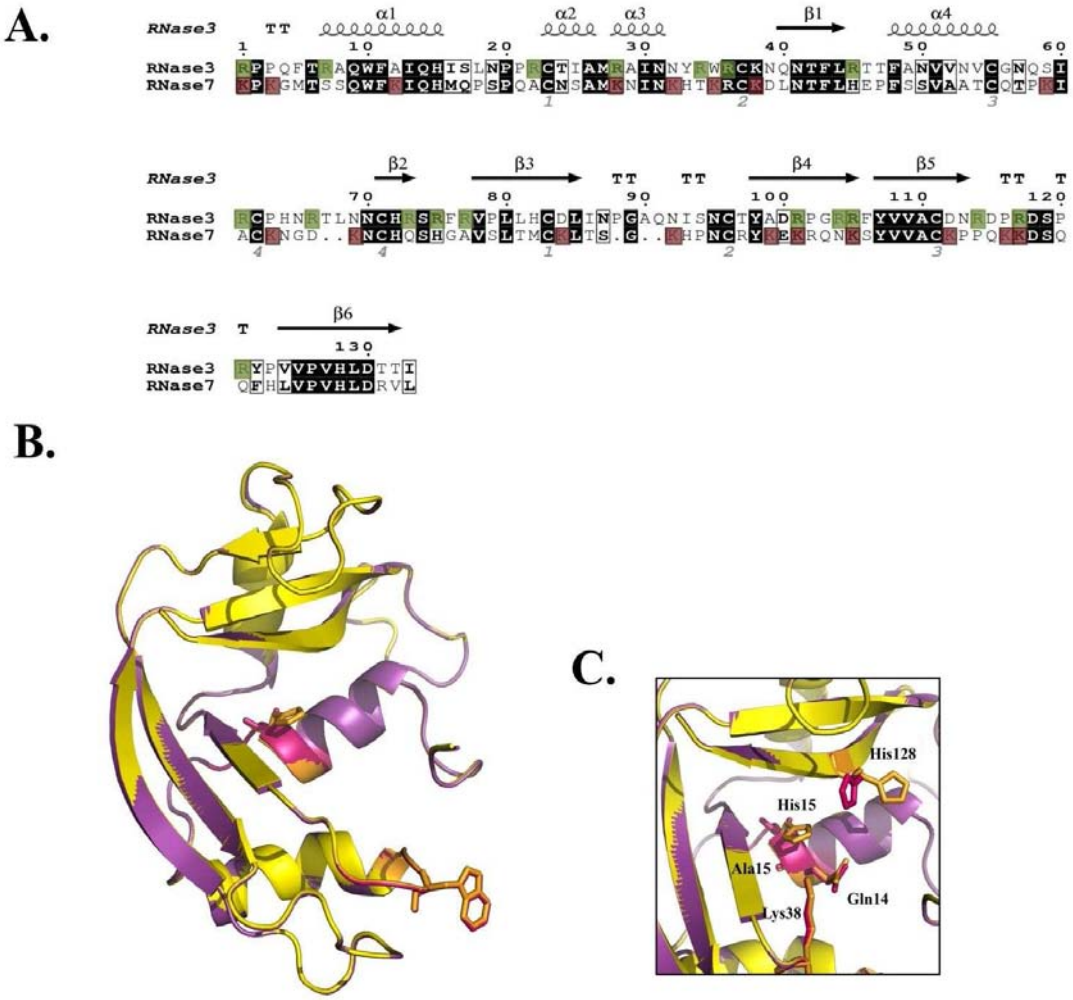

Figure 2

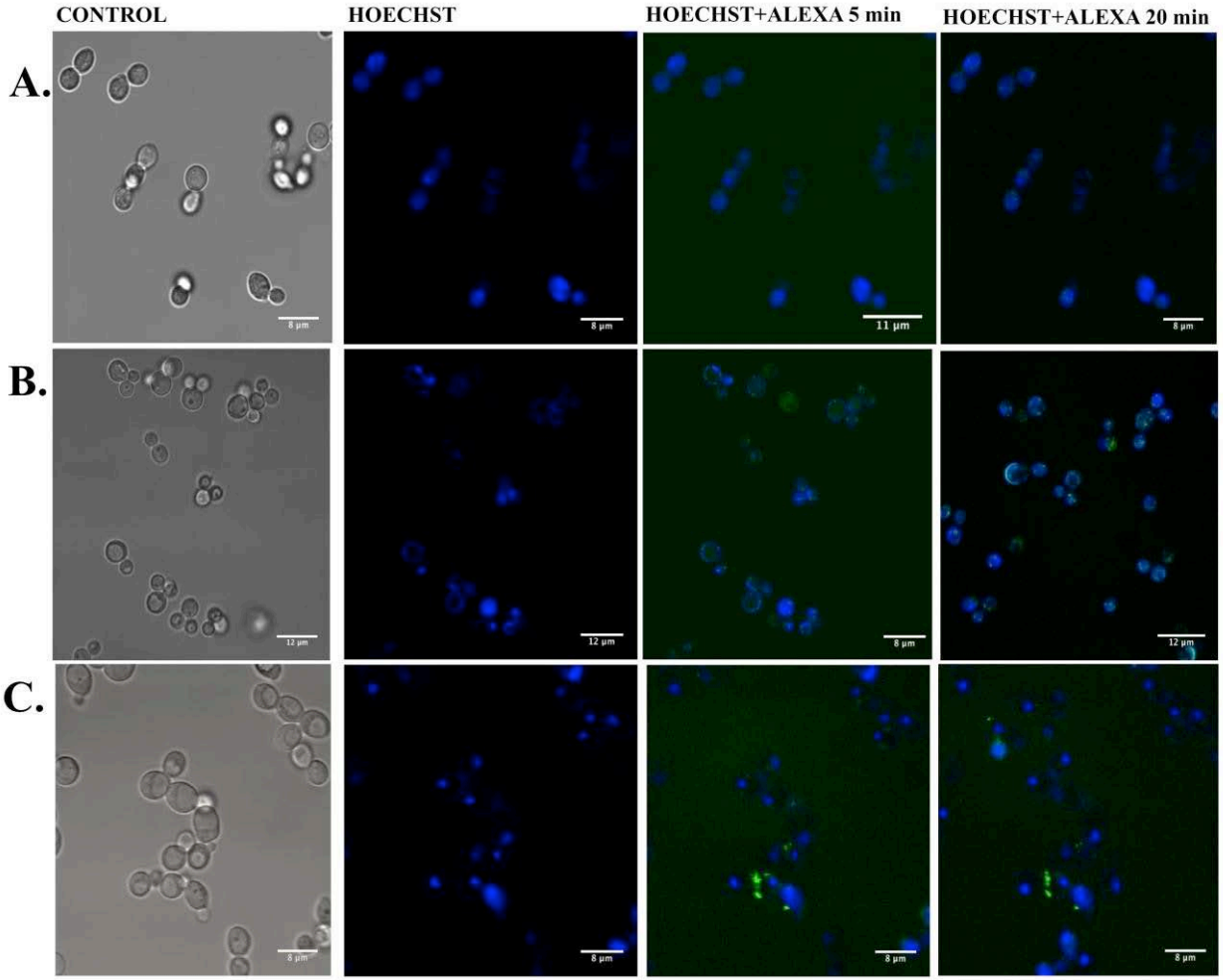
CONTROL
HOECHST
HOECHST+ALEXA 5 min
HOECHST+ALEXA 20 min
A.
B.
C.

Figure 3

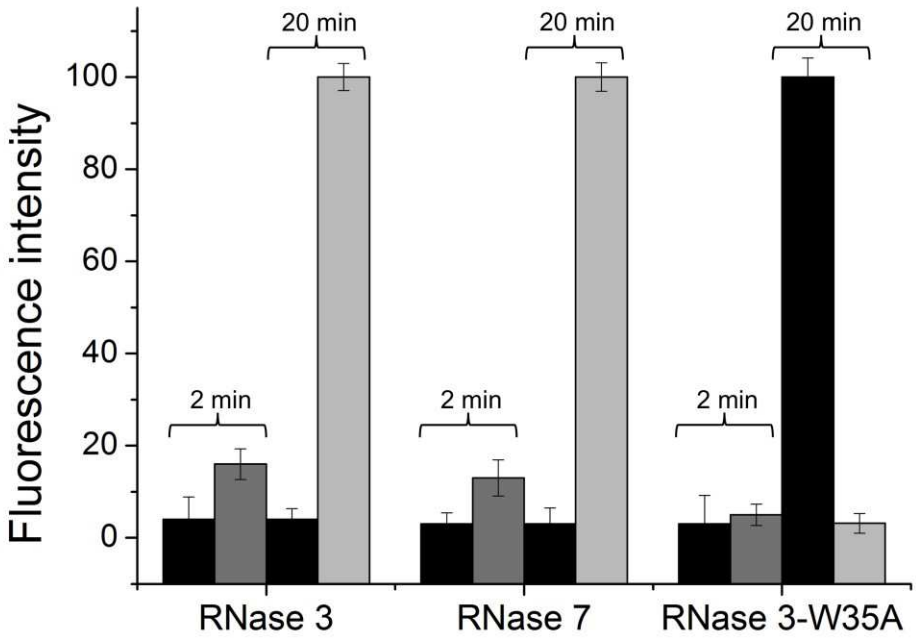

Figure 4

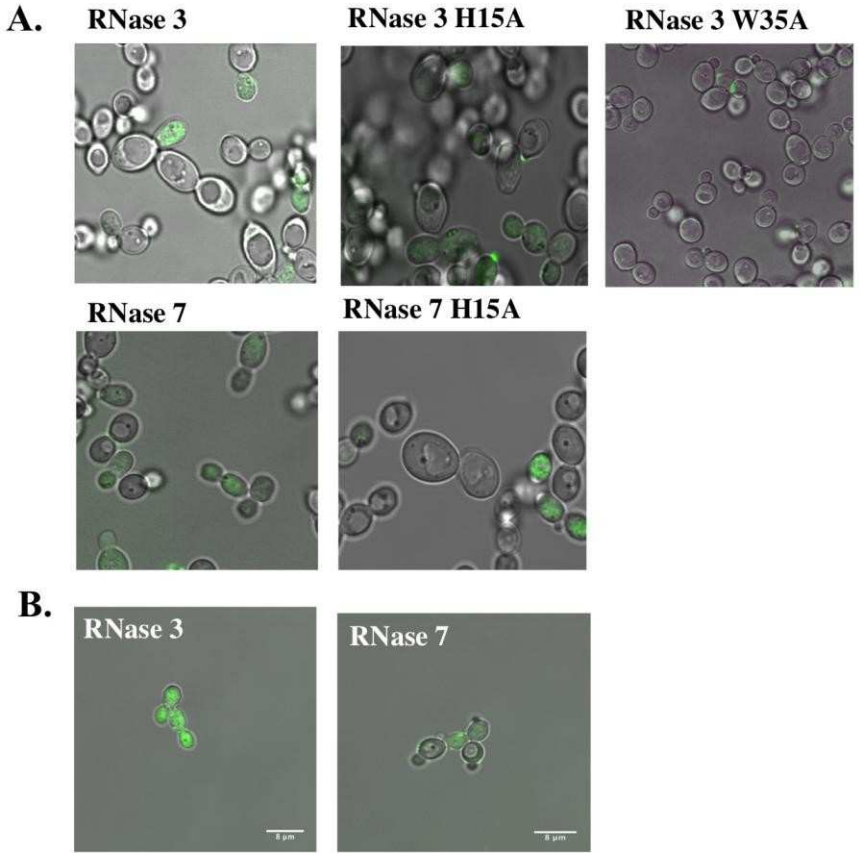

Figure 5

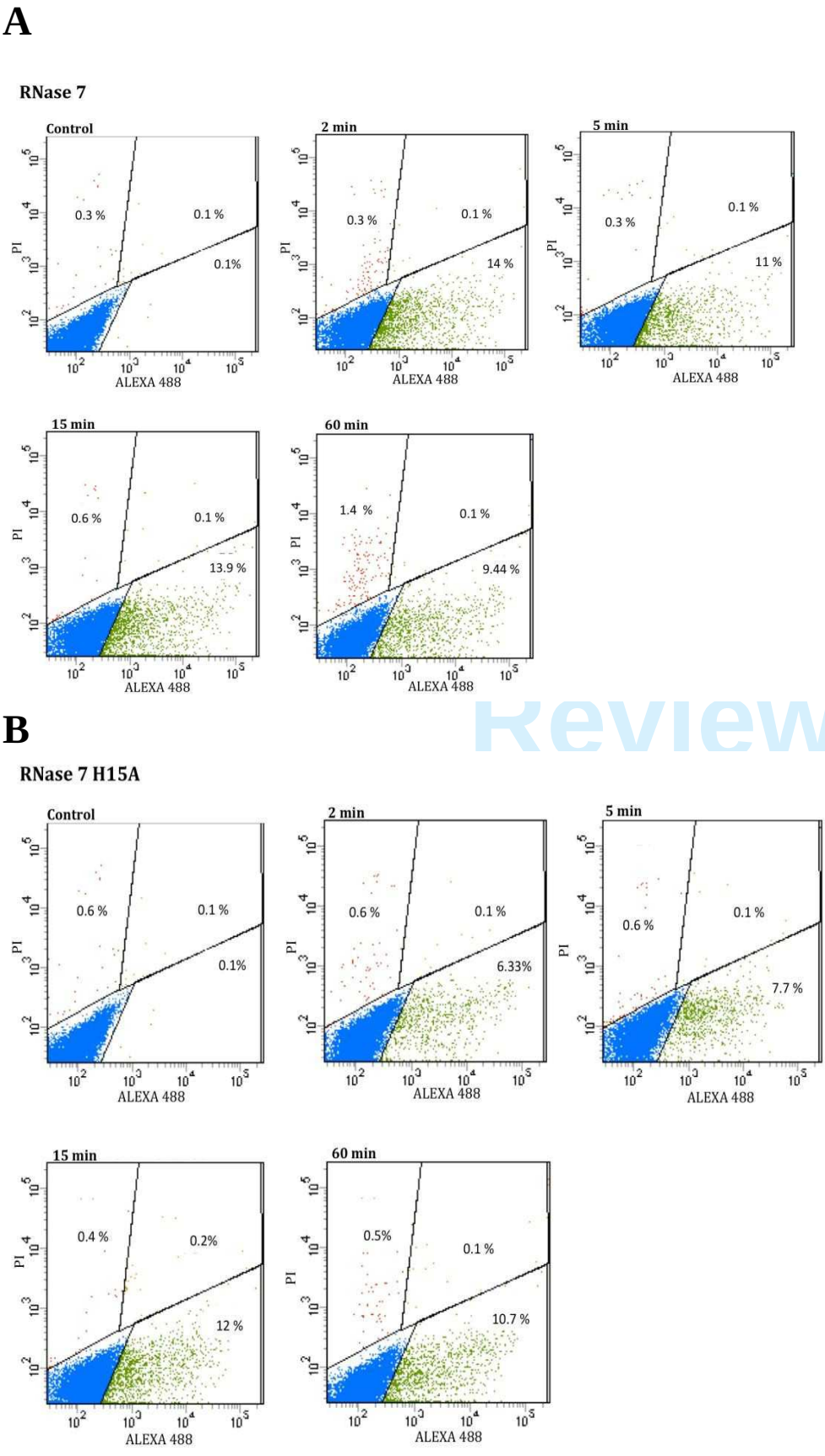

Figure 6

A

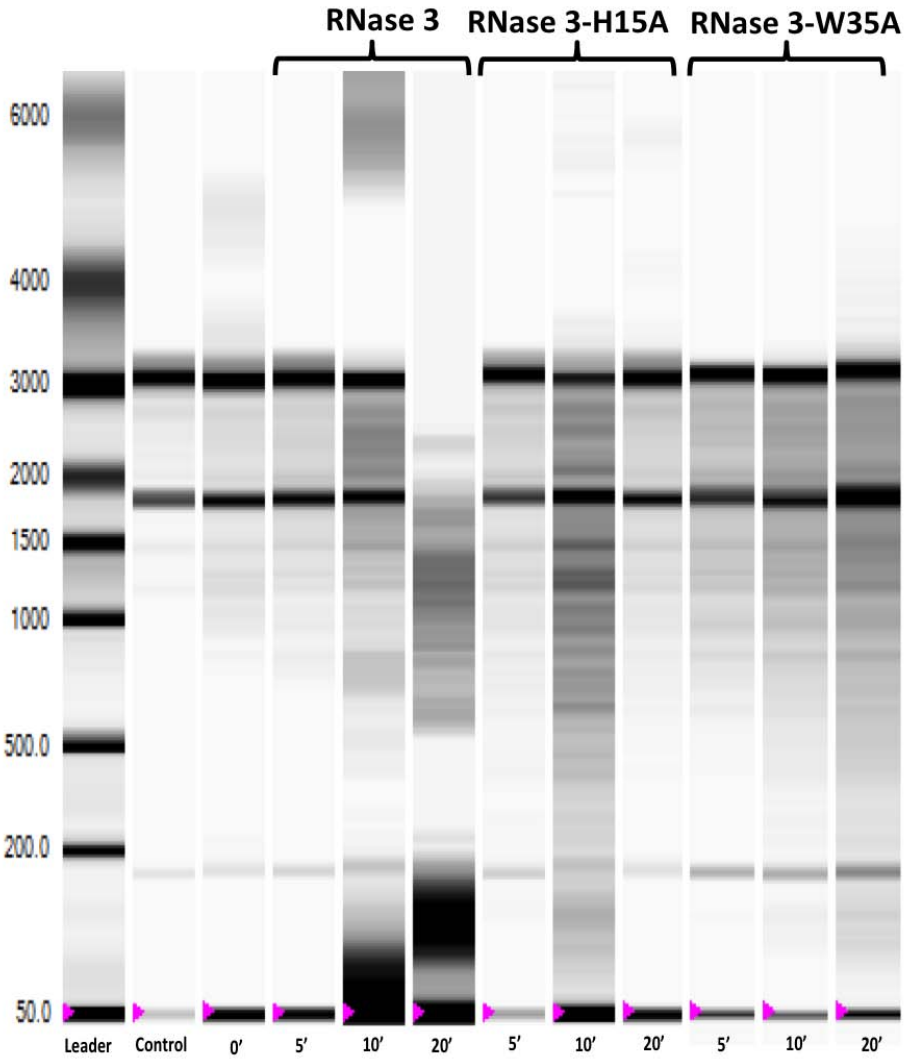

B

	RNase 3	RNase 3-H15A	RNase 3-W35A
5 min	26.81/48.92	10.32/23.75	12.36/23.15
10 min	5.08/7.93	14.32/19.16	16.58/11.75
20 min	1.01/0.15	15.20/26.30	16.42/22.14

Figure 7

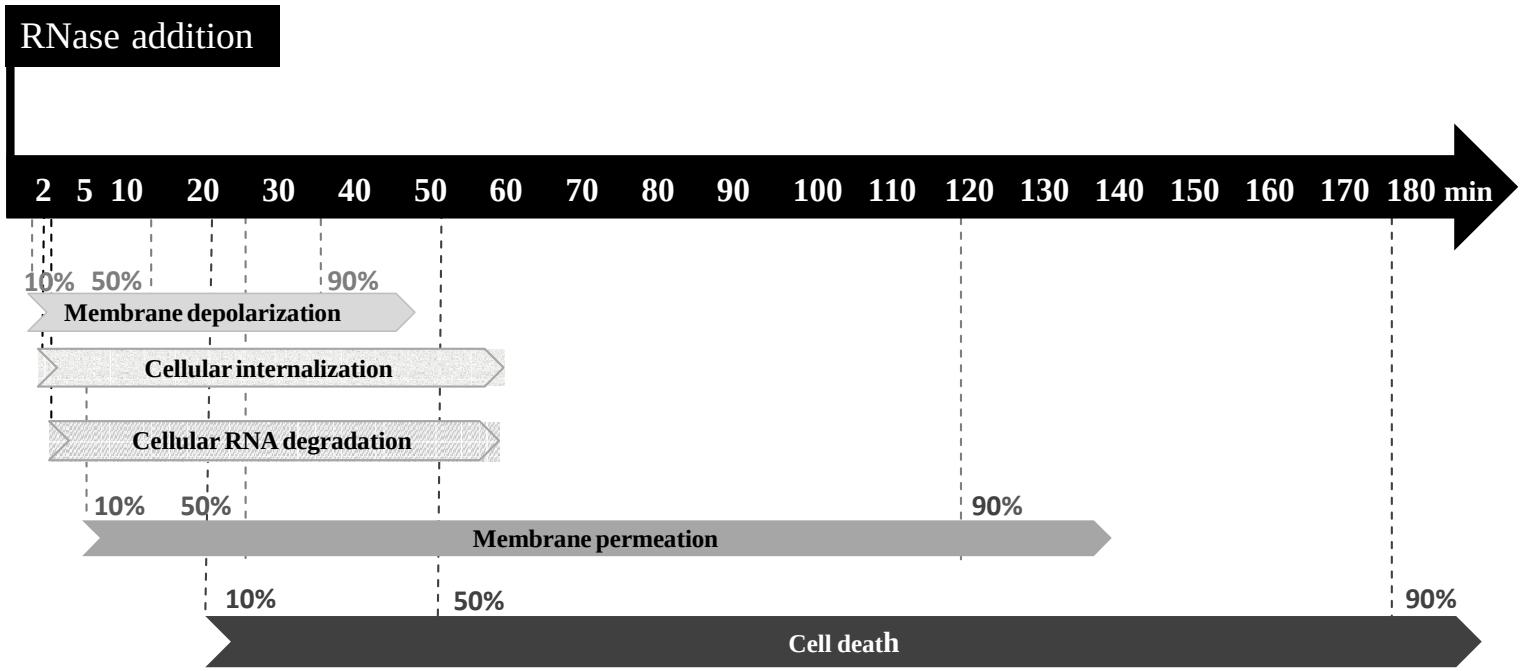
RNase addition
2 5 10 20 30 40 50 60 70 80 90 100 110 120 130 140 150 160 170 180 min
10% 50% 90%
Membrane depolarization
Cellular internalization
Cellular RNA degradation
10% 50% 90%
Membrane permeation
10% 50% 90%
Cell death